ADAPTIVE FORWARD ERROR CORRECTION CODING FOR DIVERSITY COMMUNICATION SYSTEMS

BY

SAAD SAEED AL-ABEEDI

A Thesis Presented to the

DEANSHIP OF GRADUATE STUDIES

KING FAHD UNIVERSITY OF PETROLEUM AND MINERALS

DHAHRAN, SAUDI ARABIA

In Partial fulfillment of the

Requirements for the Degree of

MASTER OF SCIENCE

In

ELECTRICAL ENGINEERING

DEC 2003

KING FAHD UNIVERSITY OF PETROLEUM AND MINERALS
DHAHRAN 31261, SAUDI ARABIA

DEANSHIP OF GRADUATE STUDIES

This thesis, written by **Saad Saeed Al-Abeedi** under the direction of his Thesis Advisor and approved by his Thesis Committee, has been presented to and accepted by the Dean of Graduate studies, in partial fulfillment of the requirements for the degree of **MASTER OF SCIENCE IN ELECTRICAL ENGINEERING.**

Thesis Committee

_____
Dr. Maan A. Kousa (Chairman)

_____
Prof. Asrar-Ul-Haq Shaikh (Member)

_____
Dr. Saud Al-Semari (Member)

_____
Department Chairman
Dr. Jamil M. Bakhashwain

_____
Dean of Graduate Studies
Prof. Osama A. Janadi

_____
Date

To my parents,

to my wife, Umm Jassir,

and to my little son, Jassir.

ACKNOWLEDGMENTS

All Praises and thanks be to ALLAH who enabled me to carry out this work and helped me to complete it.

Next, I would like to express my abbreviation to Dr. Maan Kousa, my thesis advisor, for his careful guidance and encouragement through this research.

I am also grateful to the committee members, Professor Assrar-Ul-Haq sheikh and Dr. Saud Al-Semari, for their useful suggestions and valuable comments.

Last but not least, thanks to Umm Jassir for her support, patience, and sacrifice.

TABLE OF CONTENTS

CHAPTER 3

Performance of MC-AFEC System under Realistic Conditions

CHAPTER 4

Conclusions and Suggestions for Further Work

LIST OF FIGURES

LIST OF TABLES

Table **Page**

LIST OF SYMBOLS

α	: Attenuation factor of the channel
AF	: Amount of fading
ARQ	: Automatic Repeat Request
BER	: Bit-error rate
β_q	: The q^{th} ranked channel estimate
CSI	: Channel State Information
ε	: Channel bit-error rate
f_D	: Doppler frequency
γ	: Instantaneous signal to noise ratio per bit
$\overline{\gamma}$	: Average signal to noise ratio per bit
Γ	: Set of channel quality estimates, γ_i's
h	: Adaptation period
L	: Number of diversity channels
k	: Number of information symbols
m	: Number of bits per symbol
m	: Nakagami fading parameter
MC-AFEC	: Multi-Channel Adaptive Forward Error Correction
MRC	: Maximal Ratio Combining
n	: Length of a code
N_s	: Number of scatterers in Jakes model
P	: Post-decoding symbol error probability
$\overline{P}$	: Overall average symbol error probability

$\bar{P}_b$: Overall average bit error probability

ϕ_i : Phase of the i^{th} scatterer in Jakes model

R : Throughput

ρ : Correlation coefficient

SC : Selective Combining

SER : Symbol-error rate

Ω : Mean square value of α

SNR : Signal-to-noise ratio

t : Error correction capability

τ : Duration of adaptation period

θ_i : Incident angle of the i^{th} scatterer in Jakes model

ζ : Channel symbol-error rate

ملخص الرسالة

اسم الطالب: سعد بن سعيد العبيدي

عنوان الرسالة: التشفير التكيُّفيّ المتقدم لتصحيح الخطأ في أنظمة الاتصالات اللاسلكية باستخدام قنوات استقبال التنوع

التخصص: هندسة كهربائية

تاريخ التخرج: شوال 1424هـ

السلوك المتغير بالنسبة للزمن لقنوات الاتصال المتأثرة بظاهرة الخبو الدوري (Fading) يمكن أن يسبّب تدهور شّديد لأداء النّظام. التشفير (Coding) و استقبال التنوع (Diversity) تعتبر تقنيات فعّالة لتحسين أداء النّظم المتأثرة بالخبو الدوري. عادةً ما تستخدم قنوات استقبال التنوع لتزويد جهاز الاستقبال بأكثر من نسخة للإشارة المرسلة. و لكن في هذه الرّسالة، سنستغلّ هذه القنوات بإدراج تشفير متقدم لتصحيح الخطأ (Forward Error Correction Coding) بطريقة تكيّفيّة لكي نحدّ من معدّل الخطأ في النّظام. الهدف الرئيسي هو تصغير احتمال الخطأ الكلّيّ لتحديد أفضل شفرة ممكنة لتستَخْدَم على كلّ قناة على أساس جودتها، بشرط أن يبقى معدل الطاقة الكلي ثابت.

في هذا البحث قمنا باستخدام نوعين من التشفيرRS و BCH، و كلاهما يُستخدمان بطريقة الفك بالقرار الصّعب (Hard-decision decoding). تمت دراسة أداء هذا النّظام على نوعين من القنوات هما: Rayleigh و Nakagami-*m* باستخدام النمذجة الحاسوبية، و الحسابات الرقمية في بعض الأحيان. هذه الرسالة تبحث أيضاً تأثير الارتباط بين القنوات، و تأخر تقييم جودة القنوات، و مدى قوة الخبو الدوري، على الأداء العام للنظام.

درجة الماجستير في العلوم
جامعة الملك فهد للبترول و المعادن الظهران
المملكة العربية السعودية

ABSTRACT

Name:	SAAD SAEED AL-ABEEDI
Title:	ADAPTIVE FORWARD ERROR CORRECTION FOR DIVERSITY COMMUNICATION SYSTEMS
Major field:	Electrical Engineering
Date of Degree:	October 2003

Time-varying behavior of fading channels can cause severe degradations of the system's performance. Coding and Diversity are found to be efficient techniques to improve the performance of faded systems. Typically, diversity channels are used to provide the receiver replicas of transmitted signal. In this thesis, we will utilize the available diversity channels by incorporating forward error correction coding in an adaptive way in order to minimize the bit error rate of the system. Minimization of the overall error probability will be considered to determine the optimum code rate to be used over each channel based on its quality, subject to the constraint of fixed overall throughput rate.

Both BCH and RS coding with hard-decision decoding will be considered for the purpose of forward error correction. The performance of this system over Rayleigh and Nakagami-m fading channel models will be studied by means of computer simulation, and by numerical calculations whenever possible. The effect of channel correlation and the impact of outdated channel state information on the performance of the system will be also investigated.

KING FAHD UNIVERSITY OF PETROLEUM AND MINERALS

DHAHRAN, SAUDI ARABIA

CHAPTER 1

INTRODUCTION AND LITERATURE REVIEW

Interest in wireless communication has increased in recent years. In particular, microwave radio has been gaining in importance as a transmission medium. One of the main problems associated with the radio channel is its randomly time-variant impulse response. The time dependence of the transmission properties of the channel, principally the fluctuation of the attenuation, is known as fading.

Fading can cause very poor performance on wireless communication systems. If we compare the bit error probability (BER) of communication over a Rayleigh fading channel to the nonfading case, we observe that, for the Rayleigh fading case, it

decreases only inversely (linearly) with the transmitted energy while it decreases exponentially in the nonfading case. Diversity and error-control coding are two well-known techniques to improve the performance of faded systems. Combining these two techniques in an adaptive way can be highly effective in reducing the effect of fading.

This chapter will introduce the concept of fading and its mitigation techniques. In Section 1.1, a general background of fading channel is presented followed by a literature review of fading mitigation techniques in Section 1.2. The statement of the problem of this work and the layout of the thesis are furnished in Section 1.3.

1.1 General Background of Fading Channels

Consider sending a narrow pulse across a link that has a time-varying multipath response at two different times. The level of the received signal may vary. In addition, several versions may arrive at different instants of time, due to reflections from different layers in the inhomogeneous atmosphere and/or the reflection and scattering from buildings, trees and other obstacles creating multiple paths. The relatively delayed signal components at the receiver interfere with each other. Because of the random time variations, these signals could add constructively at times and destructively at other times, resulting in variation of the received signal power levels. This is known as multipath fading which is the main source of fading attenuation.

The channel can be frequency-selective or non-selective. It is frequency-selective if it affects different spectral components differently, causing channel induced intersymbol interference (ISI) distortion. On the other hand, the channel is said to be frequency non-selective if the attenuation of all frequency components of the transmitted signal is essentially the same, and their phase shift is linearly proportional to frequency.

Fast fading and slow fading describe the characteristics of the time variation. If the characteristics of the channel change rapidly during the signaling interval, the fading is considered fast, otherwise it is slow. Fast fading results in distortion of the baseband pulse shape [1].

The performance may be severely degraded as a result of fading specially if the channel is both fast and frequency-selective. As we mentioned earlier, the BER performance of the system that experiences Rayleigh fading decreases linearly with SNR. However, in the non-fading case, the performance decreases exponentially with SNR. In fact, even when the average transmitted power of a fading channel is high there is still a significant probability that the actual received signal power for any transmission is very small causing what is known as a deep fade. Deep fades are known to be the main cause of the poor performance of fading channels. In the literature, many systems and techniques have been proposed to mitigate the degradation in the performance caused by multipath fading. In the following section, an overview of fading mitigation techniques is presented.

1.2 Fading mitigation techniques

If the channel has fast and/or frequency-selective fading, the system will suffer from an irreducible BER caused by signal distortion as a result of these types of fading. If this is the case, no amount of E_b/N_0 will help to reach the desired level of performance. The general approach in this case is to use some form of mitigation to remove or reduce the distortion. For example, if the distortion is introduced as a result of frequency-selective fading, you can use equalization to compensate for the channel-induced Inter-symbol Interference (ISI) that is seen in frequency-selective fading. As another example, spread spectrum techniques can be used to combat this type of distortion because of their ability of rejecting interference, and ISI is a type of interference.

Fast fading causes distortion to the base band pulse shape, leading to an irreducible error rate. Such distorted pulses usually create synchronization problems, such as failure of phase-locked loop (PLL) receivers. Robust modulation, error-correction coding, and interleaving are examples of the methods of combating fast fading distortion. Once the distortion has been mitigated, another mitigation techniques can be applied to compact the loss in SNR. [2]

When the channel has flat and slow fading, there will be no distortion; the system will undergo a loss in SNR only. Diversity and error control coding are two powerful techniques to combat the loss in SNR. If we could avoid using a channel when it is in deep fade, the performance will be improved significantly. Diversity will provide such

solution where the signal is transmitted over independently fading channels, making it very improbable that all the received versions of the signal are simultaneously affected by a deep fade. Conversely, coding is a well-known approach to reduce the BER for both faded and unfaded systems. A combination of these two techniques has been considered in the literature and found to provide improved performance. The performance will be further improved for time-varying channels if we adapt the transmission parameters to match the prevailing channel conditions. An overview of some of these techniques is presented in the following subsections.

1.2.1 Diversity systems

Classical diversity techniques consist of receiving several replicas of the same information-bearing signal over independently fading channels followed by combining these replicas at the receiver to increase the overall received SNR. As mentioned above, the idea behind diversity techniques is to have a low probability of occurrence of deep fade and hence, the performance of the system will be improved. [3]

Diversity can be obtained by extracting the signals via different radio paths:

- In space, through the use of multiple receiver antennas (space or antenna diversity).
- In frequency, by using multiple frequency carriers, where the separation between successive carrier is at least the coherence bandwidth of the channel (frequency hopping or multi-carrier systems)

- In time, by transmitting the information over different time slots that are separated by at least the coherent time of the channel. (coded systems).

- Through multipath, as in direct sequence spread-spectrum systems with RAKE receiver where the multipath components are resolved at different delays.

There are three types of classical diversity combining techniques: Maximal Ratio Combining (MRC), Equal Gain Combing (EGC), and Selection Combining. These techniques differ basically in the complexity restrictions put on the communication system, and available amount of channel state information (CSI) at the receiver. [3]

MRC is known to be the optimal combining scheme in the absence of interference regardless of fading characteristics. However, the cost of this optimal performance is the increased complexity since MRC requires knowledge of all channel fading parameters. [3]

A suboptimal and a less complex scheme is the EGC where the estimation of fading amplitude is not required. The phase information in each diversity branch is the only information needed to process the different replicas of the information-bearing signal at the receiver. [3]

MRC and EGC require all or some of the CSI from all the received signal replicas. Moreover, all of diversity channels need to be processed. On the other hand, selective combing (SC) scheme requires processing only one of the diversity channels, the branch with the highest SNR. SC is often implemented in the form of switched and

stay diversity (SSC), in wich rather than continually selecting the best channel, the receiver selects a specific channel until SNR drops below certain threshold and then it selects the best branch again. [3]

Newly hybrid techniques have been proposed for their promising offer to meet the specifications of emerging wireless. These techniques can be classified into two groups: Generalized diversity schemes and multidimensional diversity techniques. More information about these diversity systems can be found in [3].

1.2.2 Error-Control Coding

Error-Control Coding has been recognized as an important approach to improve the reliability of digital communication system over fading and non-fading channels. Analysis shows that communication channels have a definite capacity for information transmission. In 1948, Shannon proved that if the data source rate is less than the channel capacity, it is possible to communicate over noisy channel with an error probability as small as desired with proper encoding and decoding. [4]

Error control coding improves the reliability of data by adding a redundancy to the data delivered to the user. A codeword is formed by adding parity bits to the information bits at the encoder. This redundancy can be used for error detection and/or error correction. In error detection, the decoder tries to identify the erroneous codeword at the receiver. Any valid codeword is assumed to be correct. Therefore, the decoder will fail in error detection if and only if the errors cause the codeword to be decoded as

another valid codeword. On the other hand, in error correction, the decoder will try to correct the received invalidcodewords.

Basically, there are two error control strategies, namely Automatic Repeat Request (ARQ) and Forward Error Correction (FEC). In ARQ, coding is devoted for the purpose of detection only. If the decoder didn't detect errors, the original information bits can be recovered and delivered to the user. Otherwise, the receiver discards the received codeword and sends back a negative acknowledgment (NACK) through a feedback channel requesting a retransmission of that erroneous codeword. Theoretically, this process is repeated waiting for a valid codeword.

In ARQ systems, the throughput efficiency is very sensitive to the retransmission protocol. Fundamentally, there are three protocols of retransmission: stop-and-wait (SW), go-back-N (GBN) and selective-repeat (SR). In SW-ARQ, the transmitter stops after a packet transmission and stays idle until an acknowledgment (ACK) is received back. If ACK is received, a new packet is transmitted, whereas NACK indicate that the same packet needs to be retransmitted. On the other hand, in both GBN-ARQ and SR-ARQ, the transmitter continuously transmits packets until it receives NACK. In GBN-ARQ, the system retransmits the negatively acknowledged packet and the successive ones as well. However, in the case of SR-ARQ, only the negatively acknowledged packets are retransmitted.

In FEC systems, information bits are encoded for the purpose of error correction only. In the case of block coding, for example, a block of k information bits is encoded

into a codeword with a block length of *n* bits. The redundancy added by the encoder will be used at the decoder to correct the invalid codeword. When the decoder detects the presence of errors in a received codeword it attempts to locate and correct them, and delivers the decoded word to the user. Generally, if the number of errors that the decoder can correct need to be increased, then the number of parity check bits have to be increased as well. Increasing the parity bits expands the code length, which leads to expanding the required transmission bandwidth. Also, as the code length is expanded it becomes increasingly difficult and expensive to design good decoders.

"Throughput" and "reliability" are the two parameters usually used to evaluate the performance of digital communication systems. Throughput can be defined as the ratio of the average number of information bits accepted by the receiver per unit time, to the total transmitted bits per unit time. On the other hand, the reliability of a system may be deduced from more than one quantity. The probability of error of the received information bits is commonly used as a measure of the reliability of communication systems.

Both error control techniques, ARQ and FEC, enhance the reliability of communication systems at the expense of decreasing the throughput. In FEC the throughput is sacrificed by the added redundancy, while in ARQ the throughput is sacrificed mainly by the request of retransmission. As a result, FEC gives a constant throughput, set by the code rate, while the throughput of ARQ is strongly dependent on channel quality. From reliability point of view, the decoded word in FEC must be delivered to the user even if it not correct, whereas ARQ doesn't accept the detected

erroneous packets. The only degradation in reliability in ARQ is when the erroneous packet passes undetected. This means that the reliability of ARQ systems is higher than FEC systems especially for bad channels. To sum up, both techniques have their relative advantages and disadvantages. ARQ schemes maintain a highly reliable system at the cost of a low throughput for poor channels; while FEC schemes maintain fixed throughput at the cost of lower reliability for poor channels. The two schemes can be combined as in "Hybrid ARQ". In such system, the information bits are initially encoded for error detection, which is used for ARQ. Then, the encoded word is further encoded for FEC. At the receiver, the decoder performs error correction followed by error detection to test the validity of the decoded codeword. If no errors are detected, the message is delivered to the user. Otherwise, the receiver discards the codeword and asks for a retransmission of that discarded codeword.

FEC can be considered as a form of time diversity that can be effective in reducing the loss in SNR caused by fading. There are two different types of FEC codes: convolutional codes and block codes. In convolutional coding, the system operates on information sequence without breaking it up into segments. Rather, the encoder for the convolutional coding processes the information continuously and associates each long information sequence with a code sequence containing more bits.

On the other hand, the encoder for block coding breaks the continuous sequence of information bits into *k*-symbol segments called blocks. It then operates on these blocks independently by associating certain redundancy bits to the information block to form an n-symbol block called a codeword. A coding scheme is referred to as being

linear if the sum of two code vectors is also a code vector. Similarly, a coding scheme is referred to as being cyclic if all cyclic shifts of a code vector result in valid code vectors. In our work, we will consider two widely used linear cyclic block codes: Binary Bose–Chaudhuri–Hocquenghem (BCH) codes and non-binary Reed–Solomon (RS) codes. In the following subsections these two codes will be explained briefly. More examples and comprehensive studies on error-correction coding can be found in [4 – 7].

1.2.2.1 BCH codes

BCH codes are one of the most important and powerful classes of multiple-error-correcting linear block codes with wide variety of coding parameters. They were discovered by Bose and Ray-Chaudhuri in 1960 and independently by Hocquenghem in 1959. One of the advantages of BCH codes is that there exist very elegant and powerful algebraic decoding algorithms for BCH codes that have been realized in a reasonable performance and amount of hardware. BCH codes take an important position in the theory and practice of multiple-error correction [7].

BCH codes are a sub-class of linear cyclic codes. One of the basic properties of a q-ary (n, k) cyclic code is that every code polynomial $c(x)$ can be expressed as $c(x) = i(x)g(x)$, where $g(x)$ is the generator polynomial with degree $n - k$ and $i(x)$ is a polynomial of degree $k-1$ in GF(q).

When constructing an arbitrary cyclic code, there is no guarantee that the resulting code has a certain minimum distance. Given an arbitrary generator polynomial

$g(x)$, we have to conduct a computer search of all nonzero code words $c(x)$ to determine the minimum-weight code word and thus the minimum distance of the code. BCH codes, on the other hand, ensure a minimum "design distance" d given a particular constraint on the generator polynomial. The actual minimum distance of the code is then greater than or equal the designed distance, that is $d_{min} \geq d$.

Given a finite field GF(q), a block length n, and the correction capability t ($t = \left\lfloor \frac{d-1}{2} \right\rfloor$, $1 \leq t \leq (n-1)/2$), an (n,k,t) BCH code can be generated cyclically by the generator polynomial,

$$g(x) = LCM\left\{ m_0(x), m_1(x), \ldots, m_{2t-1}(x) \right\}. \tag{1.1}$$

Here $LCM\{.\}$ is the least common multiple polynomial. Also $m_i(x)$ (i = 0,1,…,2t-1) is the minimal polynomial of α^i, where α is the field element whose order is n in some extension field GF(q^m) for some integer $m \geq 3$. Usually, the field element α is a primitive element in GF(q^m) which is corresponding to a primitive BCH code. On the other hand, if α is not a primitive element, the resultant code is a nonprimitive BCH code and α is replaced by β. In our work, we consider primitive BCH codes with q = 2, which is called primitive binary BCH codes. With such codes we have the following parameters [7]:

Block length	$n = 2^m - 1$	(1.2)
Number of information bits	$k = n - \deg(g(x)) \geq n - mt$	(1.3)
Minimum distance	$d_{\min} \geq 2t + 1$	(1.4)

1.2.2.2 Reed-Solomon codes

Reed Solomon codes are an important subclass of nonbinary BCH codes. They are often abbreviated as RS codes. They were invented by Irving Reed and Gustave Solomon in 1960. The generator polynomial of a t-error-correcting RS code defined over GF(q) has as roots the $2t$ consecutive powers of α, so that the generator polynomial is of the form,

$$g(x) = \prod_{j=0}^{2t-1} \left(x - \alpha^j \right) \tag{1.5}$$

In almost all of coding literature RS codes are discussed over the finite field GF(2^m), for some integer m, because of the simplicity of their implementation using binary devices. A t-error-correcting RS code over GF(2^m) has the following parameters,

Block length $n = q\text{-}1 = 2^m\text{-}1$ symbols

Message size $k = n - \deg(g(x)) = n - 2t$ symbols (1.6)

Error correction capability $t = \lfloor (n-k)/2 \rfloor$ symbols (1.7)

Minimum distance $d_{min} = 2t+1 = n\text{-}k+1$ (1.8)

In 1964, Singleton derived an upper bound of the minimum distance of any linear block code. The Singleton bound is give by,

$$d_{\min} \le n - k + 1. \tag{1.9}$$

When the equality in Equation (1.9) is satisfied, the code is said to be a maximum distance separable (MDS) code. From Equation (1.8), it is clear that RS codes are MDS codes. MDS codes have important properties that result in several practical consequences.

It is known by Rieger Bound that Maximum burst-error-correction capability for an (n,k) linear code can't exceed $\lfloor (n-k)/2 \rfloor$. Once again, the equality is achieved in RS codes, Equation (1.7). Therefore, RS codes are powerful burst-error-correction codes [7].

In addition to there powerful correction capabilities, RS codes have other reasons for being one of the most popular codes. One of those reasons is the ability to be used efficiently for large block length because of the existence of efficient hard-decision decoding at relatively long codes [8]. Also, RS codes provide a wide range of code rates that can be chosen to optimize the system's performance. For these reasons, RS codes have been used extinsively in many applications such as storage devices (DVD or compact desks), high-speed modems, wireless and mobile communications, and satellite communications.

1.2.3 Combined coding and diversity systems

As mentioned earlier, combining coding and diversity is a powerful way to improve the performance of faded systems. There have been many examples in the literature taking this approach. The simplest way of combining coding and diversity is to encode the

information using any coding method, such as block coding, convolutional coding or turbo coding. Then, the encoded bits are transmitted via multiple channels using any diversity schemes. At the receiver, distorted versions of the transmitted bits are combined using maximal ration combining (MRC), selective combining, or other combining techniques. Hard decision or soft decision decoding is then employed to recover the transmitted signal.

In [9], the effect of combined MRC diversity and RS/BCH concatenated coding on the performance has been investigated experimentally for quadrature differential phase shift keying (QDPSK) system over frequency-selective Rayleigh fading. The effects of correlation on the M-ary DPSK (MDPSK), two-branch EG diversity systems were studied in [10], [11], and [12]. The BER performance has been analyzed in presence of uncorrelated-scattering frequency-selective slow Rayleigh fading. It has been shown that the two-branch diversity system performs better than short block codes (such as (7,4) Hamming code and (23,12) Golay code) with perfect bit interleaving when the correlation coefficient is 0.5. However, combined diversity and block coding with perfect bit interleaving are found to be effective in combating the effects of frequency-selective fading .

In [13], a scheme of combined MRC diversity reception and convolutional coding employing hard decision decoding is proposed for QDPSK mobile radio system. Another scheme of decoding is also proposed in [13] employing error-and-erasure correction Viterbi decoding. In the second scheme, the received signal envelope is sampled and used as CSI that results in an effective error-and-erasure correction

decoding operation at the receiver. The noisy versions of the transmitted code word from different diversity branches is combined using a simple code combiner to form a more reliable code word. The performance is analyzed over Rayleigh fading channels with AWGN.

The impact of CSI on both uncoded and coded systems with EG/MRC diversity receptions has been studied in [14]. The authors concluded that there is no effect of the lack of CSI on the BER for uncoded signal sets with equal energy [e.g. PSK]. On the other hand, for coded systems, lack of CSI reduces the performance. It has been proven that the channel tends to become Gaussian as the diversity order grows. The results are obtained for slow flat Rayleigh fading channels.

The effect of combining forward error correction (FEC) and diversity on the performance of BPSK direct sequence/code-division multiple access (DS/CDMA) system has been investigated in [15]. The BER performance of three coding schemes ((7,4) Hamming, (15,7) BCH, and a1/2-rate convolutional coding with constraint length of three) has been compared. The channel is modeled as Rayleigh fading and lognormal shadowing, and corrupted by both self and mutual interferences, assumed Gaussian. MRC microscopic and selection macroscopic diversity are considered. It has been found that with only micro diversity, the performance of the convolutional coded system is superior to that of (7,4) Hamming coded system and inferior to the one of (15,7) BCH coded system in Rayleigh fading channel with no lognormal shadowing. Convolutional coded system is affected most by lognormal shadowing and it makes its performance worse than the other two coding schemes. However, with enough order of macro

diversity, convolutional coded system showed improved performance in Rayleigh fading and lognormal shadowing, and it became better than (7,4) Hamming system, but still inferior to the (15,7) BCH system.

In [16], a diversity receiver scheme has been proposed for demodulation and decoding of mobile radio signals. The proposed demodulation scheme uses a new distance-combination technique based on classical MLSE Viterbi algorithm. A new soft-decoding algorithm combining the signals coming from frequency-diversity channels has been also proposed. Gaussian minimum-shift-keying (GMSK) modulation scheme has been used. The channel coding system used in GSM has been assumed. The results showed that this proposed system achieves reliable BER performance on many fading conditions, better than the system employing hard decoding in the expense of modest increase in receiver complexity.

A diversity-combining scheme is proposed for a combined multiple turbo codes and multiple antenna diversity for synchronous DS/CDMA systems over fading channels [17]. This combining scheme is composed of a modified parallel mode decoding process and a reduced MAP algorithm using TCM structure. The performance is investigated by means of simulation for QPSK DS/CDMA system on flat Rayleigh fading channel. In addition, the performance of a combined turbo coding and diversity has been studied in [18] in a hybrid direct-sequence/slow frequency hopping CDMA (DS/SFH CDMA) system.

Diversity can be achieved by hopping as in [19]. Wang and Moeneclaey have analyzed the BER performance of multiple hops per symbol fast-frequency-hoping spread-spectrum multiple access (FFH-SSMA) system employing MFSK modulation with non-coherent square-law envelope detection and RS coding over multipath Rayleigh and Rician indoor fading channel. The receiver uses diversity by linearly combining the squared envelops of the different hops of the same MSFK symbol. By employing RS coding, a significant improvement in BER performance was obtained compared with uncoded one, and the improvement increases as the number of (M) of MFSK signals increases.

Diversity can be employed in a non-classical way, i.e. it is not just a matter of repetition. In [20], A pre-diversity (diversity at the transmitter) scheme has been proposed using coding, multi carrier, and multi antenna for slow flat fading channel with burst errors. This scheme does not need interleaving and hence it does not introduce considerable delay. K bits is encoded by (N,K) block code. Each of the N bits is modulated on one of N different carriers and transmitted via one of N different antennas, The authors proved that this system provides fixed BER characteristics for both slow fading and fast fading channels. In contrast to interleaving systems, they do not perform well in slow fading. By simulation, the authors showed that, for BPSK modulation system, and using (7,4) Hamming code, 7 carriers, and 7 transmitters, the performance is 15dB better than the interleaving systems.

Orthogonal frequency division multiplexing (OFDM) can introduce Diversity [21]. In OFDM the signal bandwidth is subdivided into many narrow band subchannels.

Coding and modulation is employed on each channel. In [21], three coding strategies were proposed for an OFDM system with MRC diversity. Interleaving is used in two-dimensional frequency and time domain to maximize coding efficiency. The three coding strategies were compared and it was found that, based on the best interleaving method, the ½-rate convolutional code requires a constraint length of at least 6, with soft decisions, to achieve better performance than ½-rate (40,20) RS code with 6-bit symbols and a combination of erasure and error correction. A concatenated coding scheme employing convolutional and RS coding was proposed as the third coding strategy and was found to outperform the other two strategies. Simulation was used to obtain the results for the proposed schemes with QPSK modulation. Rayleigh fading with a two-ray, equal amplitude, power delay profile was assumed for the channel.

1.2.4 Adaptive systems

An alternative approach to reliable communication over time varying channels is to use adaptive techniques. Adaptation of transmission parameters is a technique that has been used a lot in communication theory. ARQ scheme is an adaptive system where a retransmission request is made whenever the received signal has an error. Another example is the Maximal-ratio combining diversity, which uses the channel quality information to estimate the continuously updated weighting factors. If we can use a channel state estimator, which monitors the channel quality and delivers this information to the transmitter, it will be possible to continuously adjust one or more transmission parameter according to the current channel state. An obvious expense is the need of a

reliable feedback channel to transmit the channel state information from the transmitter to the receiver. However, the main advantage is that using traditional techniques will be possible, by essentially decomposing the time-varying channel into a number of time-invariant channels.

Adaptation of transmission parameters has been proposed in the literature. Hays, in his early work [22], could optimize the transmitted power for the Rayleigh channel using the information about the channel state obtained through a noiseless feedback channel. In [23-26], Goldsmith and others tried to solve the problem of maximizing the capacity of fading channel by adapting the transmitted power, signaling scheme and rate according to the channel state information (CSI) at the transmitter.

Adaptation can be employed in Antenna as in [42], where an adaptive beamforming scheme is proposed for the receiver of up-link W-CDMA with narrow-band sub-coding. This system shows a significant improvement over classical RAKE receivers in terms of BER and algorithm complexity.

Modulation can also be adapted. In [44], adaptive modulation and coding (AMC) have been combined with a truncated auto repeat request (ARQ) protocol, in order to maximize spectral efficiency over Nakagami-*m* block fading channels. Numerical results reveal that retransmissions reduce stringent error-control requirements and thereby enable considerable spectral efficiency gains.

In [45], the authors proposed an adaptive time-diversity system equipped with adaptive modulation and retransmissions over Nakagami-*m* block fading channels. Their

system maximizes the spectral efficiency for a prescribed average packet error rate (PER), without imposing feedback latency to be less than the wireless channel's coherence time which is a stringent requirement in most existing adaptive modulation schemes.

An OFDM-CDM (orthogonal frequency division multiplexing code division multiplexing) system with adaptive symbol mapping has been developed in [42]. This combination enables a robust transmission with flexible error protection and data rate adaptation for parallel data streams by exploiting additional diversity due to CDM.

In [46], the authors have developed an adaptive multi-input multi-output (MIMO) space-time (ST) OFDM transmissions capable of adapting to partial channel state information (CSI) that is available at the transmitter. Their proposed transmitter includes an outer stage (adaptive modulation), and an inner stage (adaptive beamforming).

Coding can be adapted too, as in [27], where an adaptive scheme employing code combining through packet retransmissions has been studied. The receiver uses CSI to perform error-and-erasure correction Viterbi decoding. An adaptive forward error coding scheme has been proposed in [28]. A predictive algorithm is used to estimate the fading level on the channel and this estimate is used to adapt the code rate. A set of BCH codes having the same codeword length but different correcting capabilities, and hence different code rates has been determined. According to the channel quality, one code of the BCH codes set will be chosen. The achieved performance is analyzed for both the bit

error rate and the throughput. The same adaptive system is proposed in [29] but with different prediction algorithm.

Diversity can be combined with adaptive coding as in [30] and [31]. In [30], an adaptive FEC scheme referred to as Multi-Channel Adaptive Forward Error Correction (MC-AFEC) system has been proposed, where a discrete optimization of the overall error probability is used to determine the code rate over each diversity channel based on the state of these channels. The performance of the proposed adaptive system with binary BCH coding and Hard-decision decoding has been analyzed over a flat slowly fading channels. The effect of correlation on the same system has been analyzed in [31]. This system achieves a better performance compared to selective diversity system.

1.3 Proposed work and thesis layout

The research in this thesis is based on the multi-channel adaptive forward error correction (MC-AFEC) system proposed in [30,31], taking the advantages of the three techniques: coding, diversity and adaptation to reduce the bit-error probability of a communication system with fading. The system assumes the availability of number of independent parallel channels. Instead of using the classical diversity channels as a repetition coding, the information symbols will be optimally divided on the diversity channels according to their quality. Then, these information symbols will be encoded using block codes with fixed length keeping the throughput fixed. The main objective of

the MC-AFEC system is to minimize the overall error probability under the constraint that the throughput is fixed.

We were motivated to choose this system for the following reasons. First, this system has a promise to provide an improved performance compared to classical diversity systems. Second, it was proposed to be an adaptive form of diversity; adaptive in the sense of assigning the codes according the quality of channels and adaptive in the sense of controlling the throughput, a feature which the classical diversity systems lack. Third, some important points need to be covered, which were not considered in the original work.

We can summarize our contribution in this work in the following:

1. The original work in [30] was analytical. In this work, the analytical results are verified by simulation.

2. The original work used BCH codes only. In our work, two different codes are adopted: Binary BCH and RS with more emphasis is put on the RS codes. We were motivated to use RS codes because, in addition to their good distance properties, they can be generated for any k with known t. Unlike BCH codes, where it is not possible to get all the required values of k. This feature is extremely important in our system since we need to establish a group of certain number of code sets of certain number of codes that satisfy certain rate. Table 1.1 shows the possible k's for the two coding schemes that form sets of 3 codes of length n satisfying the

rate 1/3. In the case of BCH coding, n = 63 bits and $K=k_1+k_2+k_3$ = 63 while in the case of RS coding, n = 15 symbols= 60 bits and K=15 symbols. It can be noticed that RS coding produces more code sets in a structured manner.

3. The previous work evaluated the system performance over Rayleigh fading channel. In our work, we generalized the channel model to Nakagami-*m* fading of which Rayleigh fading is a special case. This generalization allows us to study the effect of fading severity on the system's performance.

4. While the original work in [30] assumes independent diversity channels, and the extension in [31] considered the effect of correlation for two channels only, in our work, we studied the effect of mutual correlation between any set of channels.

5. The previous work assumed perfect estimation of the instantaneous CSI. In this work, the impact of outdated CSI is studied using computer simulation and assuming Jakes-like channel model.

k_1	k_2	k_3
63	0	0
45	18	8
39	24	0
36	16	7

BCH code sets

k_1	k_2	k_3
15	0	0
11	3	1
9	5	1
9	3	3
7	7	1
7	5	1
5	5	5

RS code sets

Table 1.1 Number of information symbols of the 3 codes of the valid sets satisfying the rate of 1/3 for BCH coding (n=63 bits) and RS coding (n=15 symbols).

The proposed work is organized in two chapters. The description, the analysis and the optimization procedure of the MC-AFEC system are furnished in Chapter 2. In this chapter, the behavior and the performance of the MC-AFEC system are studied over Rayleigh fading channels. In Chapter 3, the MC-AFEC is compared with Selective Combining diversity in the following aspects: the performance over Rayleigh channel, the effect of correlation between diversity branches and the effect of outdated CSI estimates. In addition, the effect of fading severity on the MC-AFEC system is studied over Nakagami-m channels and compared with MRC and SC. We conclude with Chapter 4, where we summarize the findings of this work and suggest directions of future work.

CHAPTER 2

RELIABILITY STUDY OF MC-AFEC SYSTEM

2.1 Introduction

As was stated earlier, error control coding and diversity are two powerful techniques that are used individually or together to combat fading effect on communication systems. In addition, adaptation of the parameters of faded systems have been proposed and employed to improve their performance. In this work, an adaptive system referred to as multi-channel adaptive forward error correction (MC-AFEC) system is employed. This

system combines the use of diversity channels and error control coding to combat the fading effect on communication channels. This system was proposed in [30] and found to be better than the classical selective combing technique (SC) in terms of BER performance, and flexible in terms of the choice of the throughput regardless how many diversity channels are available, which the classical diversity systems lack. The available diversity channels were utilized by forward error correction coding in an adaptive way to improve the reliability of the system. This system does not introduce any significant or variable delay, which enables fixed-rate information flow to be achieved without buffering.

This chapter is devoted for a reliability study of the MC-AFEC system. In the next two sections, the system and the adopted channel model are described. In Section 2.4, we present an analysis of the system. Code grouping and discrete optimization method are furnished in Section 2.5 followed by a description of the adopted evaluation methods in Section 2.6. In Section 2.7, the performance of the system is studied over Rayleigh fading channels. Finally, the effect of using only one code set is investigated in Section 2.8.

2.2 System description

It is assumed that L diversity channels are available for transmission. These channels are utilized equally, i.e. the transmission rate (*pbs*) is identical. These L channels are not necessarily independent. The system is illustrated in Figure 2.1.

Information will be processed in blocks of K symbols. Unlike the conventional diversity systems in which the block of K symbols is sent in replica over the diversity channels, the block of K symbols will be split into L segments according to the relative qualities of the channels in order to utilize the L channels in an optimal way. Then, each segment is encoded into a codeword of a fixed length of n symbols before transmission over the assigned channel.

The availability of Channel State Information (CSI) is assumed. The information gained about channel state at the receiver will be sent back to the transmitter over a feedback channel. In fact, CSI is employed in existing diversity systems, like maximal ratio combining (MRC) and selective combining (SC) systems. In SC, the CSI provides the receiver with the estimated gains of the available channels so that the channel with the largest gain is selected. On the other hand, both the gain and the phase must be estimated for each branch for the MRC. Other systems that require the use of CSI can be found in [23–29].

Based on the available CSI of each of the L channels, the number of information symbols, and hence the number of check symbols that are to be sent over each channel is determined. Channels with poor quality will be allocated fewer information symbols and more check symbols, while channels of better quality are allocated more information symbols and a reduced number of check symbols. This is done subject to the constraint of fixed throughput where the K information symbols are transmitted through the transmission of L codewords keeping the overall throughput fixed at $K/(nL)$. In other

words, the code rates are adjusted to match the current channel conditions, subject to the constraint of constant average rate over the L channels.

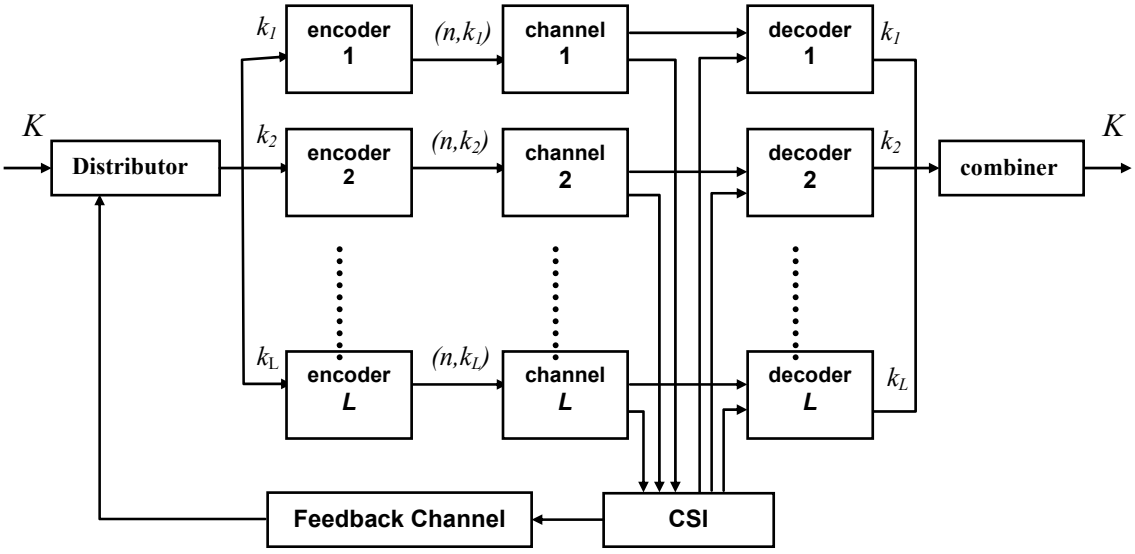

Figure 2.1: Block Diagram for the MC-AFEC System

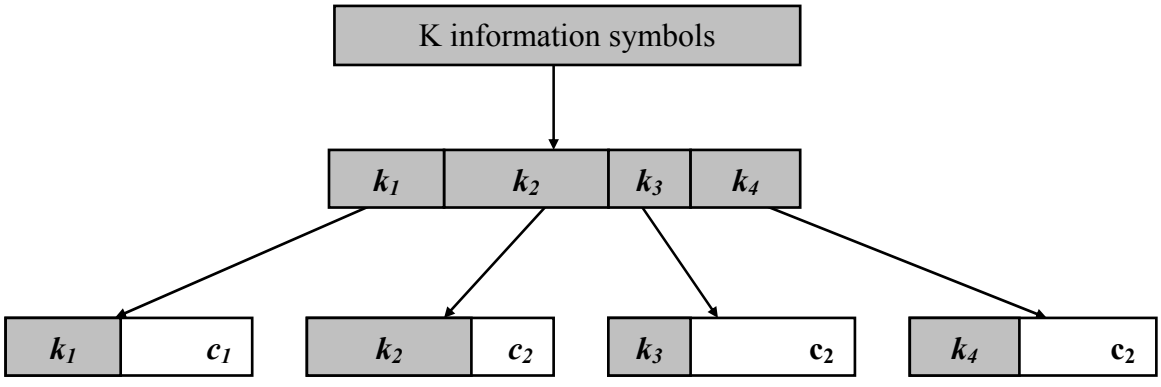

Figure 2.2: Distributing K information symbols for transmission over four channels

Figure 2.2 illustrates this process for $L=4$, where K information symbols are divided into four segments: k_1, k_2, k_3 and k_4. Then c_1, c_2, c_3, and c_4 check symbols are appended to the information segments, respectively, so that each channel carries n symbols. Note that for the setup in Figure 2.2, channel 2 has the best quality; hence it has the largest number of information symbols and the smallest number of check symbols. On the contrary, channel 3 is the worst channel and hence it has the smallest number of information symbols. A new distribution may be obtained whenever the CSI is updated.

To distinguish between diversity channels in MC-AFEC system, we will use multi-carriers, where the encoded symbols on each channel are modulated by a different carrier. Diversity can be realized as frequency diversity or antenna diversity.

Frequency Diversity:

Frequency diversity can be achieved if the separation between the carriers is greater than the coherence bandwidth of the channel. In this case, you require only one antenna at both the transmitter and the receiver. See Figure 2.3-a.

Antenna Diversity:

If the separation between carriers is less than the coherence bandwidth of the channels, you can still achieve diversity by using multiple antennas. This setup is analogous to the one used in [20]. The multiple antennas can be mounted at the transmitter or at the receiver depending on your needs. For example, if the transmitter were at a base station,

then it is better to have multiple antennas at the base station and one antenna at the mobile unit. This setup is illustrated in Figure 2.3-b.

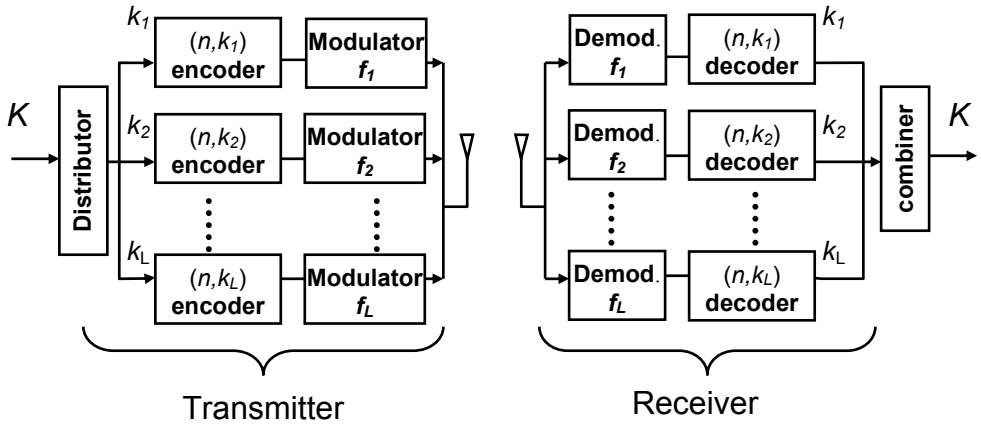

(a)

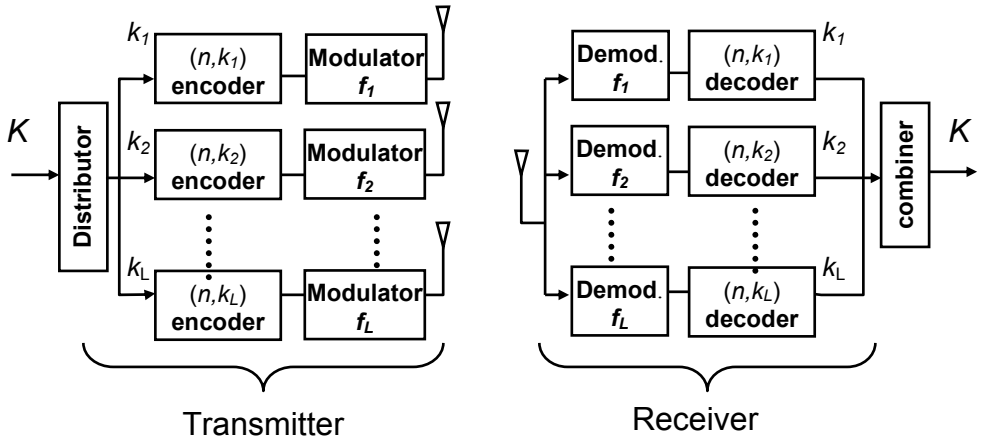

Figure 2.3: Realization of diversity channels: (a) Frequency Diversity, and (b) Antenna Diversity.

2.3 Channel Model

When a narrowband system is affected by fading, the received carrier amplitude is modulated by the fading amplitude α, where α is a random variable with mean square value $\Omega = \overline{\alpha^2}$ and probability density function (PDF) $p_\alpha(\alpha)$ which is dependent on the nature of the radio propagation. At the receiver the signal is perturbed by additive white Gaussian noise (AWGN) which is characterized by a one-sided power spectral density N_0 (W/Hz). The AWGN is typically assumed to be statistically independent of the fading amplitude α. Similarly, the received instantaneous signal power is modulated by α^2. Hence, the instantaneous signal-to-noise power ratio (SNR) per bit is defined by $\gamma = \alpha^2 E_b / N_0$, where E_b is the energy per bit.

Our performance evaluation of digital communications over fading channels will be a function of the average SNR per bit $\overline{\gamma}$, which is given by $\overline{\gamma} = \Omega E_b / N_0$. For slowly varying channels, we can obtain the PDF $p_\gamma(\gamma)$ of γ by introducing a change of variables in the expression for the fading PDF $p_\alpha(\alpha)$ of α, yielding

$$p_\gamma(\gamma) = \frac{p_\alpha(\sqrt{\Omega\gamma / \overline{\gamma}})}{2\sqrt{\gamma\overline{\gamma} / \Omega}} \tag{2.1}$$

There are different models describing the statistical behavior of the multipath fading envelope, depending on the nature of the radio propagation environment. In this thesis, the following points should be considered about the model of fading channels:

(i) It is assumed that the estimates of channel qualities (based on the received SNR, γ) are updated periodically, with τ being the adaptation period. Let the L estimates of channel qualities be denoted by the vector $\mathbf{\Gamma}_h = \{\gamma_{h1}, \gamma_{h2}, \ldots, \gamma_{hL}\}$, where γ_{hi} is the SNR per information bit on the i^{th} channel $(1 \le i \le L)$, measured over the h^{th} adaptation period.

(ii) Let $\underline{\alpha}_h = \{\alpha_{h1}, \alpha_{h2}, \ldots, \alpha_{hL}\}$, where α_{hi} is the fading envelop of the i^{th} channel during the h^{th} adaptation period. It is assumed that the diversity channels are slowly varying so that fading envelops are considered constant during one adaptation period. That is $\underline{\alpha}_h$ remains unchanged during the adaptation period τ. That is,

$$\underline{\alpha}_h = \text{constant}; \qquad h\tau \le t \le (h+1)\tau \tag{2.2}$$

As a result, $\mathbf{\Gamma}_h$ can be considered constant during τ, which means that

$$\mathbf{\Gamma}_h = \text{constant}; \qquad h\tau \le t \le (h+1)\tau \tag{2.3}$$

However, $\underline{\alpha}_h$ and $\mathbf{\Gamma}_h$ can change from one period to the next but in a slow mode. It should be noted that the adaptation period τ is assumed to be equal to the duration of transmission of one block.

(iii) The channels are assumed to be non-selective over the bandwidth of transmission; the same attenuation factor affects all frequency components of the signal transmitted within the bandwidth.

(iv) The channels are assumed to follow Rayleigh fading model.

The Rayleigh distribution is commonly used for modeling multipath fading with no direct line-of-sight (LOS) path. In this case, the channel fading amplitude α_{hi} is distributed according to the probability density function (PDF):

$$p_{\alpha_{hi}}(\alpha_{hi}) = \frac{2\alpha_{hi}}{\Omega}\exp\left(-\frac{{\alpha_{hi}}^2}{\Omega}\right), \qquad \alpha_{hi} \geq 0 . \tag{2.4}$$

Therefore, the instantaneous SNR per bit of i^{th} the channel during the h^{th} adaptation period, γ_{hi} , is distributed according to an exponential distribution PDF given by

$$p_{\gamma_{hi}}(\gamma_{hi}) = \frac{1}{\overline{\gamma}}\exp\left(-\frac{\gamma_{hi}}{\overline{\gamma}}\right), \qquad \gamma_{hi} \geq 0 \tag{2.5}$$

The Rayleigh distribution typically match very well the channel models of mobile systems that have no LOS path between the transmitter and receiver antennas. It also fits the propagation of reflected and refracted paths through the troposphere, ionosphere, and to ship-to-ship radio links [3].

2.4 System Analysis

Based on Γ_h, a block of K information symbols will be partitioned into L segments of lengths $\{k_{h1}, k_{h2}, \ldots, k_{hL}\}$. Then, the system will add c_{hi} check symbols to the k_{hi} information symbols that are allocated to the i^{th} channel. The set of information symbols k_{hi} and check symbols c_{hi} will form an (n, k_{hi}, t_{hi}) error correcting code, where $n=k_{hi}+c_{hi}$; $i=1,2,\ldots, L$. This (n, k_{hi}, t_{hi}) code is capable of correcting a number of errors $\leq t_{hi}$ symbols. In this work, it will be assumed that the code rate over the i^{th} channel is changed at the beginning of each adaptation period τ, and the codes so chosen are kept unchanged for the reminder of the adaptation period. Let R be the system throughput, which is defined as the ratio of average number of information symbols accepted by the receiver per unit time, to the total transmitted symbols per unit time. In our system, the throughput will be held constant at all times at

$$R = \frac{\sum_{i=1}^{L} k_{hi}}{n \times L} = \frac{K}{n \times L} \qquad (2.6)$$

Let P_{hi} denote the post-decoding symbol error probability on the i^{th} channel during the h^{th} adaptation period. If we let P_h denotes the average symbol error probability at the system's output in respect to the h^{th} adaptation period, then

$$P_h = \frac{\sum_{i=1}^{L} k_{hi} P_{hi}}{K} \qquad (2.7)$$

The aim of adaptation process is to select the set of k_{hi}'s that yeilds the minimum error probability P_h during the h^{th} adaptation period. In other words, the system should obtain the optimum set of k_{hi}'s as a function of Γ_h, while maintaining the throughput R constant.

Let ζ_{hi} be the symbol error rate (SER) of the i^{th} channel, during the h^{th} adaptation period, which is determined by the modulation technique in use and subject to the received SNR γ_{hi}. For a given class of error correcting codes, and according to the value of $\{\gamma_{hi}\}$, the set $\{k_{hi}\}$ determines the set $\{t_{hi}\}$. Now, the set $\{t_{hi}\}$ and the set $\{\zeta_{hi}\}$ will be used to determine $\{P_{hi}\}$. The exact Equation relating P_{hi} to ζ_{hi} is a function of the weight structure and the decoding algorithm.

Let $f(\Gamma_h)$ denote the joint PDF of Γ_h. By averaging Equation (2.7) over $f(\Gamma_h)$, the overall average post-decoding symbol error probability $\overline{P}$ can be obtained, that is

$$\overline{P} = \int_0^{\infty}\int_0^{\infty}\cdots\int_0^{\infty} P_h \times f(\Gamma_h) d\Gamma_h \qquad (2.8)$$

In this chapter, two coding schemes will be considered: BCH coding and RS coding, both with hard decision decoding. For RS code, the post-decoding symbol error probability P_{hi} is given by

$$P_{hi} = \frac{1}{n} \sum_{j=t_{hi}+1}^{n} j \cdot \binom{n}{j} \zeta_{hi}^{j} (1-\zeta_{hi})^{n-j} \tag{2.9}$$

Let ε_{hi} be the bit error rate (BER) of the i^{th} channel on the h^{th} adaptation period. Within the adaptation period h, the fading envelope α_{hi} is considered constant as we assumed earlier and the only random process that perturbs the channel during a transmission of a block is the AWGN. That is for a given α_{hi} the channel is assumed AWGN. AWGN in a bit is considered independent to the one in other bits. Hence, we can relate ζ_{hi} to ε_{hi} by

$$\zeta_{hi} = 1-(1-\varepsilon_{hi})^{m} \tag{2.10}$$

For binary BCH codes, the upper bound given in [6] is used to determine P_{hi}, which is

$$P_{hi} < \frac{1}{n} \sum_{j=t_{hi}+1}^{n} \min(j+t_{hi}, n) \cdot \binom{n}{j} \varepsilon_{hi}^{j} (1-\varepsilon_{hi})^{n-j} \tag{2.11}$$

In this upper bound, we are assuming that all incorrect decoding events introduce t more additional errors; that is if j errors are present in a received word ($j \geq t$), the decoder can insert at most t additional errors.

To evaluate ε_{hi}, we have to assume a modulation scheme. To simplify the analysis binary coherent phase shift keying (BPSK) will be used as our modulation technique. Assume that the channel fading is sufficiently slow that the phase can be estimated from the received signal without errors to achieve ideal coherent modulation. Hence, ε_{hi} can be written as

$$\varepsilon_{hi} = Q\left(\sqrt{2\gamma_{hi}}\right) \tag{2.12}$$

The task now is to minimize the overall post-decoding error probability, Equation (2.8), subject to the constraint $R = \frac{\sum_{i=1}^{L} k_{hi}}{n \times L}$, Equation (2.6). In the following section, a method of optimizing such Equation is presented.

2.5 Code grouping and discrete optimization

The objective of the adaptation process is to minimize Equation (2.8) subject to the constraint in (2.6). It should be noted that P_h is a function of k_{hi} and ε_{hi} that are functions of γ_{hi}'s, the elements of $\mathbf{\Gamma}_h$. The aim of adaptation process is to obtain a set of relations between k_i's and γ_{hi}'s.

Generally, the method of Lagrange multiplier is used to solve the problem of minimizing a function subject to constraints. However, this method is extremely difficult to be applied in our case because the variables k_{hi} and t_{hi} in Equations (2.7), and consequently in Equation (2.8), are discrete. Furthermore, the variable t_{hi} appears as the lower limit of the summation of Equation (2.9). Instead, a method of discrete optimization proposed in [32] is adopted here. The two issues of constraint on throughput, R, and the minimization of the overall average error probability, $\overline{P}$, are treated separately as follows.

First, a set, S, of error correcting codes of a fixed codeword length, n, but with different rates, has to be chosen. For a given throughput R and L diversity channels, a group G of all sets of L codes (denoted as L-code sets) is formed so that each member of G satisfies the rate constraint in (2.6). Each L-code set corresponds to an information set $\{k_{hi}\}$ that is different from the one in any other L-code set. Let N_G denotes the total number of the L-code sets in G, that is, G contains N_G members.

Next, the transmitter should select the L-code set that yields the minimum P_h, Equation (2.7), for a given estimate of $\mathbf{\Gamma}_h$, and hence minimizes $\overline{P}$. The selected L-code set is used during the adaptation period τ. A new L-code set will be selected in the next adaptation period at which the new estimate of $\mathbf{\Gamma}$, say $\mathbf{\Gamma}_{h+1}$ is obtained. Minimization is thereby achieved by selecting the best L-code set between the N_G different sets based on the current estimate of $\mathbf{\Gamma}$.

Undoubtedly, both the transmitter and the receiver must know the selected optimized set of codes, in order for the system to operate properly. This implies that a reliable feedback channel must exist. The feedback channel will be assumed noise-free. This assumption can be made true by applying adequate coding on the information sent back over the feedback channel, which is simply the L-code set number. In the unlikely event of the transmitter not using the L-code set expected for the receiver, the error will be restricted to one block and will not propagate to the consequent blocks.

To illustrate the process of L-code grouping, consider S to be the set of all RS codes of length n = 15 including the two trivial codes (n,n,0) and (n,0,--). The (n,0,--)

code represents the case when all the n bits are dummy which carry no information whereas the $(n,n,0)$ code correspond to the case when all n bits are information bits. For the purpose of illustration, suppose that $L = 2$ and $R = 0.5$. By applying this rate constraint, 8 sets can be formed, five of such code sets are shown below in Table 2.1 in the form (n,k,t). It is clear from Table 2.1 that the total number of information bits in each raw is equal to 15, which keeps the overall throughput constant.

The process of error minimization, discussed earlier, implies selecting the appropriate L-code set and assigning its L codes to the appropriate channels. This process requires allocating the higher-rate code to the best channel and continuing down to the poorest channel to which the lowest-rate code is assigned. In practice, this can be accomplished simply by ordering the codes in a L-code set in descending order of their rates. Then, each code of the selected L-code set is assigned in a simple direct associative manner to the L-channels that have been arranged in descending order of quality.

The question now is which L-code set should be chosen for a given channel quality vector Γ_h. One way for performing this selection is to partition the L-dimensional space associated with the vector, Γ_h, into cells, and then associate each cell with the optimum L-code set. This might be implemented by quantizing the elements of Γ_h, and then using the quantized vector as the address in a ROM, where a number associated with the best performance L-code set has been stored.

Figure 2.4 illustrates the partitioning for the case of L=2 and using the five pairs given in Table 2.1. The outer region, denoted by *, corresponds to the case where one channel is in relatively deep fade. Using the set number 1, which is the case of avoiding the channel with deep fade, yields to the best performance compared to the use of other sets. On the other hand, when the two channels have approximately the same quality, i.e. the most inner region, denoted by Δ, the two channels have to be utilized equally, that is set number 5 will the optimum set in this case. The other regions correspond to the cases between these two extremes.

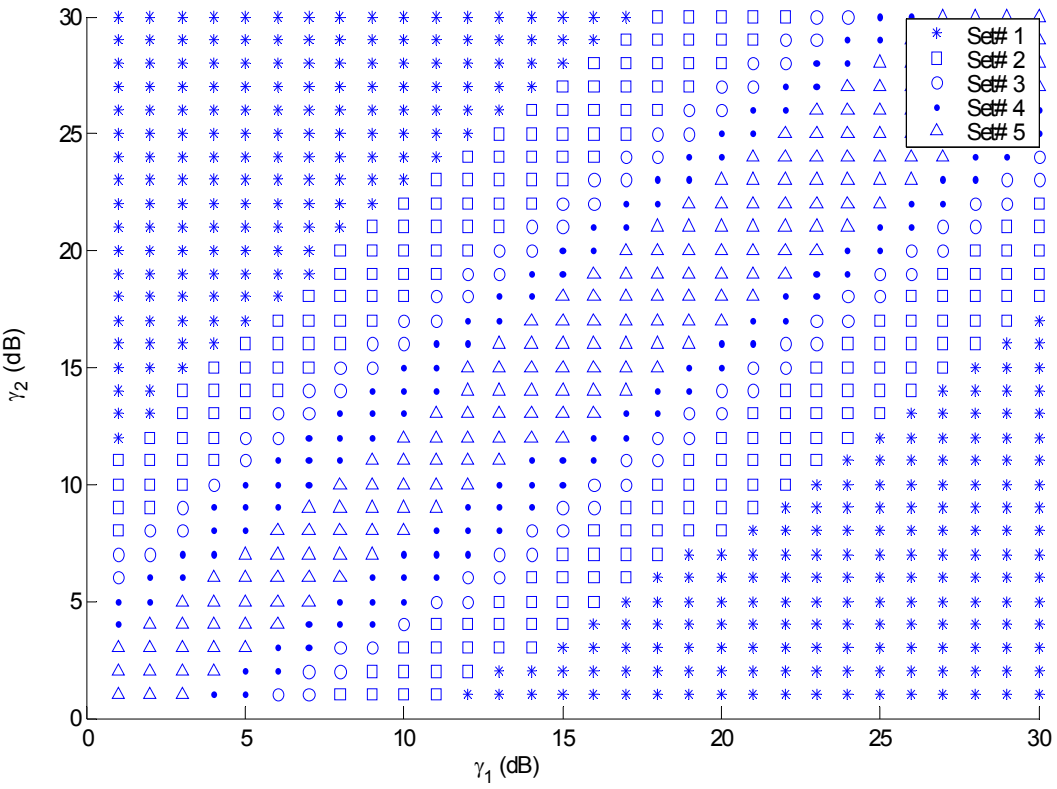

Figure 2.4: The optimum set for a given Γ for $L = 2$, $R = 0.5$.

Set number	Code 1	Code 2
1	(15,15,00)	(15,00,---)
2	(15,13,01)	(15,02,06)
3	(15,12,01)	(15,03,06)
4	(15,10,02)	(15,05,05)
5	(15,08,03)	(15,07,04)

Table 2.1: Five 2-code sets satisfying $R = 0.5$.

2.6 Evaluation models

For a given number of diversity channels, L, throughput rates, R, and average signal to noise ratio per information bit, $\overline{\gamma}$, a multidimensional integration has to be employed to evaluate the performance. The analytical integration of (2.8) is very difficult since we need to optimize the integrand for each value of Γ_{hi} and, as discussed in the previous section, such optimization is very difficult to be performed analytically. Hence, numerical multidimensional integration is employed to estimate the value of $\overline{P}$, the overall symbol error probability. A software simulation has also been performed to estimate the performance and to validate the numerical results.

2.6.1 Numerical Evaluation

In the numerical estimation, a multidimensional integration algorithm found in [34] has been deployed. At the h^{th} evaluation instance $(\gamma_{h1},\gamma_{h2},\ldots,\gamma_{hL})$, we have to choose the code set that results in a minimum P_h, the post decoding error probability at instance h. So, P_h has to be calculated for each code set. To evaluate P_h, the symbol error rate ζ_{hi} has to be calculated for each channel. Then the channels have to be ordered according to their qualities. The channel with lower ζ_{hi} will be better. For a certain code set, the channel with highest ζ_{hi} will be assigned the lowest rate code. On the other hand, the one with lower ζ_{hi} will have higher rate code. The pairs of (k_i , t_i) (i=1,2…,L), in addition to the value of ζ_{hi} 's will be applied into Equations (2.9) or (2.110) to get the value of P_{hi} associated with each code on the code set. Then, we calculate P_h according to Equation (2.7). This process is repeated for all sets to choose the one that produces the lowest P_h.

Multiplying P_h by $f(\Gamma_h)$ will generate the estimation of the integral at the h^{th} evaluation instance $(\gamma_{h1},\gamma_{h2},\ldots,\gamma_{hL})$. The process has to be repeated by the integration algorithm to span all the dimensions until the required accuracy is reached. It should be noted that the diversity channels are assumed to have independent Rayleigh fading for this chapter. Hence, $f(\Gamma_h)=f(\gamma_{h1})f(\gamma_{h2})\ldots f(\gamma_{hL})$.

The channels are assumed to be equivalent on the average; i.e., $E[|\alpha_{hi}|]=1$, i = 1, 2, …,L. For fair comparison between systems with different rates, their total

transmitted power has to be equal. For that reason the SNR per channel, $\overline{\gamma}_c$, should equal to SNR per information bit, $\overline{\gamma}$, multiplied by the rate,

$$\overline{\gamma}_c = R\overline{\gamma} \tag{2.13}$$

To evaluate the system's bit error probability $\overline{P}_b$, we assume that the bits within a symbol are independent even after decoding. Although the decoding may induce some correlation between the bits in a symbol, this assumption gives a reasonably accurate results especially for high $\overline{\gamma}$ and large block length *n*. Thus, we can relate $\overline{P}_b$ to $\overline{P}$ by

$$\overline{P}_b = 1-(1-\overline{P})^{1/m} \tag{2.14}$$

where *m* is the number of bits per symbol ($n = 2^m$-1).

2.6.2 Simulation:

Simulation has been also conducted for the purpose of validating the numerical results. For a certain value of $\overline{\gamma}$, *L,* and *R,* the simulation is conducted in the following manner. First, according to the throughput *R = NL/K*, the *L*-code sets has to be assigned. Then, the variance of the AWGN has to be normalized according to the value of *R= NL/K,* giving

$$\sigma^2 = \frac{1}{2\overline{\gamma}_c} = \frac{1}{2R\overline{\gamma}} \tag{2.15}$$

Again, this normalization is required to compare several systems with different rates and with equal energy transmitted. On each branch, the Rayleigh fading is generated with $E[|\alpha_{hi}|]=1, i=1,2,\ldots L$ by using two Gaussian sequences; both of them have 1/2 variance and zero mean.

It should be noted that in our simulation no actual coding/decoding algorithm has been implemented. That is because it would be a very lengthy simulation especially for large L and high $\overline{\gamma}$. Instead, we generate a block of N symbols that will be transmitted on each diversity channel. We assumed that the system is using a certain L-code set according to the performance of each channel. After passing the blocks over the fading channels, a comparison between the transmitted and the received blocks is performed to get the number of erroneous symbols. If the number of erroneous symbols for one block on channel i is less than or equal to t_i, the error capability of the used code, then the block is correctable. Otherwise, it is not.

Decoding may alter the number of errors from the actual received errors, which may increase or decrease. In the literature many bounds and approximations on the post-decoding errors have been proposed [32]. Here, we adopt the approximation that, on the average, the number of post-decoding erroneous symbols remain equal to the number of pre-decoded ones.

Figure 2.5 shows the detailed block diagram of our simulation procedure. The symbols used in that figure are defined in Table 2.2. Our simulation procedure involves the following steps:

I. n, k, L, $s_{\max}$ and $\overline{\gamma}$ have to be initialized.

II. According to R ($R= K/nL$), A group G of code sets has to be formed. Each set contains L codes with overall information symbols equal to K, i.e. $\sum_{i=1}^{L} k_i = K$.

III. The counters: C, v_i, T_i, $s_{cs,i}$, $b_{cs,i}$ have to be reset to zero. i=1,2,…L and cs = 1,2,…N_G.

IV. A set of L fading envelopes, denoted as $\{\alpha_w\}$; w = 1,2,… L, will be generated assuming Rayleigh distributed with $E[|\alpha_w|^2]= 1$. Then, these α_w 's are sorted to form the set $\{\alpha_i\}$ of ranked fading envelops such that the highest fading envelope is α_L and the lowest is α_1. The best code set number, sc, will be determined according to the set $\{\alpha_i\}$. The codes within this set will be also sorted according to their rates, where the code with lowest rate will be assigned the lowest rank and the code with higher rate is assigned a higher rank. As a result, the symbols in the i^{th} channel will be encoded by the i^{th} ranked code, $(n,k_{cs,i},t_i)$ and then it will be perturbed by the i^{th} ranked fading envelope.

V. Over the i^{th} channel (i= 1,2,…L), the i^{th} block of symbols will be transmitted according to the following steps:

A. The counters: j_i, eb_i and es_i have to be reset to zero.

B. Within each symbol, the bits are generated and processed according to the following steps:

   1. Reset the flag S_i.
   2. c_i , a binary bit (0 or 1 with equal probability) is generated.
   3. The bit is modulated (BPSK is assumed). Let the modulated signal be cm_i.
   4. The modulation signal, cm_i, is multiplied by α_i.
   5. A Gaussian random variable with variance equal to $1/(R\overline{\gamma})$ is generated and added to the signal.
   6. At the receiver, the signal is demodulated and demapped. The received bit after demapping is denoted by r_i.
   7. In the decoding process, r_i is compared with c_i. If they are equal, go for the next step. Otherwise, increment eb_i and set S_i to 1.
   8. The steps 2 to 7 have to be repeated for m times, where m is the number of bits per symbol. v_i is used as a counter for the number of bits per symbols.

C. After processing a symbol, reset v_i and increment j_i.

D. Check if the flag S_i is set or not. If S_i equals one, increment es_i.

E. Repeat steps B to D for n times. j_i is used as a counter for the number of symbols per block.

F. The number of erroneous symbols, es_i, is compared with the correction capability of the code, $t_{cs,i}$. If es_i is less than or equal to $t_{cs,i}$, then the errors

are correctable. Otherwise, they cannot be corrected. In this case, we will assume that the number of uncorrected symbols after decoding is equal to the number of erroneous symbols before decoding.

G. If $es_i > t_{cs,i}$, then the error counters will be incremented as follows:

$$T_{\mathrm{i}}=T_i+es_{\mathrm{i}}$$

$$s_{cs,\mathrm{i}} = s_{cs,\mathrm{i}} +es_{\mathrm{i}}$$

$$b_{cs,\mathrm{i}} = b_{cs,\mathrm{i}} +eb_1$$

VI. T, the overall erroneous symbols ($T = \sum_{i=1}^{L} T_i$),is compared to $s_{\max}$, the maximum required erroneous symbols. In our simulation, we let $s_{\max}$ to be at least 100. If the maximum number of erroneous symbols is achieved, count the overall symbol error probability and bit error probability. Other wise, increment C and return to Step IV.

The average symbol error rate of the system is calculated as follows. From Equation (2.7), it is found that P_h is a function of P_{hi} where P_{hi} is the post decoding symbol error probability of the i^{th} channel using one of the codes in the chosen set, which is equal to,

$$P_{hi} = \frac{\text{The number of erronous symbols of the } i^{th} \text{ block withen the } h^{th} \text{ adaptation period}}{\text{The number of symbols in a block}}$$

$$= \frac{s_{hi}}{n} \tag{2.16}$$

where s_{hi} is the number of erroneous symbols of the i^{th} block during the h^{th} adaptation period. Substitute Equation (2.16) in (2.7), to get

$$P_h = \frac{\sum_{i=1}^{L} s_{hi} k_{hi}}{n K} \tag{2.17}$$

As we stated earlier, P_h is the post decoding symbol error probability associated with the h^{th} adaptation period. Replacing the notation h by cs as an indication to the selected code set, we get

$$P_{cs} = \frac{\sum_{i=1}^{L} s_{cs,i} k_{cs,i}}{n K} \tag{2.18}$$

where P_{cs} is the post-decoding symbol error probability associated with the code set cs and $s_{cs,i}$ is the number of errors associated with the code number i of the set number cs. Finally, by averaging $s_{cs,i}$ over all codes, we can calculate the overall system's symbol error probability $\overline{P}$, as

$$\overline{P} = \sum_{cs=1}^{N_G} \sum_{i=1}^{L} \frac{s_{cs,i} k_{cs,i}}{n K C} \quad , \tag{2.19}$$

where N_G is the total number of sets and C is the total number of simulation runs.

To get the overall bit error probability, $\overline{P}_b$, the number of erroneous bits associated with the code number i of the set number cs, $b_{cs,i}$, need to be averaged over all codes, yielding

$$\overline{P}_b = \sum_{cs=1}^{N_G} \sum_{i=1}^{L} \frac{b_{cs,i} k_{cs,i}}{n m K C} \quad , \tag{2.20}$$

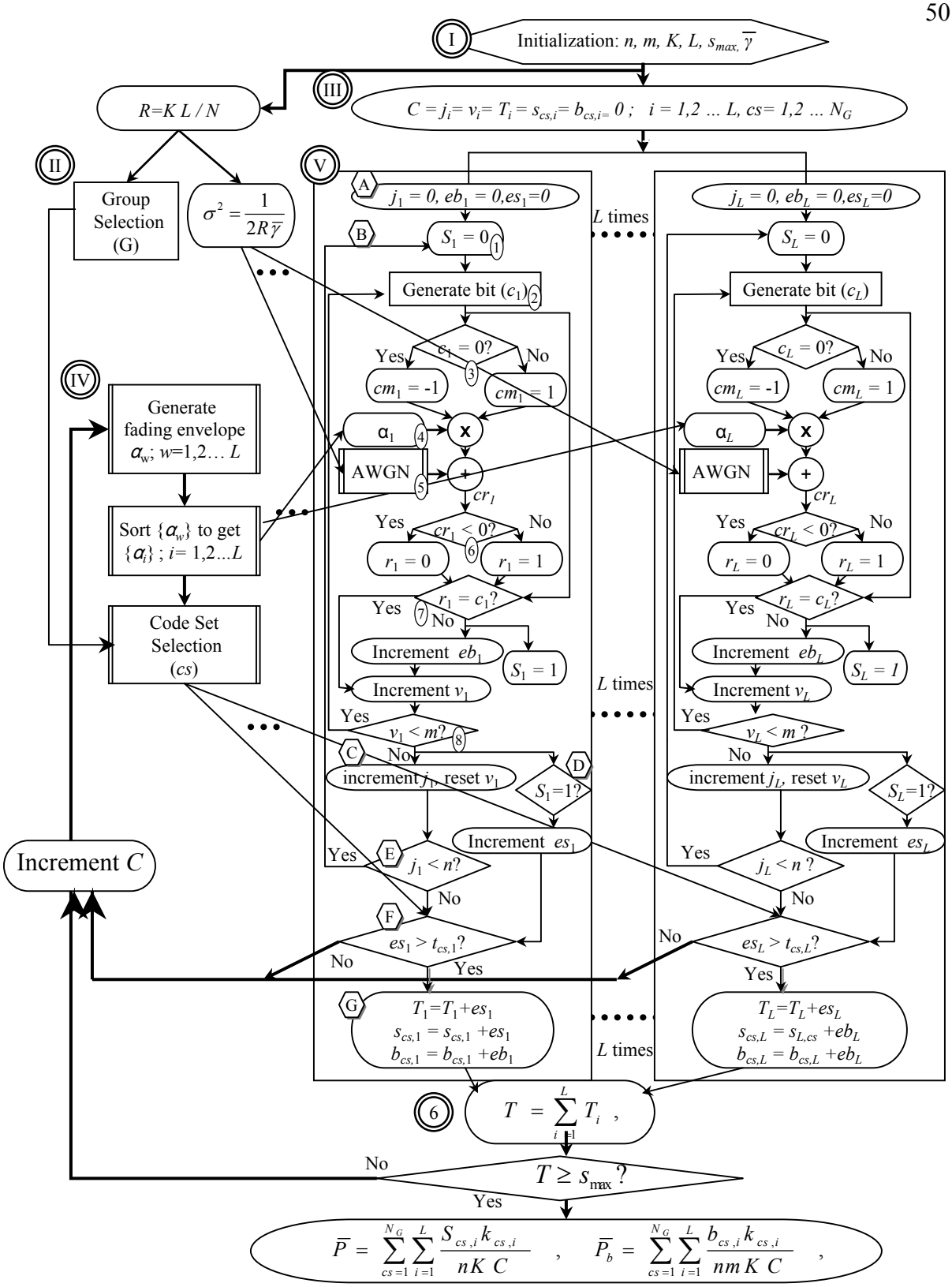

Figure 2.5: Block diagram of the adopted simulation model.

α_I	: The i^{th} ranked fading envelope.
α_w	: The w^{th} unranked fading envelope.
$b_{cs,i}$	: Overall number of errounous bits associated to the i^{th} ranked code of the set number *cs*.
C	: Counter for the number of simulation runs.
c_i	: Coded bit associated to the i^{th} channel.
cm_i	: Modulated bit associated to the i^{th} channel.
cr_i	: Received signal associated to the i^{th} channel.
Cs	: Selected code set number.
eb_i	: Counter for the number of erroneous bits within a block.
es_i	: Counter for the number of erroneous symbols within a block
$\overline{\gamma}$	: Average SNR per bit.
j_i	: Counter fo the number of symbols within a block.
K	: Total number of information symbol transmitted during 1 simulation run.
L	: Number of diversity channels.
m	: Number of bits per symbol.
n	: Number of symbols per block.
N_G	: Maximum number of code sets per group.
P	: Overall symbol error probability.
P_b	: Overall bit error probability.
R	: Throughput.
r_i	: Demapped received bit associated with the i^{th} channel.
$s_{cs,i}$	: Overall number of erroneous symbols associated to the i^{th} ranked code of the set number *cs*.
S_i	: a symbol in error flag.
$s_{\max}$	: Maximum tolerable number of erroneous symbols.
T	: Total number of erroneous symbols
T_i	: Total number of erroneous symbols associated to the i^{th} channel.
v_i	: Counter for the number of bits within a symbol.

Table 2.2: List of symbols used in the simulation model in Figure 2.5.

In order to validate the numerical results of the BCH coded system proposed in [30, 31], a comparison between the numerical and simulation results is performed. In the evaluation, the set S was taken to have all the BCH codes of length n = 63. The number, N_G, of L-codes sets in G was limited to a maximum of eight sets. Figure 2.6 shows the BER performance of the BCH-coded MC-AFEC system for different number of channels, L, and R= 1/L. It can be noticed from Figure 2.6 that both the simulation and numerical results are matched. In the next section, the performance and the behavior of RS-coded system will be studied in details for different values of $\overline{\gamma}$, R and L.

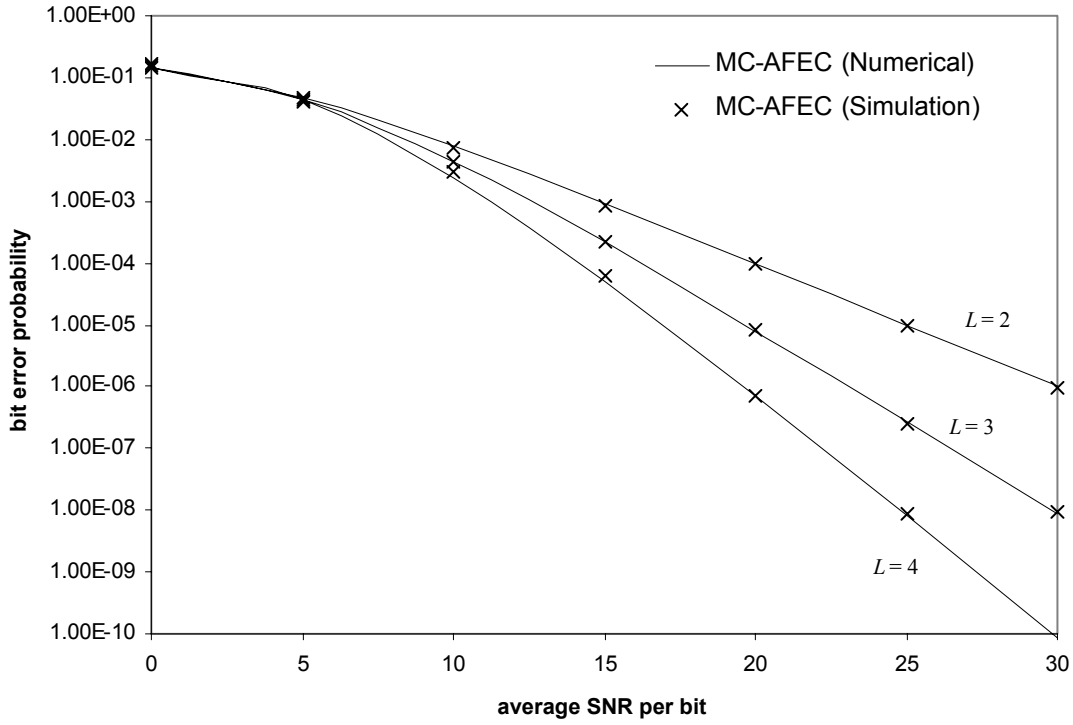

Figure 2.6: Comparison between the numerical results of the BCH-coded MC-AFEC system and the simulation results for L= 2, 3, and 4 and R = 1/L.

2.7 System performance

The Models of evaluating the performance of the MC-AFEC system has been described in the last section for both numerical and simulated techniques. In this section, these models will be used to examine the performance of the system with different values of average SNR, $\overline{\gamma}$, throughput rate, R, and number of channels, L.

In the evaluation, the set S contains all the RS codes of length $n = 2^4\text{-}1=15$ symbols. Here, the number of bits per symbol m is 4. As an example, consider the 3-code sets presented in Table 2.3 for the case of R=1/3. Here, we also restrict N_G, the number of L-code sets in G, to a maximum of eight sets.

Set number	Code 1	Code 2	Code 3
1	(15,15,00)	(15,00,---)	(15,00,---)
2	(15,13,01)	(15,02,06)	(15,00,---)
3	(15,11,02)	(15,04,05)	(15,00,---)
4	(15,11,02)	(15,03,06)	(15,01,07)
5	(15,09,03)	(15,06,04)	(15,00,---)
6	(15,09,03)	(15,03,06)	(15,03,06)
7	(15,07,04)	(15,05,05)	(15,03,06)
8	(15,05,05)	(15,05,05)	(15,05,05)

Table 2.3: Eight RS 3-code sets satisfying R ≈0.33.

The number of sets is restricted to eight after it has been found that using more sets doesn't lead to a considerable improvement in the performance. For eight sets, 3 bits are sufficient to identify the chosen set that will be communicated to the transmitter over the feedback channel. These bits can be highly protected with little cost making them almost error free.

Figures 2.7-a to 2.7-c show the SER performance of the RS-coded system with respect to the average SNR, $\overline{\gamma}$, for L = 2, 3 and 4, respectively. Observing the figures, it is clear that the results generated by numerical integration is close to the ones generated by simulation, which indicate that both methods is capable of evaluating the SER performance of the system.

In Figure 2.7-a, where L = 2, it can be noticed that a rate-reduction of 0.1, from R = 0.6 to 0.5, introduces a major improvement on $\overline{P}$ of about two orders of magnitude (from the range of 10^{-4} to 10^{-6} at $\overline{\gamma} = 30\,\text{dB}$). A much smaller improvement can be observed in the case of L = 3 (Figure 2.7-b) where the improvement is less than one order of magnitude.

Along the same lines, a reduction from R = 0.4 to 0.33 did not lead to a significant improvement for L = 4 (Figure 2.7-c), where $\overline{P}$ has been reduced only from 1.8×10^{-8} to 1.1×10^{-8}, while for L = 3 the same reduction in rate results in a significant improvement of more than one order of magnitude.

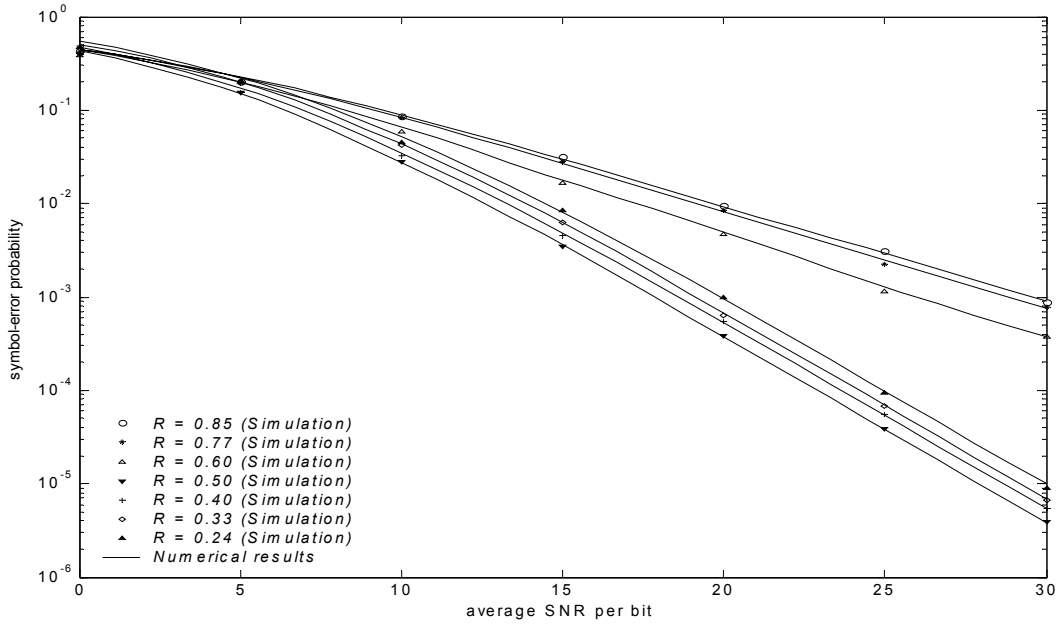

(a)

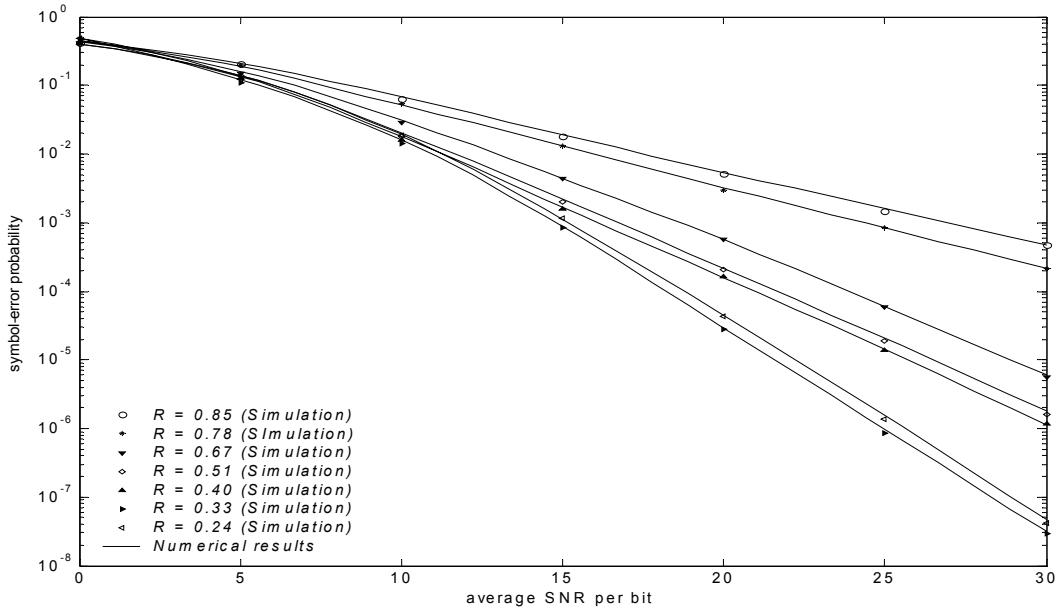

(b)

Figure 2.7: Symbol-error probability of the RS-coded MC-AFEC system vs. average SNR per bit, for different throughput rates and with (a) $L = 2$, (b) $L = 3$, and (c) $L = 4$ diversity channels.

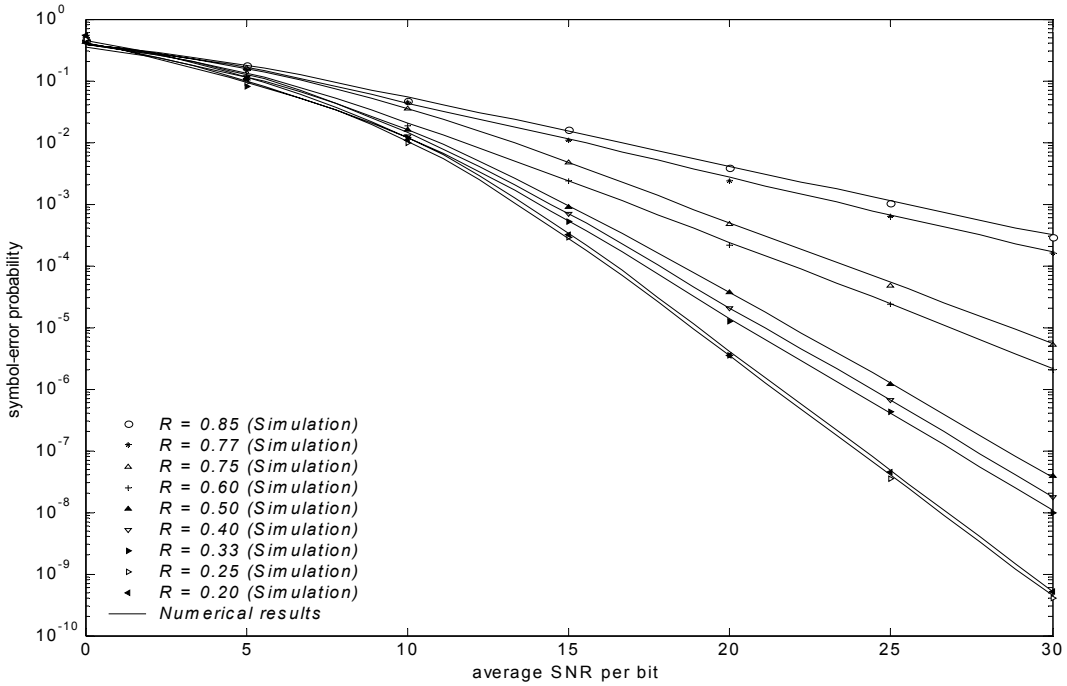

(c)

Figure 2.7: (Continued)

From the above observations, it is clear that the relation between R and $\overline{P}$ is not straightforward, and it is dependent on the value of L. For example, in Figure 2.7-a (L=2), it is apparent that the curves are grouped into two clusters. The cluster with better performance corresponds to R equal to or less than 0.5, while the other cluster corresponds to rate $R > 0.5$. The clustering pattern is related to the number of possibly avoidable channels. For $R \leq 0.5$, one of the two channels can be voided, while for $R > 0.5$ both channels must be utilized. For the case $L = 3$, the BER curves are grouped in three clusters; see Figure 2.7-b. The best cluster corresponds to $R \leq 0.33$, where two of the three channels can be avoided. The second cluster corresponds to the case where one

bad channel can be avoided. This corresponds to $0.33 < R \le 0.67$. The worst cluster is for $R > 0.67$ where no possibility to avoid any channel. The same discussion applies to Figure 2.7-c for $L = 4$. In this case, the curves are grouped into four clusters. This clustering behavior is observed in the ranges $R \le 0.25$, $0.25 < R \le 0.5$, $0.5 < R \le 0.75$ and $R > 0.75$.

To generalize, the clustering behavior depends on the relative values of R and L. It is found that for a given L, the curves corresponding to the rates in the range $(\frac{i-1}{L}, \frac{i}{L}]$ are grouped in a cluster. This behavior can be noticed clearly in Figures 2.8 to 2.10 where the Symbol-error probability versus the throughput rate is presented for L= 2,3 and 4, respectively, for different values of $\bar{\gamma}$. Each cluster of curves, in Figures 2.7-a to 2.7-v, corresponds to a smooth curve of gradual changes over the interval $\frac{i-1}{L} < R \le \frac{i}{L}$. Large changes can be noticed at $R = \frac{i}{L}$,which is another illustration of the gap between clusters.

As mentioned earlier, the clustering behavior is related to the number of channels that can be avoided without violating the throughput constraint. That is, the reduction in $\bar{P}$ caused by decreasing R depends on whether this change enables the system leave out the worst channel or not; if yes, the improvement will be significant. Otherwise, it is minor. The justification behind this type of behavior is connected to the instance of deep fade. The performance of the system is dominated by the occurrence of deep fades on a channel. In case of deep fade and in view of the slow fading model adopted here, the

reduction in the code rate will have a little effect. As an example, in the case of $L = 3$ (Figure 2.9), the slow change of $\bar{P}$ with R can be seen in the interval $0.67 < R < 1$ where there is no possibility to avoid any channel when it suffers from a deep fade. When the rate is dropped to 0.67, a remarkable improvement can be noticed, as it is then possible to avoid one channel when it is deeply faded.

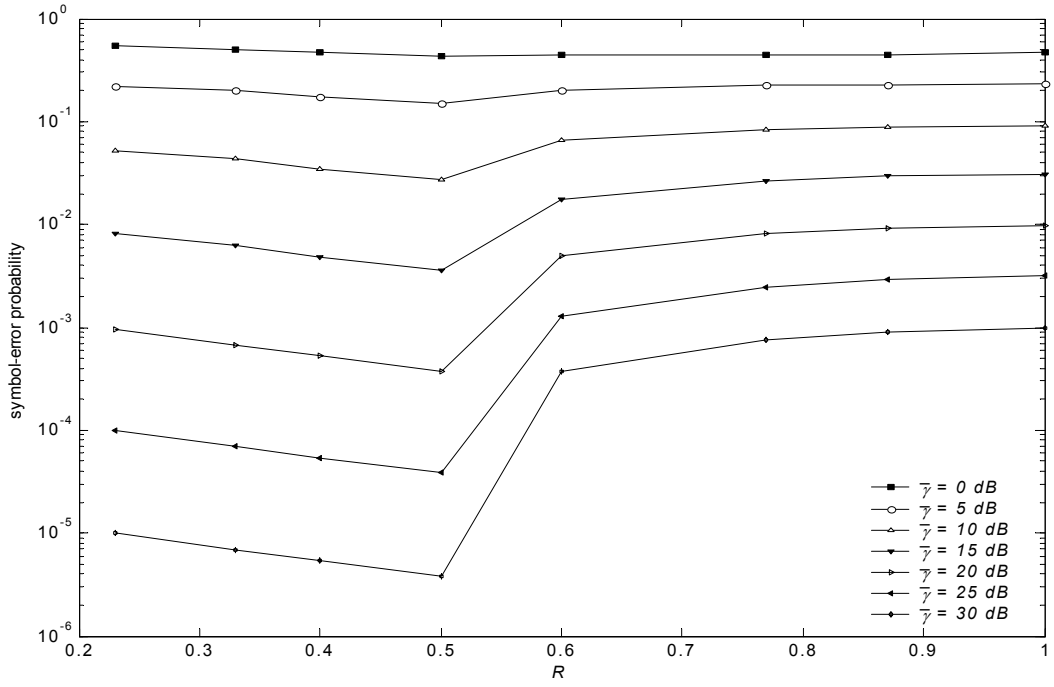

Figure 2.8: Symbol-error probability of the RS-coded MC-AFEC system with $L = 2$ vs. rate, for different SNR values.

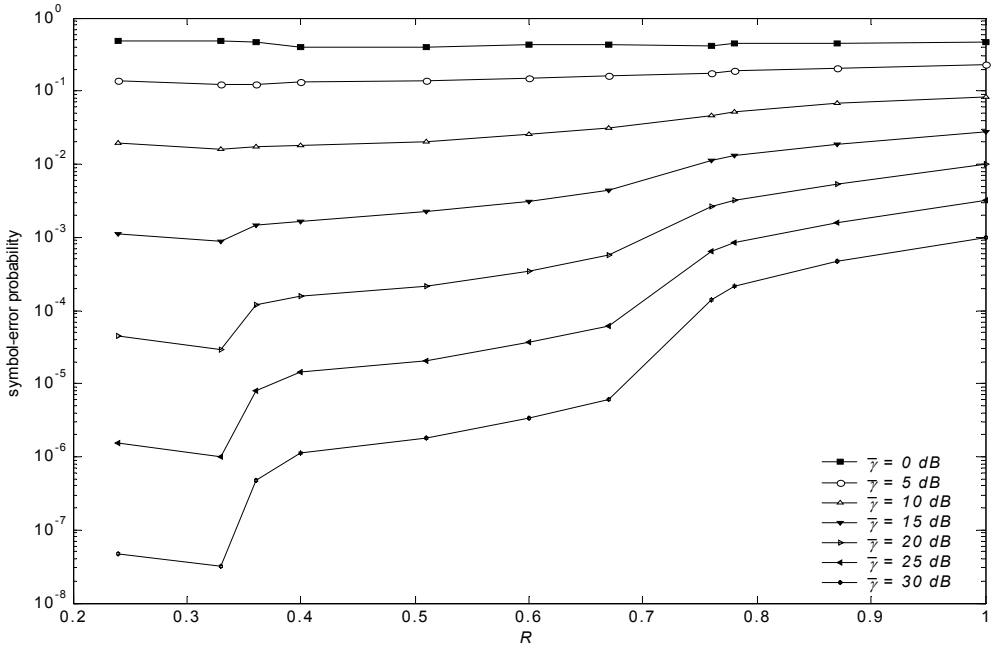

Figure 2.9: Symbol-error probability of the RS-coded MC-AFEC system with $L = 3$ vs. rate, for different SNR values.

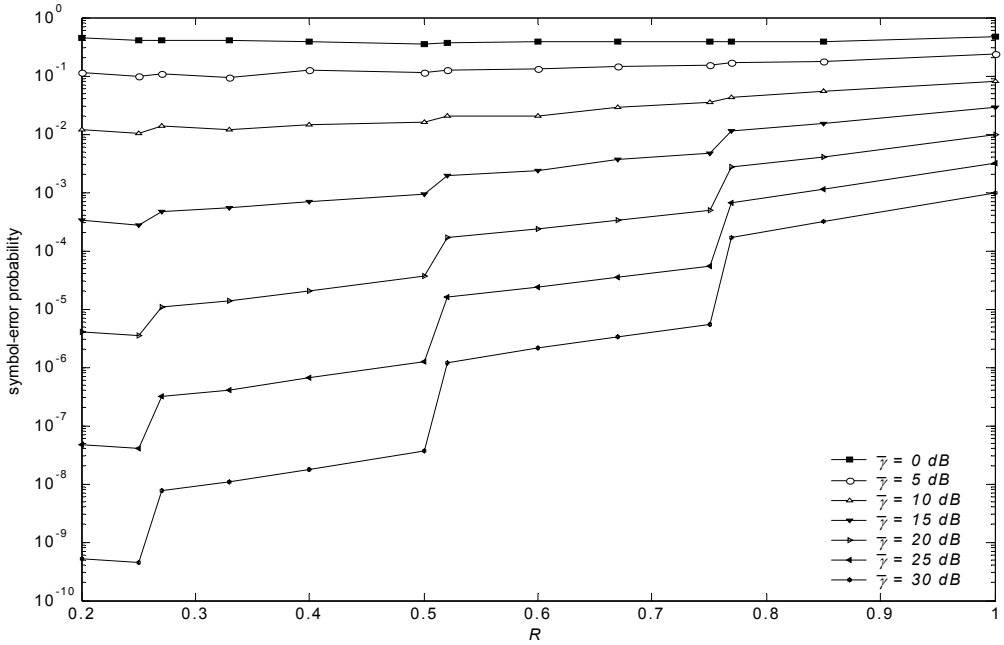

Figure 2.10: Symbol-error probability of the RS-coded MC-AFEC system with $L = 4$ vs. rate, for different SNR values.

The trend of gradual improvement is resumed within the region $0.33 < R \leq 0.66$, since still only one bad channel can be avoided. Once the rate falls to 0.33, another significant improvement is observed where it is possible to leave out two channels when they experience deep fades. The same observations is noted when $L = 2$ (Figure 2.8) for intervals $0.5 < R \leq 1$ and $R \leq 0.5$, and for $L = 4$ (Figure 2.10) for the intervals: $0.75 < R < 1$, $0.5 < R \leq 0.75$, $0.25 < R \leq 0.5$, and $R \leq 0.25$.

Unexpectedly, reducing R doesn't lead always to better performance. For example, consider the system with L =2 in Figure 2.8. It is observed that the system of R = 1/2 has a better performance than the cases of R < 1/2. This can be seen also in the case of L = 3 where the best performance is obtained when R = 1/3, and in the case of L = 4, R = 1/4 is the rate of the best system. Hence, one can conclude that $R = 1/L$ is the optimum code rate. The reason of this behavior is related to the efficiency of coding. That is the effect of added redundancy doesn't compensate for the effect of reduction in $\bar{\gamma}$. As a result, the coding gain will be negative.

The effect of increasing the number of channels while the rate is constant is shown in Figures 2.11 to 2.17 for different RS code rate. These Figures demonstrate the significance of improvement in $\bar{P}$ with respect to R and compare this adaptive system with L = 2, 3 and 4 with the case of fixed-rate at L = 1 (with the same rate). The following observations can be made about Figures 2.11 to 2.17.

(i) Generally speaking, increasing the number of channels L will always result in improved performance at any rate R.

(ii) The performance of fixed-rate system (L = 1) is unacceptable. In fact, it is worse than the uncoded system and it gets worse as the rate is reduced. This is due to the power of coding is taken from the randomness of the noise. In our channel model, the fade envelope covers the whole block and no matter what the rate of code is, it will perform worst than the uncoded case since the deep fades will severely diminish the performance. Therefore, the coding becomes a waste since it cannot suppress the effect of deep fading.

(iii) The amount of improvement of the adaptive system over the fixed-rate system increases as the rate decreases. It is so because the decrease in the rate means more freedom for adaptation.

(iv) Clustering effect referred to earlier appears here again. In the following lines, a discussion on the effect of R and L on this phenomena will be presented.

At R = 0.85 (Figure 2.11), and for L = 2, 3 and 4, the system cannot avoid using any channel when it has an instant deep fade. Hence, in the three cases, the curves are close and there is no significant improvement from increasing the number of channels over the system of fixed-rate (L = 1).

In the case of R = 0.75 (Figure 2.12), the situation is different. Here at L= 4, the system has the ability to avoid one channel, while for L = 2 and 3, the system doesn't have this ability. Avoiding a channel is accomplished by transmitting no information,

only redundant symbols are transmitted, i.e. the code (n,0,--) is used on that channel. As a result, the $L = 4$ case has a significant gain over the other cases.

At $R = 0.6$ (Figure 2.13), the systems with $L = 3$ and 4 can avoid one bad channel while for $L = 2$ there is no possibility to avoid the deeply faded channel at this rate. Consequently, the curves of $L = 3$ and $L = 4$ are close to each other while the curve for L=2 is considerably worse.

In the case of $R = 0.5$ (Figure 2.14) and $R = 0.4$ (Figure 2.15), one bad channel can be avoided in the cases of $L = 2$ and 3. Therefore, a significant improvement over the fixed system ($L = 1$) is obtained. Moreover, for $L = 4$ two bad channels can be avoided. Therefore, another major improvement is also recorded.

For the case of $R = 0.33$ (Figure 2.16), the systems of $L = 3$ and 4 have the ability of avoiding two channels. Hence, the two curves are close to each others, while the curve for $L = 2$ is far worse.

In Figure 2.17, the throughput rate is equal to 0.25. At $L = 4$, the flexibility of channel avoidance is very high (3 channels), in $L = 3$ the flexibility is moderate (2 channels), in $L = 2$ the flexibility is low (1 channel) while in the fixed-rate system there is no possibility to avoid any channel. Consequently, all curves are significantly separated. The curve of $L = 2$ has a significance improvement over the fixed-rate system, the curve of $L = 3$ is considerably far from $L = 2$, and the curve of $L = 4$ is far better than all others.

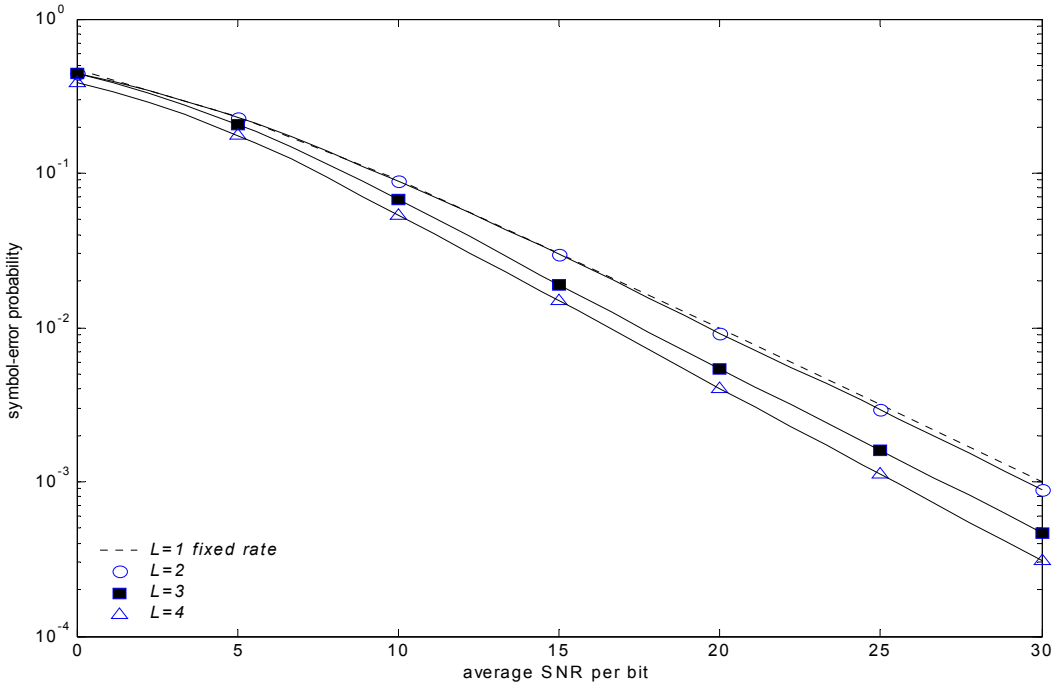

Figure 2.11: Symbol-error probability of the RS-coded MC-AFEC system at $R = 0.85$.

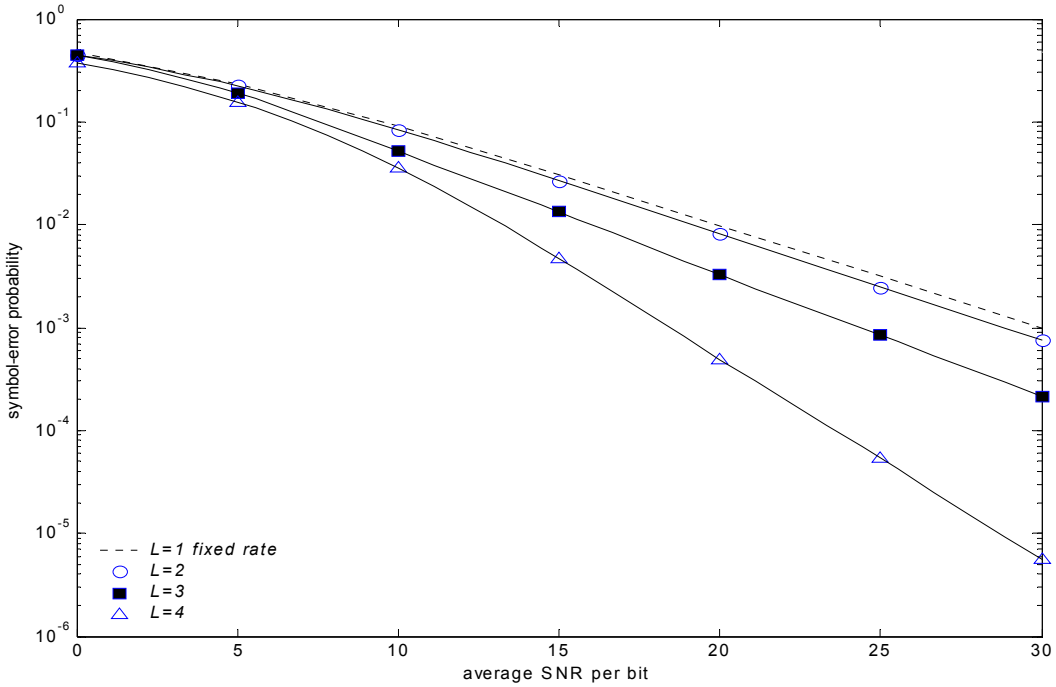

Figure 2.12: Symbol-error probability of the RS-coded MC-AFEC system at $R = 0.75$.

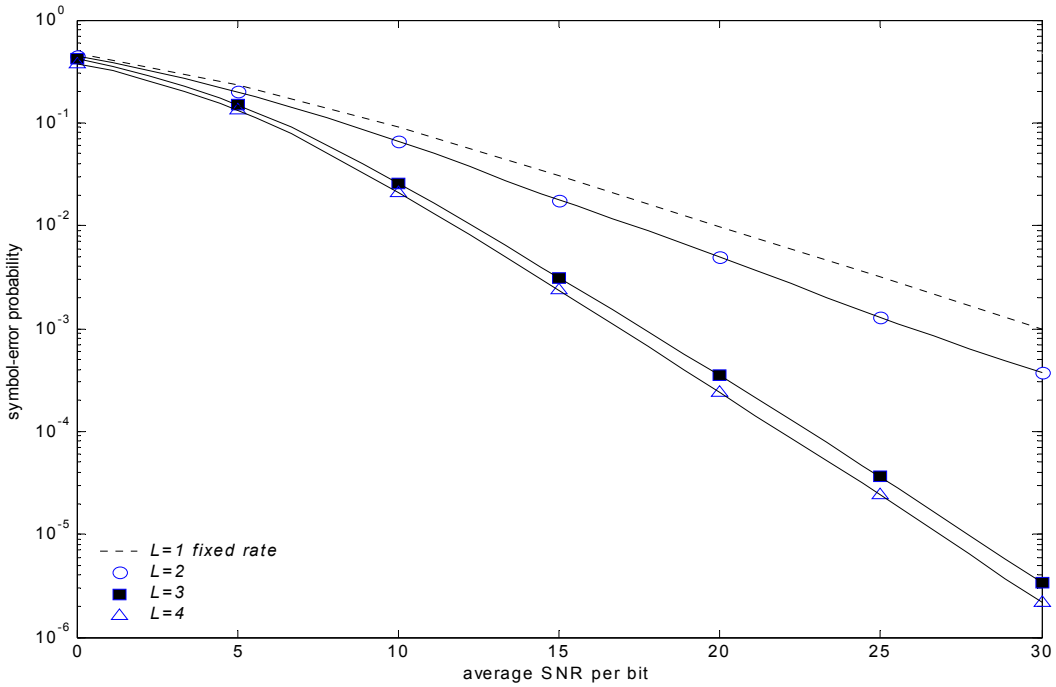

Figure 2.13: Symbol-error probability of the RS-coded MC-AFEC system at $R = 0.6$.

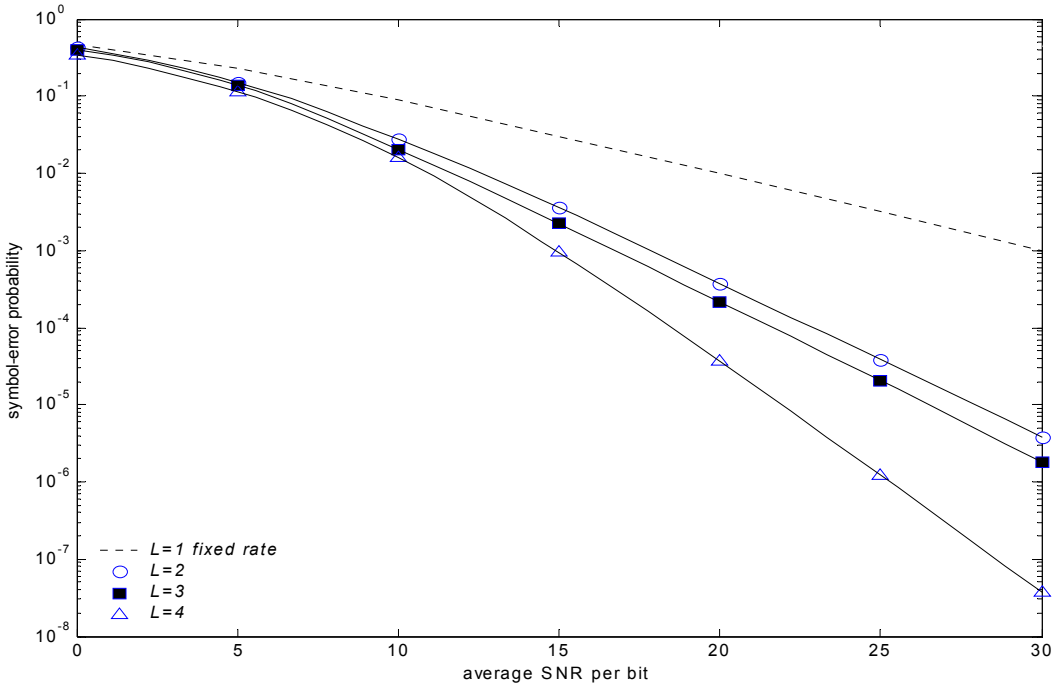

Figure 2.14: Symbol-error probability of the RS-coded MC-AFEC system at $R = 0.5$.

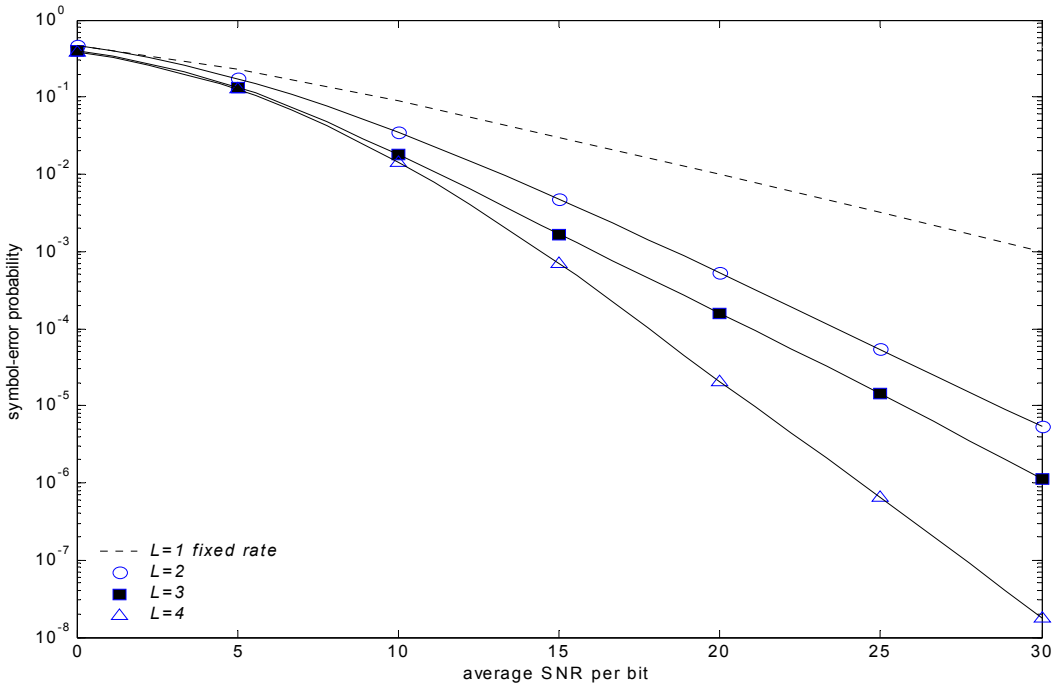

Figure 2.15: Symbol-error probability of the RS-coded MC-AFEC system at $R = 0.4$.

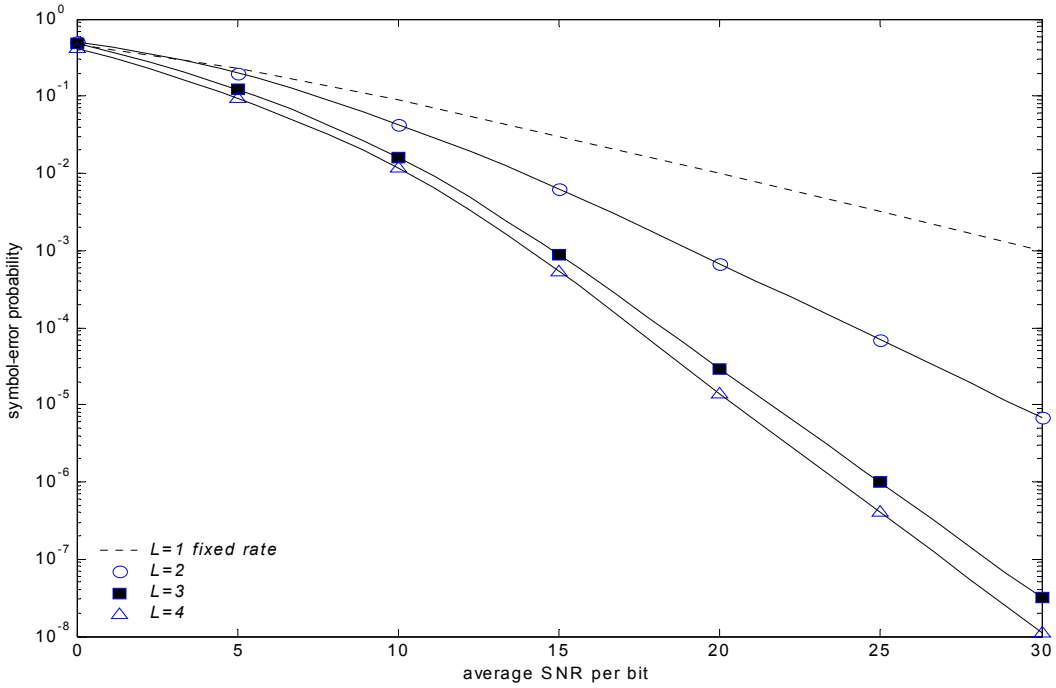

Figure 2.16: Symbol-error probability of the RS-coded MC-AFEC system at $R = 0.33$.

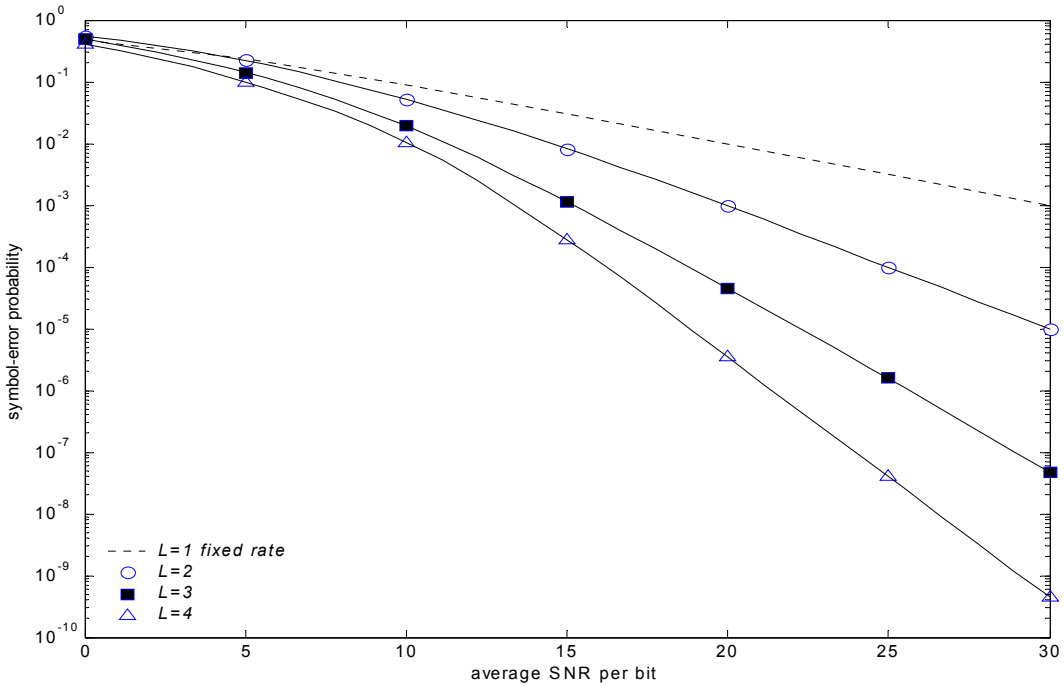

Figure 2.17: Symbol-error probability of the RS-coded MC-AFEC system at $R = 0.25$.

2.8 System performance using One *L*-code set

Instead of utilizing eight *L*-code sets for adaptation, the use of a single *L*-code set will be studied in this section. The system is still adaptive in terms of allocating the codes on each channel according to their qualities, where the highest rate code is assigned to the best channel and the lower rate codes to the poorer channels. Let γ_i; i = 1,2,…, L be the estimates of the SNR of the i^{th} channel and let βq denotes the *qth* ranked estimate of those γ_i's, where q = 1,2,…,L. To illustrate the relationship between γ_i's and βq's, consider for example, the case when L = 3. In this case the relation will be

$$\beta_1 = \gamma_x \,;\; \beta_2 = \gamma_y \,;\; \text{and } \beta_3 = \gamma_z \,, \quad \text{when} \quad \gamma_x < \gamma_y < \gamma_z \tag{2.21}$$

Let $g_q(\beta_q)$ be the probability density function of the q^{th} ranked of the L independent identically distributed random variables. From order statistics [33], $g_q(\beta_q)$ can be expressed as

$$g_q(\beta_q) = \binom{L}{q}\left[\int_0^{\beta_q} f(\gamma)d\gamma\right]^{q-1} f(\beta_q)\left[\int_{\beta_q}^{\infty} f(\gamma)d\gamma\right]^{L-q} \tag{2.22}$$

The pdf of γ, $f(\gamma)$, in Rayleigh fading channel is given in Equation (1.12). Substitute this pdf in the above Equation and carry out the integration to get $g_q(\beta_q)$. After some manipulations, $g_q(\beta_q)$ can be written as

$$g_q(\beta_q) = \frac{q}{\overline{\gamma}}\binom{L}{q}\left[1-\exp\left[-\frac{\beta_q}{\overline{\gamma}}\right]\right]^{q-1}.\exp\left[-\frac{(L-q+1)\beta_q}{\overline{\gamma}}\right] \tag{2.23}$$

In Figure 2.18, $g_q(\beta_q)$ has been drawn for different values of $\overline{\gamma}$.

Let the L codes of the set be ranked according to their rates in ascending order where the rank L will be assigned to the highest rate code. The q^{th} rank code will be always assigned to the channel with SNR of β_q. Let P_q be the post-decoding symbol error probability of the system using the q^{th} ranked code. The overall average symbol error probability is obtained by averaging P_q over $g_q(\beta_q)$, that is

$$\overline{P} = \frac{1}{K}\sum_{q=1}^{L} k_q \int_0^{\infty} P_q g_q(\beta_q) d\beta_q \qquad (2.24)$$

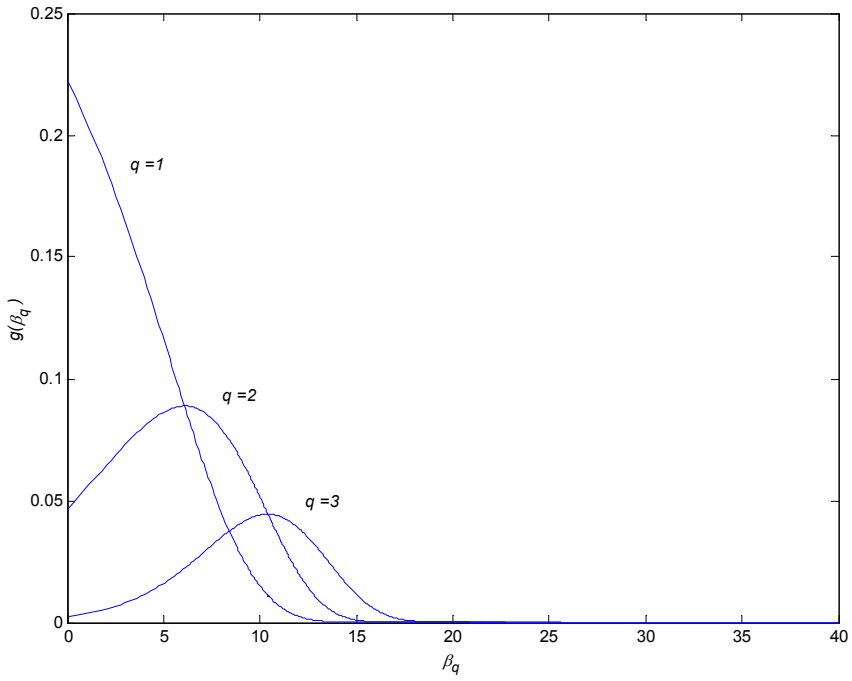

(a)

Figure 2.18: The pdf of the q^{th} ranked of SNR for three independently Rayleigh faded channels with (a) $\overline{\gamma} = 10\,\text{dB}$, (b) $\overline{\gamma} = 20\,\text{dB}$, and (c) $\overline{\gamma} = 30\,\text{dB}$.

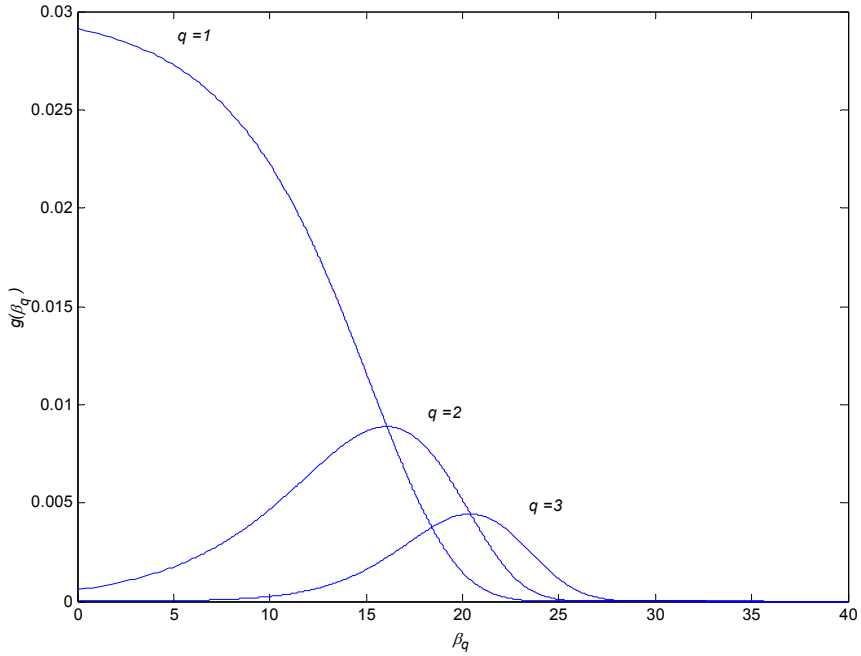

(b)

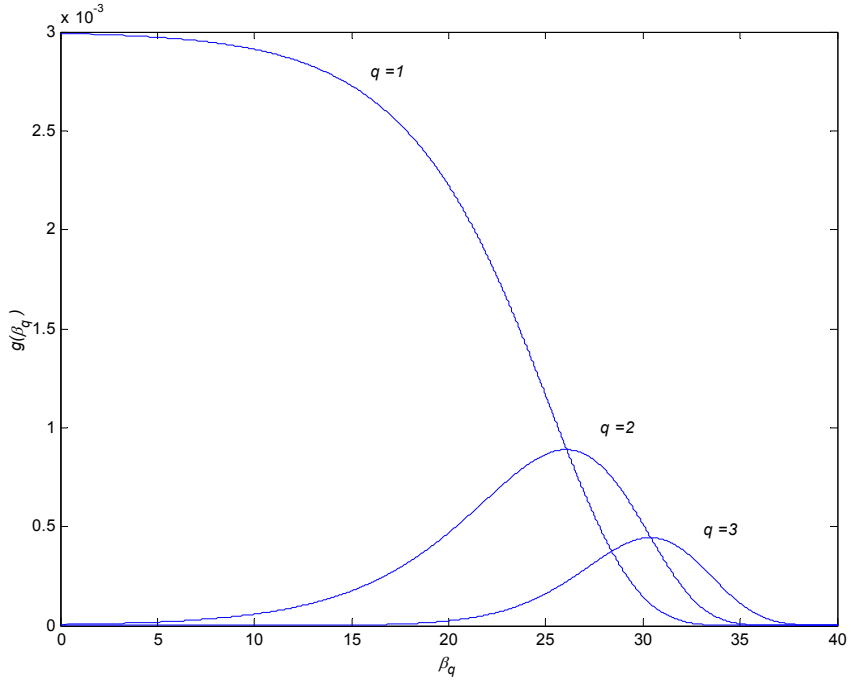

(c)

Figure 2.18: (Continued).

Set number	Code 1	Code 2	Code 3
1	(63,63,00)	(63,32,05)	(63,00,---)
2	(63,63,00)	(63,16,11)	(63,16,11)
3	(63,57,01)	(63,38,04)	(63,00,---)
4	(63,51,02)	(63,44,03)	(63,00,---)
5	(63,51,02)	(63,28,07)	(63,16,11)
6	(63,46,03)	(63,30,06)	(63,19,09)
7	(63,46,03)	(63,28,07)	(63,21,08)
8	(63,39,04)	(63,28,07)	(63,28,07)

Table 2.4: Eight BCH 3-code sets satisfying R ≈0.5.

Consider the case of BCH-coded system with $L = 3$ and $R = 0.5$. The plots of $\overline{P}$ for different code sets are shown in Figure 2.19 and compared with the original MC-AFEC system with the all eight codes given in Table 2.4. The MC-AFEC system that utilizes all of the eight sets is represented by curve A. Curve B, C and D, is the cases when we use just one code listed in Table 2.5. Observing Figure 2.19, it is clear that using all of the eight sets yields the best performance shown by curve A. A significant fall in the performance is observed for curve D compared with other cases. This is due to the code set D using all three channels, and non of them can be avoided during deep fade. On the other hand, code sets B and C have the ability to reject the deeply faded channel. A slight improvement of curve B over C is noticed and it is due to using a more powerful code over the second worst channel [32].

Figure 2.20 shows $\overline{P}$ for the RS-coded system with R =1/3 and L = 3. Similar to the above system, curve A is the optimal case as a result of providing the system with 8 code sets of Table 2.3 including the code sets of the other curves. In curve B, all the code sets of Table 2.3 is used except Set number 1. Curves C, D, and E represent the performance of the system that uses only one code set, given in Table 2.6.

The importance of the ON/OFF code set (the first set) at high $\overline{\gamma}$ can be seen clearly when we compare curve A with curve B. While the two systems have close performance at low $\overline{\gamma}$, the system in A shows remarkable improvement at high $\overline{\gamma}$. This in fact emphasizes the dominance of the effect of the number of possibly avoidable channels at high $\overline{\gamma}$. For B, only one channel can be avoided while in A the system has the ability of avoiding two channels.

Similarly, the significance of the ON/OFF code set at high $\overline{\gamma}$ can be seen clearly when we compare curve B with curve C. The system that uses all sets except the ON/OFF code set (curve B) shows better performance at low $\overline{\gamma}$ compared to the system in C, which uses the ON/OFF code set only. However, the system in C improves faster to be better than the system in B at high $\overline{\gamma}$.

Curve D refers to the case when the system can avoid one bad channel, and hence as expected, a worse performance is noticed compared to the cases when the system can avoid two channels. Finally, if the system is not given the flexibility to avoid a channel in deep fade, the performance will be severely degraded, as seen in curve E.

The results of Figures 2.19 and 2.20 can be generalized to all cases of R and L. One L-code set can be adaptively utilized with its members assigned to the diversity channels according to their quality. This set should be chosen in such a way that one of its codes is as redundant as possible, the following code is yet again as redundant as possible, and so on. This implies that the worst channel will be assigned a highly redundant code; as such as the throughput constraint permit. The optimum case would be to avoid transmission over more of the channels, as long as the throughput constraint is not violated. This will be don at the price of allowing the number of information symbols on better channels to be with weak or no coding. The code set that is chosen using this criterion will be the best of all other sets.

Let us Refer to Figure 2.1, where the code set assignment according to the instantaneous SNR of each channel in the case of $L = 2$, note that the most outer regions are when one or more channels have a low γ which corresponds to deep fades. The code set used in the outer regions is the set number 1 (the ON/OFF code set) in Table 2.1, which is the best set that employs the method that has been described above. It is known that the major source of the severe degradation in the performance is when one channel or more is in deep fade, and it is clear from Figure 2.1 that the code set that has been assigned using the method explained above will take care of these intervals very effectively providing the best performance compared with other codes. Therefore, with the method of choosing the best set explained above, the deterioration in the system's performance would be minimal compared with the system that uses all of the code set available.

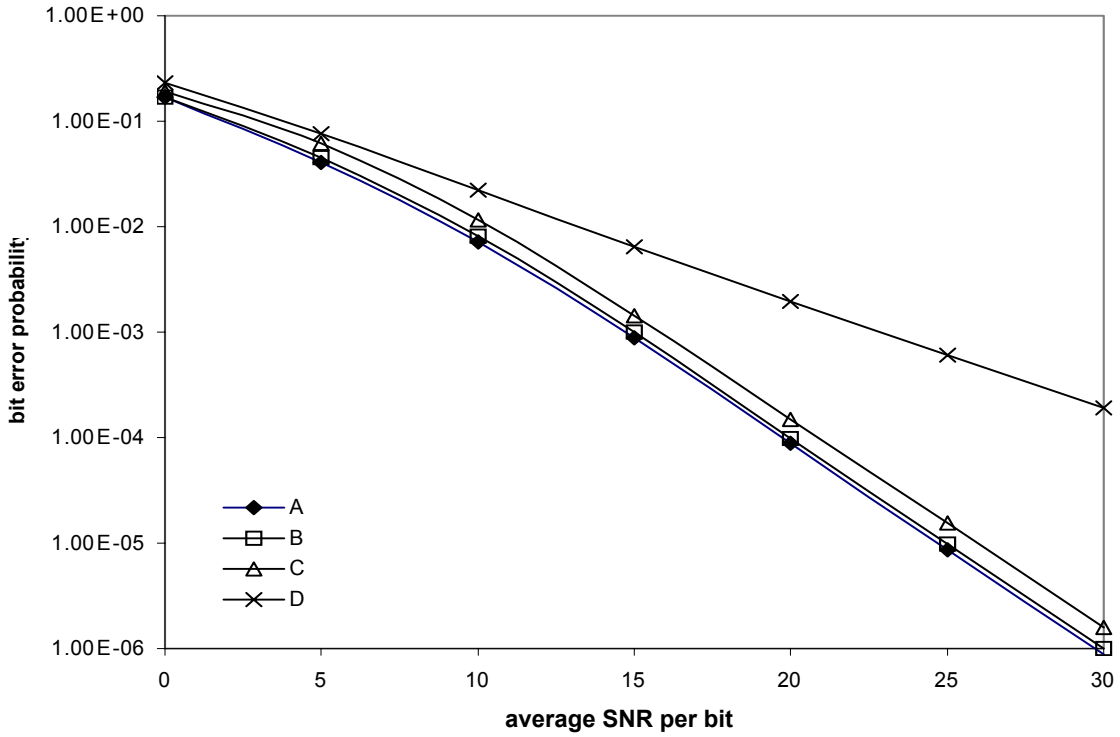

Figure 2.19: The effect of choosing the code sets on the performance of BCH-coded MC-AFEC system with $L = 3$ and $R = 0.5$.

A	All eight sets of Table 2.4		
B	(63,63,00)	(63,32,05)	(63,00,---)
C	(63,51,02)	(63,44,03)	(63,00,---)
D	(63,51,02)	(63,28,07)	(63,16,11)

Table 2.5: The code sets associated with the curves in Figure 2.19.

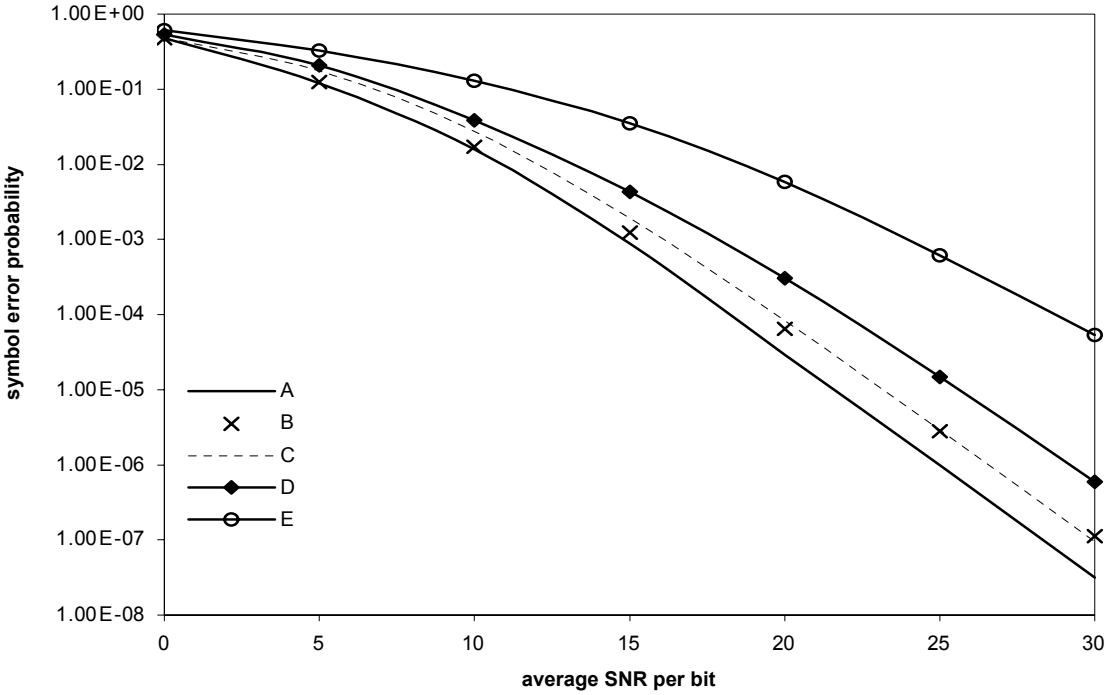

Figure 2.20: The effect of choosing the code sets on the performance of RS-coded MC-AFEC system with $L = 3$ and $R = 0.33$.

A	All eight sets of Table 2.2		
B	All eight sets of Table 2.2 except the first one		
C	(15,15,00)	(15,00,---)	(15,00,---)
D	(15,09,03)	(15,06,04)	(15,00,---)
E	(15,05,05)	(15,05,05)	(15,05,05)

Table 2.6: The code sets associated with the curves in Figure 2.20.

CHAPTER 3

PERFORMANCE OF MC-AFEC SYSTEM UNDER REALISTIC CONDITIONS

3.1 Introduction

In the previous chapter, the structure and the behavior of the MC-AFEC system has been studied. This system is a form of a diversity system in the sense of utilizing multiple channels to the effect of fading. In implementation terms, this system reduces to that of selecting the optimum set of codes for a given channel estimation. As a result, the MC_AFEC system may be viewed as wider-range selective diversity. Therefore, it would be valuable to compare this system with selective combing (SC) diversity. In addition, the performance of the MC-AFEC system is studied in some realistic conditions. For instance, correlated branches and outdated channel estimates.

This chapter is organized as follows. First, a comparison with selective combining diversity system over Rayleigh fading channels is performed. Then, the effect of the correlation between diversity channels is studied. We next examine the impact of outdated estimates of the channel state information CSI on the system's performance. In the last section, the effect of fading severity will be investigated by examining the behavior of the system over Nakagami-*m* fading channel for different values of the parameter *m*.

3.2 The performance over Rayleigh fading channels

In this section, the performance of the MC-AFEC is compared to the SC over a Rayleigh fading channel for the channel model described in Section 2.3. The following was assumed about the two systems:

- The channels are slow and non-selective.
- All the diversity channels are identical on the average.
- The diversity channels are independent.
- Perfect channel state information CSI is assumed; That is, the estimates are noise free and available on time with no delay.

In Chapter 2, two methods have been presented in order to evaluate the bit error rate $\overline{P}_b$. The first method is based on the evaluation of Equation 2.4 using numerical multidimensional integration, while the other is based on computer simulation.

According to these models the SER performance of the RS-coded MC-AFEC system has been evaluated with various rates *R* and with different number of channels *L*. The results in the form of BER for the two coding schemes: Binary BCH and RS are presented here and compared to SC with different values of *R* and *L*. Figures 3.1 to 3.3 and 3.4 to 3.6 show the BER of the RS and BCH coded systems, respectively. It can be remarked from the figures that the numerical and simulation results are matched.

Figures 3.1 and 3.4 display the performance of the MC-AFEC systems when *L*= 2. Observing these figures, it can be seen that at *R* = 0.5 the MC-AFEC system operates better than the SC system by about 1 dB. However, for other values of *R*, less or more than 0.5, the performance degrades in such a manner that the system became inferior to the SC system. As a result, the MC-AFEC system better to be in rate *R* = 0.5 to have a reasonable performance compared with the SC.

If the MC-AFEC utilizes three diversity channels as in Figures 3.2 and 3.5, the performance will improve more and it can be observed that when $R \leq 1/3$, the BER is lower than the one in SC case with the same number of channels. For the case when *R*= 1/3, the BER curve is lower than the SC curve by more than 1.6dB. However, $\overline{P}_b$ get higher when *R* is reduced below 1/3, but it is still better than the SC system. On the other hand, increasing *R* above 1/3 will make the system worse than the SC. Consequently, the rate should be less than or preferably equal to 1/3 in order for the MC-AFEC system to perform better than SC with the same number of channels.

Figures 3.3 and 3.6 demonstrate the performance of the MC-AFEC system when $L = 4$ for the RS and BCH coded systems respectively and compared with the SC with the same number of diversity channels. The MC-AFEC systems show more improvement over the SC. It can be seen from the figures that the MC-AFEC system outperform the SC by approximately 2.5 dB when $R = 0.25$ and Still, the performance is better than the SC if the rate decreases below 0.25. Unfortunately, it became inferior to the SC when $R > 0.25$ especially at high SNR. However, for lower SNR, the system with some rates higher than 0.25 shows a better performance. For example, consider the case of $R = 0.33$, the MC-AFEC system have a better performance than the SC with R=0.25 if they operate below $\overline{\gamma} \simeq 22$ dB ; to be specific, a 1.6 dB improvement can be noticed. In the same way, the system with $R = 0.4$, an improvement over the SC with $R = 0.25$ can be remarked at $\overline{P}_b \simeq 10^{-4}$ by about 1.2 dB. As a result, if the application requires the BER of about 10^{-6} or more, the MC- AFEC would be acceptable when the throughput is between 0.33 and 0.5 compared to the SC. However, lower rate may be needed if lower BER is required.

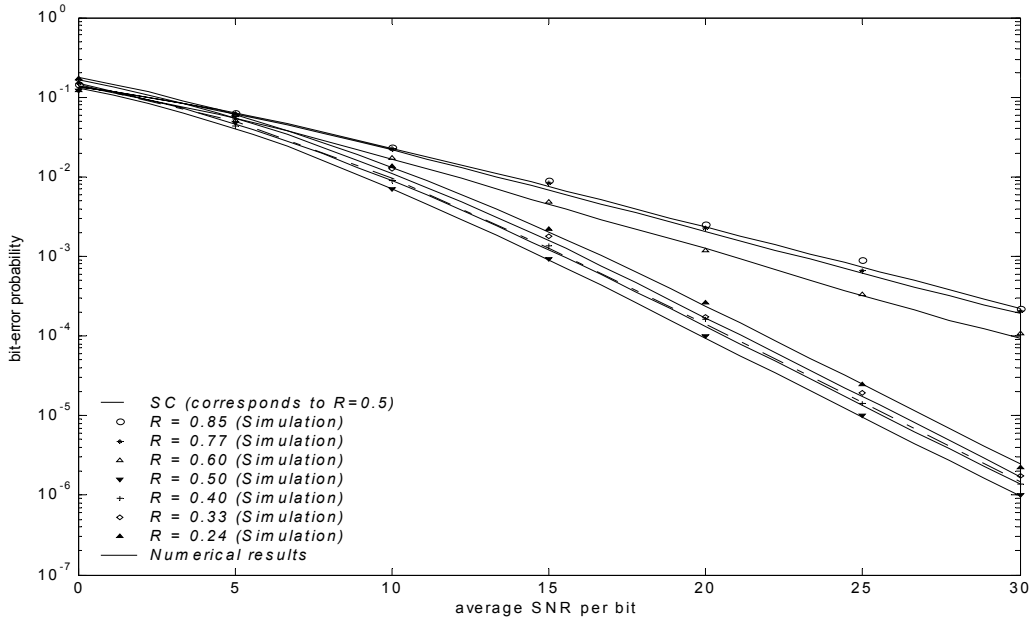

Figure 3.1: The performance of RS-coded MC-AFEC of various rates compared to the SC diversity with two diversity channels.

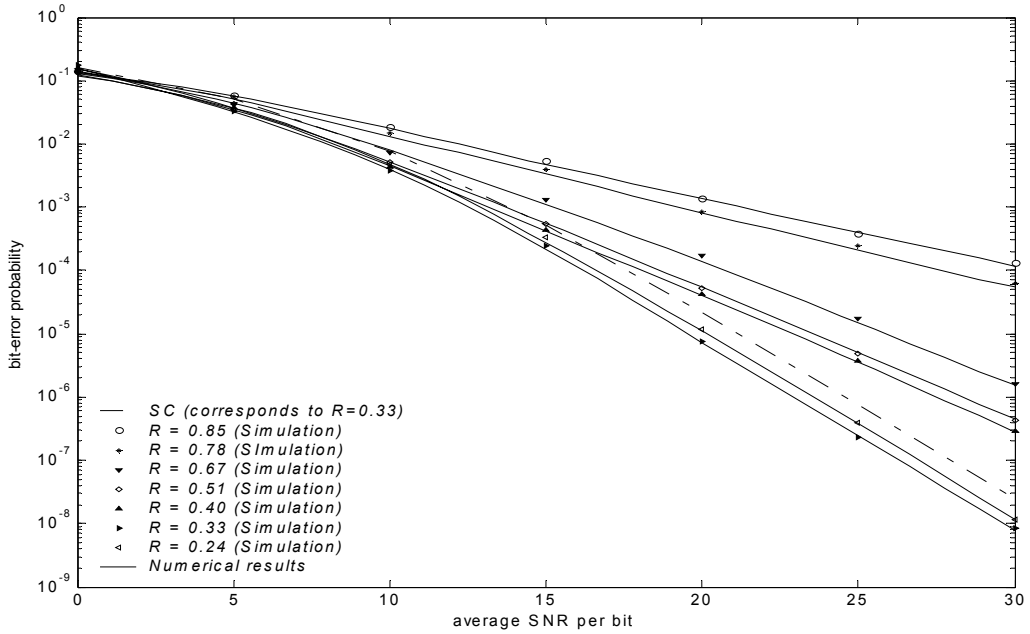

Figure 3.2: The performance of RS-coded MC-AFEC of various rates compared to the SC diversity with three diversity channels.

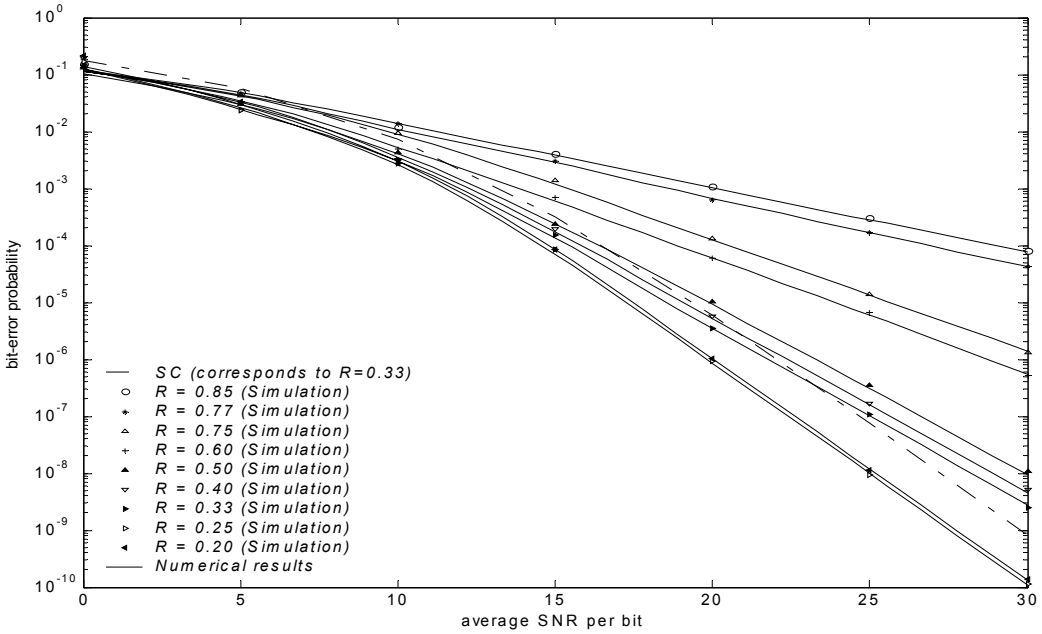

Figure 3.3: The performance of RS-coded MC-AFEC of various rates compared to the SC diversity with four diversity channels.

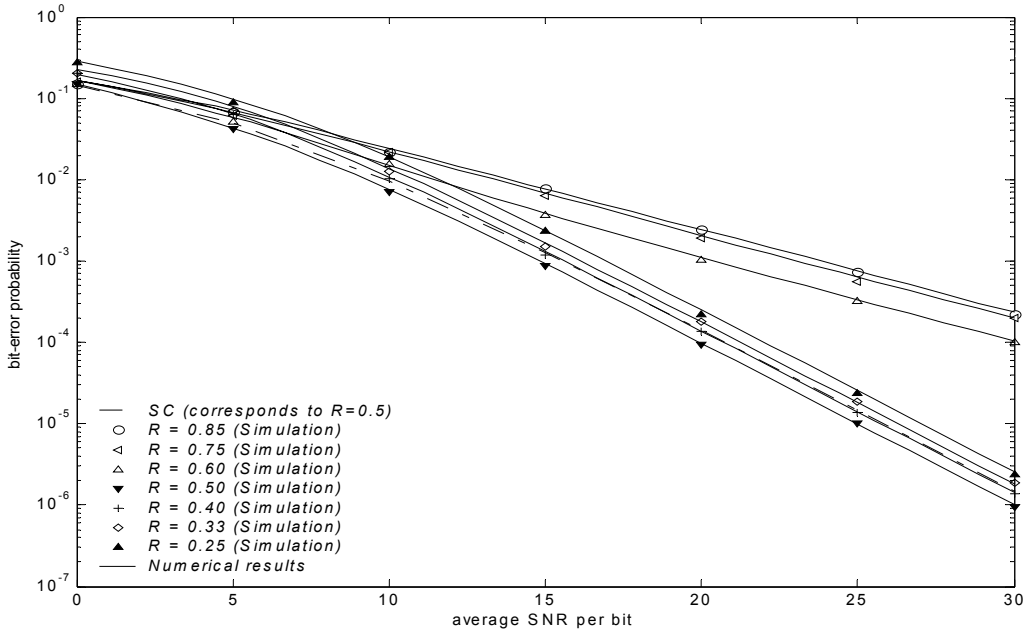

Figure 3.4: The performance of BCH-coded MC-AFEC of various rates compared to the SC diversity with two diversity channels.

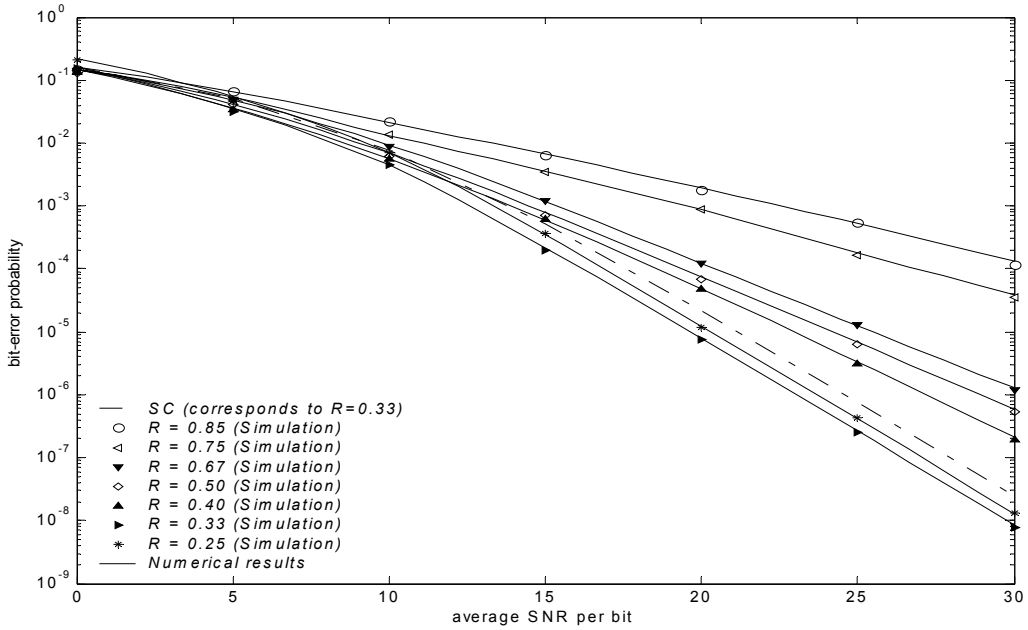

Figure 3.5: The performance of BCH-coded MC-AFEC of various rates compared to the SC diversity with three diversity channels.

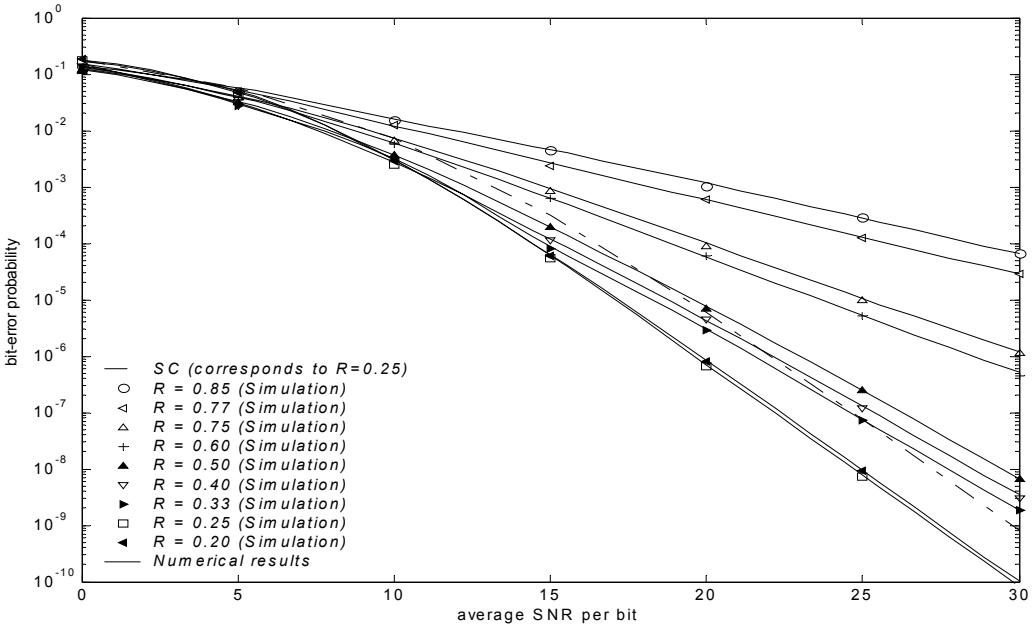

Figure 3.6: The performance of BCH-coded MC-AFEC of various rates compared to the SC diversity with four diversity channels.

3.3 The impact of branch correlation

In studying the performance of diversity systems, it is usually assumed that the diversity channels are independent. However, there are a number of real life cases in which this assumption is not valid. Consider, for instance, the case of space diversity. Due to physical limitations, correlation between branches may be introduced. In the literature, various correlation models have been proposed. For example, Nakagami [36] proposed a constant correlation model of dual diversity reception with nonidentical fading. Another model proposed by Aalo [37, sec. II-A] assumes L identically distributed branches with constant correlation between them; that is the envelope correlation coefficient ρ is the same between all pairs of channels. There are other models that adopt the exponential correlation like the one in [37, sec. II-B] where the diversity channels are assumed to be identically distributed with exponential envelope correlation coefficients between the channels pairs.

In this section, we will adopt the second realization of diversity channels presented in Section 2.2, where multiple antennas is used to achieve space diversity. We will adopt also the constant correlation model proposed by Aalo [37, sec II-A]. This model assumes that the correlation between all pairs of channels is constant which corresponds to the cases where all antennas are equidistant. Figures 3.7 and 3.8 shows the placement of equidistant antennas for the case of $L = 3$ and $L = 4$, respectively.

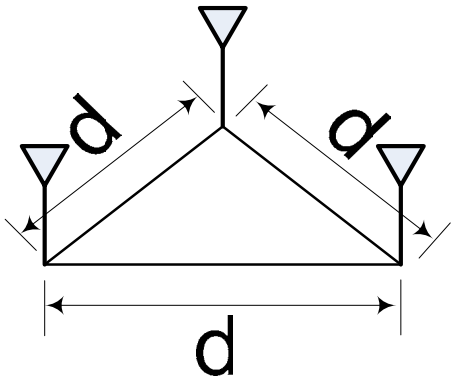

Figure 3.7: Demonstration of three equidistant antennas.

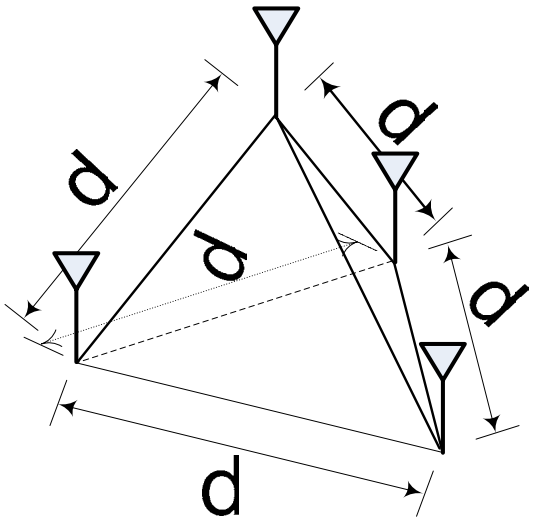

Figure 3.8: Demonstration of four equidistant antennas.

In this section, a numerical evaluation in addition to computer simulation will be presented for the case of dual diversity. Furthermore, simulation will be presented for the cases of L >2. In these evaluations the following is assumed:

- The channels are slow and non-selective.
- All the diversity channels are identical on the average; i. e., $\mathrm{E}\left[\left|\alpha_{\mathrm{i}}\right|^2\right]=1$.

- The diversity channels are correlated with the same envelope correlation coefficient ρ between channel pairs; that is

$$\rho = \frac{\text{cov}(\alpha_i^2, \alpha_j^2)}{\sqrt{\text{var}(\alpha_i^2)\,\text{var}(\alpha_j^2)}}; \qquad i \neq j,\ 0 \leq \rho < 1 \tag{3.1}$$

where, i, $j = 1, 2, \ldots L$.

- Perfect channel state information CSI is assumed.

To evaluate $\overline{P}_b$, we need to carry out the integration in Equation (2.4). It is clear that $\overline{P}_b$ is a function of $f(\Gamma)$. In Chapter 2, the channels has been considered independent; hence, $f(\Gamma) = f(\gamma_1) f(\gamma_2) \ldots f(\gamma_L)$. When the channels are correlated, we need to go for the joint pdf of γ's, $f(\Gamma) = f_{\gamma_1, \gamma_2, \ldots \gamma_L}(\gamma_1, \gamma_2, \ldots \gamma_L)$. To evaluate $f(\Gamma)$ for a given fading distribution $f_{\alpha_1, \alpha_2, \ldots \alpha_L}(\alpha_1, \alpha_2, \ldots \alpha_L)$, one needs to use the linear transformation method.

Consider the problem of finding the joint pdf for L functions of L random variables $\boldsymbol{\alpha} = [\alpha_1, \alpha_2, \ldots \alpha_L]$ [38]:

$$\gamma_1 = g_1(\boldsymbol{\alpha}); \gamma_2 = g_2(\boldsymbol{\alpha}); \ldots \gamma_L = g_L(\boldsymbol{\alpha}) \tag{3.2}$$

where $g_i(\boldsymbol{\alpha}) = \overline{\gamma}\,\alpha_i^2$; $i = 1, 2, \ldots L$. The solution of $g_i(\boldsymbol{\alpha})$ will be α_i and is given by: $\alpha_i = h_i(\Gamma)$. The set of $h_i(\Gamma)$ is the unique solution of the set of equations in (3.2) and is given by

$$h_i(\Gamma) = \sqrt{\frac{\gamma_i}{\bar{\gamma}}} \;;\; \text{(The negative solution is omitted since } \alpha_i \geq 0\text{).} \tag{3.3}$$

To get the joint pdf of Γ, the following equation need to be applied:

$$f_{\gamma_1,\gamma_2,\ldots\gamma_L}(\gamma_1,\gamma_2,\ldots\gamma_L) = f_{\alpha_1,\alpha_2,\ldots\alpha_L}(h_1(\Gamma),h_2(\Gamma),\ldots h_L(\Gamma)).\left|J(\gamma_1,\gamma_2,\ldots\gamma_L)\right| \tag{3.4}$$

Where $J(.)$ denotes the Jacobean of the transformation and is given by:

$$J(\gamma_1,\gamma_2,\ldots\gamma_L) = \begin{vmatrix} \frac{\partial h_1}{\partial \gamma_1} & \cdots & \frac{\partial h_1}{\partial \gamma_L} \\ \vdots & \ddots & \vdots \\ \frac{\partial h_L}{\partial \gamma_1} & \cdots & \frac{\partial h_L}{\partial \gamma_L} \end{vmatrix} = \left(\frac{1}{2\sqrt{\bar{\gamma}}}\right)^L \frac{1}{\sqrt{\prod_{i=1}^{L}\gamma_i}} \tag{3.5}$$

Applying Equations (3.5) and (3.3) in (3.4) to get

$$f_{\gamma_1,\gamma_2,\ldots\gamma_L}(\gamma_1,\gamma_2,\ldots\gamma_L) = f_{\alpha_1,\alpha_2,\ldots\alpha_L}\left(\sqrt{\frac{\gamma_1}{\bar{\gamma}}},\sqrt{\frac{\gamma_2}{\bar{\gamma}}},\ldots\sqrt{\frac{\gamma_L}{\bar{\gamma}}}\right)\left(\frac{1}{2\sqrt{\bar{\gamma}}}\right)^L \left(\frac{1}{\sqrt{\prod_{i=1}^{L}\gamma_i}}\right) \tag{3.6}$$

Consider the bivariate Nakagami-*m* pdf presented in [3]:

$$f_{\alpha_1,\alpha_2}(\alpha_1,\alpha_2) = \frac{4m^{m+1}(\alpha_1\alpha_2)^m}{\Gamma(m)(1-\rho)(\rho)^{\frac{m-1}{2}}} \exp\left[-\frac{m}{1-\rho}(\alpha_1^2+\alpha_2^2)\right] \mathrm{I}_{m-1}\left(\frac{2m\sqrt{\rho}\alpha_1\alpha_2}{1-p}\right) \tag{3.7}$$

where, $\Gamma(\cdot)$ is the gamma function and $\mathrm{I}_{m\text{-}1}(\cdot)$ is the modified Bessel function. Applying Equation (3.7) in (3.6), to get

$$f_{\gamma_1,\gamma_2}(\gamma_1,\gamma_2) = \mathrm{A}(\gamma_1\gamma_2)^{\frac{m-1}{2}} \exp\left[-\mathrm{B}(\gamma_1+\gamma_2)\right] \mathrm{I}_{m-1}(\mathrm{C}\sqrt{\gamma_1\gamma_2}) \;; \tag{3.8}$$

where, $\mathrm{A} = \dfrac{m^{m+1}}{\bar{\gamma}^{m+1}(1-\rho)(\rho)^{\frac{m-1}{2}}}$, $\mathrm{B} = \dfrac{m}{\bar{\gamma}(1-\rho)}$, and $\mathrm{C} = \dfrac{2m\sqrt{\rho}}{\bar{\gamma}(1-\rho)}$.

In this section, channels are modeled by Rayleigh fading. So, by setting the fading parameter m to 1, the joint PDF of γ's for Rayleigh fading environment can be reduced to be

$$f_{\gamma_1,\gamma_2}(\gamma_1,\gamma_2)=\frac{1}{\overline{\gamma}^2(1-\rho)}\exp\left[-\frac{(\gamma_1+\gamma_2)}{(1-\rho)\overline{\gamma}}\right]\ \mathrm{I}_0\left(\frac{2\sqrt{\rho}\sqrt{\gamma_1\gamma_2}}{(1-\rho)\overline{\gamma}}\right) \tag{3.9}$$

Now, by applying Equation (3.9) in the integration in Equation (2.8), the BER can be evaluated numerically. The results of this numerical evaluation can be seen in Figures 3.9 and 3.10 for the correlated dual diversity channels (L=2) of the RS and BCH coded MC-AFEC systems, respectively.

Computer simulation has also been carried out for the purpose of evaluating the BER of the MC-AFEC systems for higher L. For this objective, correlated vectors of Rayleigh r.v. has to be generated. In this work, the decomposing technique proposed in [35] is adopted. This technique is suitable for efficient generation of correlated Nakagami-m fading vectors. In the following lines, this technique is described briefly without proofs. For detailed analysis, the interested reader may refer to [35].

The technique in [35] is trying to solve the problem of how to generate an L-by-1 correlated Nakagami vector with fading parameter m and covariance matrix R_z fro independent Gaussian vectors. Let us define the notations:

$$\begin{aligned}\boldsymbol{x} &\sim N(\boldsymbol{o},\boldsymbol{R}_x)\\ \boldsymbol{y} &\sim GM(m,\boldsymbol{R}_y)\\ \boldsymbol{z} &\sim NK(m,\boldsymbol{R}_z)\end{aligned}$$

which indicate the vectors $\boldsymbol{x}$, $\boldsymbol{y}$, and $\boldsymbol{z}$ follow a joint normal (Gaussian), Gamma, and Nakagami distribution, respectively. The Gaussian process has zero mean, and the fading parameter for Gamma and Nakagami is m. $\boldsymbol{R_x}$, $\boldsymbol{R_y}$ and $\boldsymbol{R_z}$ correspond to the covariance matrix of the noted distributions. As a convention, $R(i,j)$ denotes the $(i,j)^{\text{th}}$ element of $\boldsymbol{R}$ and $\boldsymbol{x}^{\odot r}$ denotes the vector obtained by taking the power of r of each elements of $\boldsymbol{x}$; that is

$$\boldsymbol{x}^{\odot r} \triangleq [x_1^r, x_2^r, \ldots x_L^r]^T \tag{3.10}$$

where, T denotes transposition.

This technique involves a conversion from a set of independent Gaussian vectors to a set of correlated Gaussian vectors and a conversion from correlated Gaussian vectors to gamma vector then to Nakagami vector. This process is illustrated graphically below,

$$\boldsymbol{e}_k \xrightarrow{\boldsymbol{D}} \boldsymbol{x}_k \xrightarrow{\sum_{k=1}^{2m}(\cdot)^{\odot r}} \boldsymbol{y} \xrightarrow{(\cdot)^{\odot(1/2)}} \boldsymbol{z} \tag{3.11}$$

where, $\boldsymbol{e_k}$ is the k^{th} independent identically distributed (iid) Gaussian sequence with zero mean and unit variance; that is $e_k \sim N(\boldsymbol{o}, \boldsymbol{I})$, where, $\boldsymbol{I}$ is the identity matrix. The symbol $\boldsymbol{D}$ in the relation (3.11) is the coloring matrix decomposed from $\boldsymbol{R_x}$ using Cholesky decomposition; that is

$$\boldsymbol{R}_x = \boldsymbol{D}\,\boldsymbol{D}^* \tag{3.12}$$

with * denotes the Hermitian transposition. Next, the correlated Gaussian sequence $\boldsymbol{x_k}$ of covariance matrix $\boldsymbol{R_x}$ can be generated by

$$\boldsymbol{x}_k = \boldsymbol{D}\,\boldsymbol{e}_k \tag{3.13}$$

and consequently the Gamma and the Nakagami distribution can be generated using the following two equations, respectively:

$$y = \sum_{k=1}^{2m} x_k^{\odot 2} \tag{3.14}$$

$$z = y^{\odot(1/2)} = \left(\sum_{k=1}^{2m} x_k^{\odot 2} \right)^{\odot(1/2)} \tag{3.15}$$

The problem now is how to get $\boldsymbol{R_x}$, and hence $\boldsymbol{D}$ from $\boldsymbol{R_z}$. Following are the steps needed to get the value of $\boldsymbol{D}$:

1. Identify $\boldsymbol{R_z}$. For a given $\boldsymbol{R_z}$, the associated correlation coefficient equals

$$\rho(i,j) = R_z(i,j)[R_z(i,i)R_z(j,j)]^{-1/2} \tag{3.16}$$

2. Obtain the cross correlation of $\boldsymbol{y}$ $v(i,j)$ that is defined by

$$v(i,j) = R_y(i,j)[R_y(i,i)R_y(j,j)]^{-1/2} \tag{3.17}$$

To simplify the notations, the indices of $\rho(i,j)$ and $v(i,j)$ will be dropped and we will use ρ and v, respectively. The method of Newten-Raphson is used for finding the value of v that employs an iterative technique using the following equation,

$$v_{i+1} = v_i - \frac{f(v)}{\dot{f}(v)} \tag{3.18}$$

with the initial value $v_0 = \rho$ and with $f(v)$ defined as

$$f(v) \triangleq \varphi(m,1)\left\{ {}_2F_1\left(-\frac{1}{2},-\frac{1}{2};m;v\right)-1\right\}-\rho \tag{3.19}$$

and $\dot{f}(v)$ is the derivative of $f(v)$ is given by

$$\dot{f}(v) = \frac{\varphi(m,1)}{4m}\left\{ {}_2F_1\left(\frac{1}{2},\frac{1}{2};m+1;v\right)\right\} \tag{3.20}$$

where

$$\varphi(a,b) = \frac{\Gamma^2\left(a+\frac{b}{2}\right)}{\Gamma(a)\Gamma(a+b)-\Gamma^2\left(a+\frac{b}{2}\right)} \tag{3.21}$$

and the hyper geometric function is defined as

$${}_2F_1(a,b;c;z) = \sum_{n=0}^{\infty}\frac{(a)_n(b)_n}{(c)_n}\frac{z^n}{n!} \tag{3.22}$$

with $(a)_n = a\,(a+1)\ldots(a+n-1)$ and $(a)_0 = 1$.

3. Determine the covariance matrix $\boldsymbol{R_x}$ of the correlated Gaussian vectors $\boldsymbol{x_k}$'s using the following equation:

$$R_x(i,j) = \begin{cases} \xi R_z(i,i) \\ \xi\{R_z(i,i)R_z(j,j)v(i,j)\}^{1/2} \end{cases}$$

where (3.23)

$$\xi = \frac{1}{2m}\left[1 - \frac{1}{m}\frac{\Gamma^2\left(m+\frac{1}{2}\right)}{\Gamma^2(m)}\right]^{-1}$$

4. Determine the coloring matrix ***D*** by the method of Cholesky decomposition using Equation (3.12).

5. Apply Equation (3.15) to get the desired Nakagami vector ***z***. It should be noted that this step is valid for integer *m* only. For non-integer *m*, an extra step is needed before this step [35].

In our work, a Rayleigh vector is needed with the same constant correlation over all channels. To use the described technique for generating correlated vectors, one may set the parameter *m* to 1. The results are generated assuming that the correlation matrix $\boldsymbol{C}_z$ equals

$$C_z = \begin{pmatrix} 1 & \rho & \cdots & \rho \\ \rho & 1 & & \vdots \\ \vdots & & \ddots & \rho \\ \rho & \cdots & \rho & 1 \end{pmatrix} \quad (3.24)$$

Figures 3.9 and 3.10 show the BER of MC-AFEC for both RS coding and BCH coding, respectively, compared to SC, with correlated branches perturbed by Rayleigh

fading. Consider the case of L =2 in both figures. It can be noticed that the results of simulation are close to the numerical results. It is expected that the performance of the systems degrades when the channels are correlated. For the RS coded MC-AFEC and with a correlation coefficient ρ= 0.5, a reduction of about 1 dB is noticed in the performance. For ρ = 0.7 and 0.9 the performance drops by more than 2.5 dB and 5 dB, respectively. Similar observations can be noted about the BCH coded MC-AFEC and SC.

As another example, consider the case of L=3. The following observations are presented for the RS-coded MC-AFEC system, and they are valid for the other two systems with minor variations. In these figures, more reduction can be observed as compared to L = 2; for instance, about 2 dB inferiority is noticed when ρ = 0.5, compared to the uncorrelated case. If ρ increased to be 0.7 and 0.9 the system's performance drops by about 3.9 dB and 7.8 dB respectively.

All systems become even more sensitive to correlation when the number of channels increased to 4. Consider the RS coded MC-AFEC systems with L = 4 correlated Rayleigh channels. When ρ = 0.5, more than 2.5 dB reduction in the performance is introduced compared to the case of uncorrelated channels. The reduction increased to about 4.4 dB for the case of ρ=0.7 and more than 9 dB when ρ=0.9.

It is clear from the above observations that higher correlation defeats the purpose of diversity. Because larger L yields more diversity gain as compared to lower L, it is intuitive that the larger L, the more the system sensitivity to correlation.

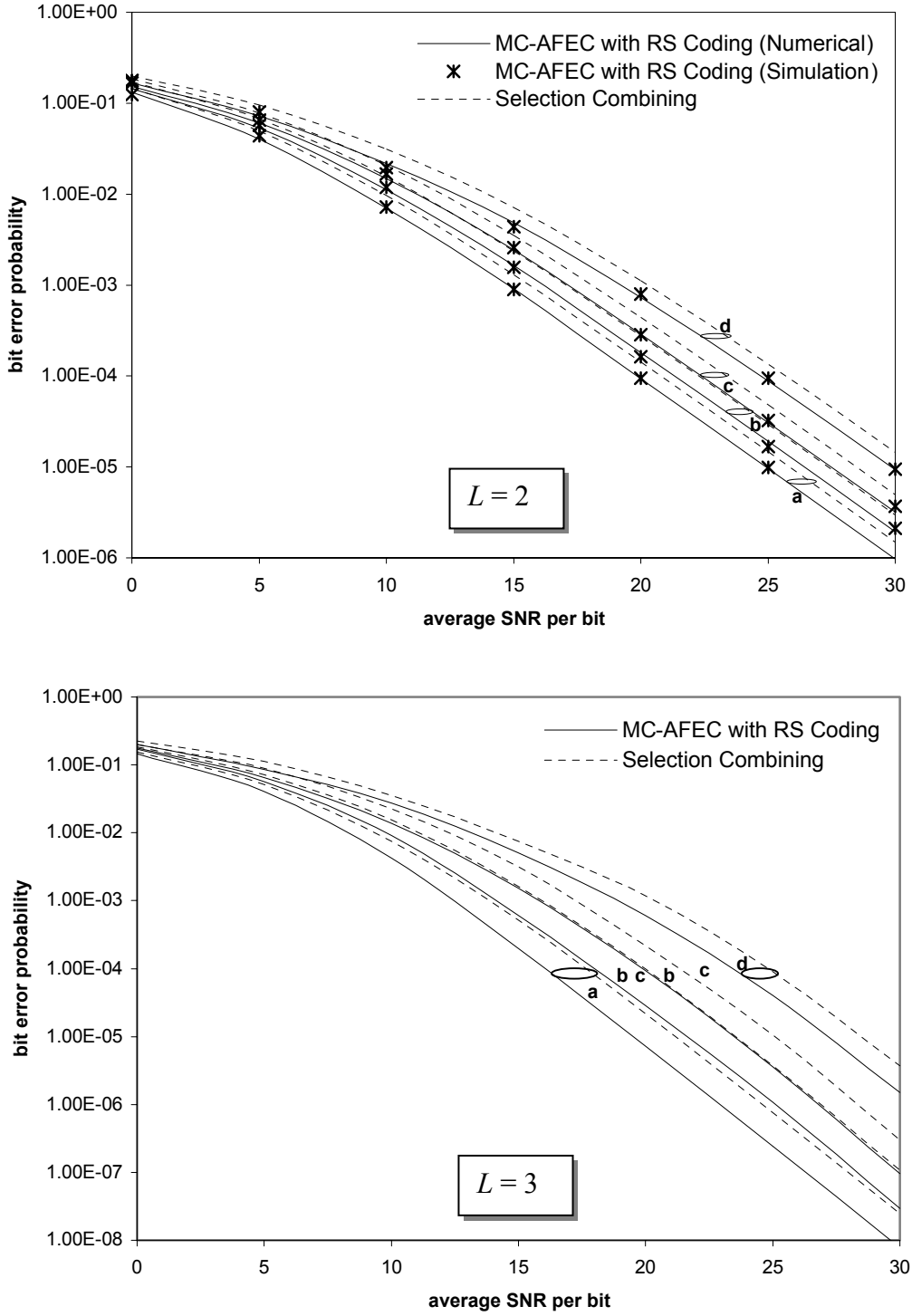

Figure 3.9: The effect of correlation on the performance of the RS-coded MC-AFEC compared to Selective Combing diversity with (a) $\rho = 0$, (b) $\rho = 0.5$, (c) $\rho = 0.7$ and (d) $\rho = 0.9$.

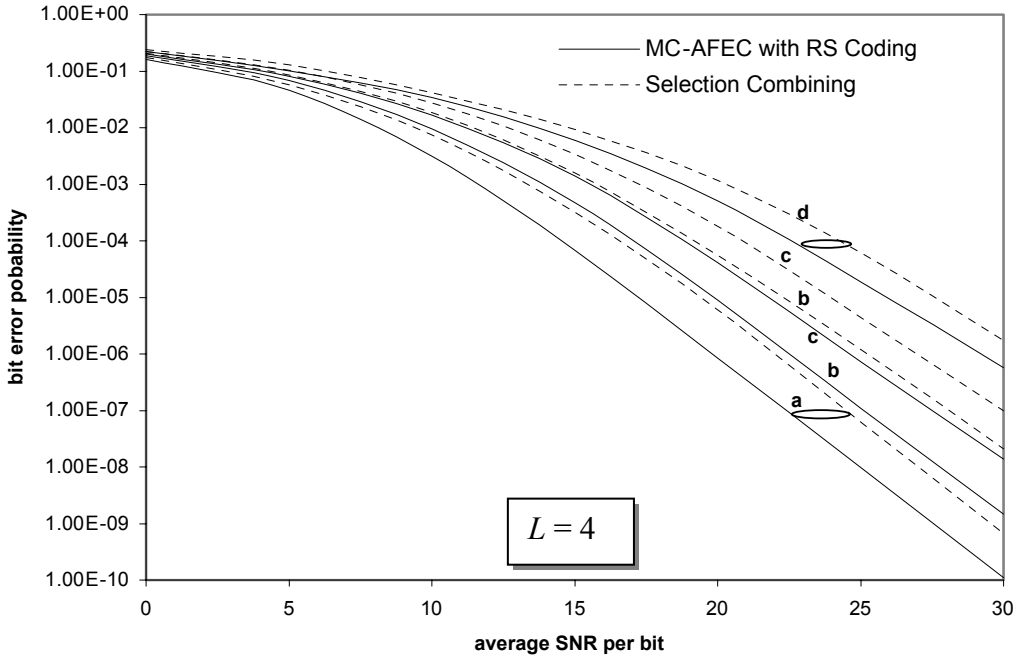

Figure 3.9: (Continued)

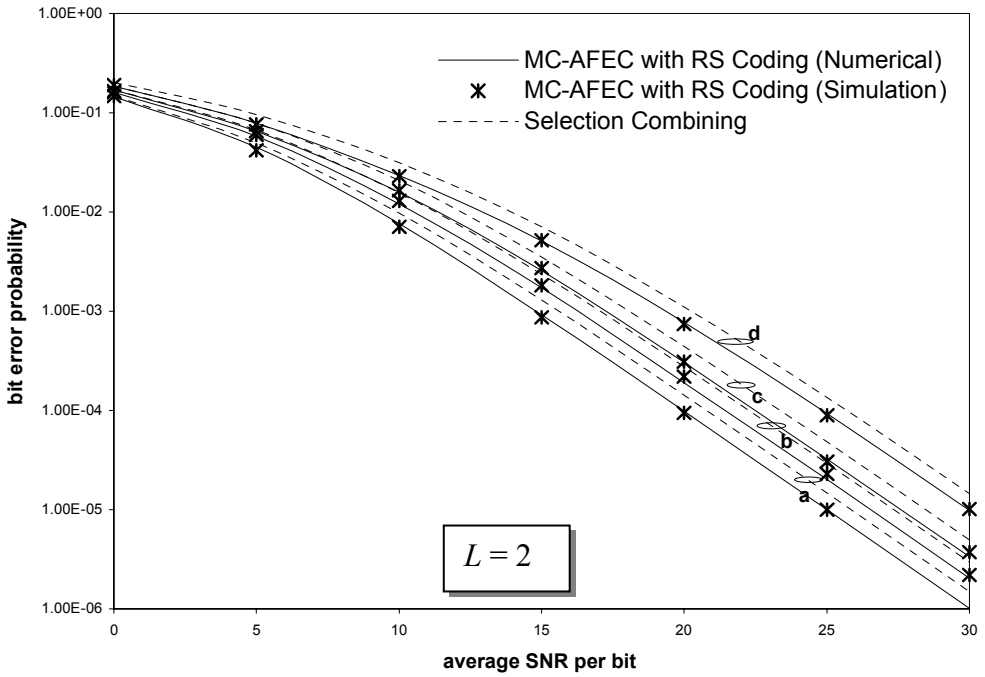

Figure 3.10: The effect of correlation on the performance of the BCH-coded MC-AFEC compared to Selective Combing diversity with (a) $\rho = 0$, (b) $\rho = 0.5$, (c) $\rho = 0.7$ and (d) $\rho = 0.9$.

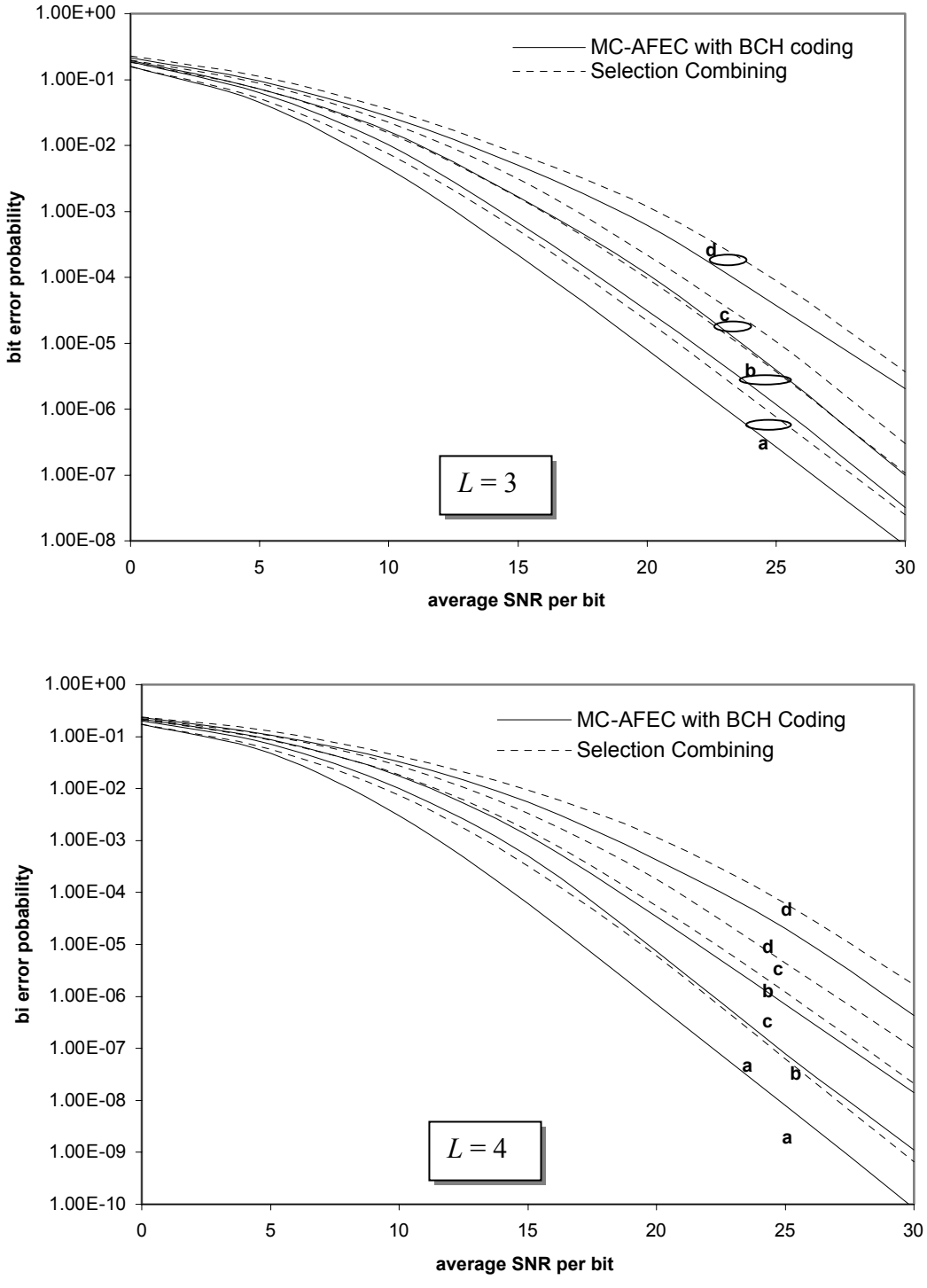

Figure 3.10: (Continued)

3.4 The Impact of Outdated Channel Estimates

In the previous sections, it has been assumed that the Channel State information CSI provides perfect estimates of the channel's SNR. However, in practice these estimates must be delivered in the presence of noise and time delay. As we stated earlier, with 8 code sets, only 3 bits are needed to be transmitted over the feedback channels. Thus, a strong coding can be applied which may validate the assumption of noiseless estimates [32]. However, time delay may not be avoided; hence, the impact of outdated channel estimates on the performance is studied in this section. With a delay of duration of 1 block transmission, the BER behavior of the RS and BCH coded MC-AFEC system will be compared with the SC through computer simulation.

In order to simulate the behavior of the system under outdated CSI, the correlation between fading samples should be considered. We will assume that the auto-correlation of the generated fading coefficients follow the Bessel function J_0 given by:

$$R(\tau) = J_0(2\pi f_D \tau) \tag{3.25}$$

All Jake's-like fading generators are designed around this auto correlation behavior. Jake's method has earned considerable popularity. In addition to its simplicity, it is computationally attractive. However, the original algorithm by Jake [41] has a problem with persistence correlation between generators. A Jake's-like fading generator has been presented in [40], which solves this problem and still has good statistical behavior: it

approximates the complex Gaussian random process very well, it is wide-sense stationary and uncorrelated generators can be created easily.

This generator assumes N_s scatterars equi-spaced in azimuth around the mobile (their distance is irrelevant). All scattered signals have the same amplitude but with random phases ϕ_i . It is also assumed that the mobile is translated a distance *x*, the angle of each scatterer *i* is θ_i with respect to the direction of movement. Under these assumptions the complex gain can be written as

$$g(t) = \frac{1}{\sqrt{N_s}} \sum_{i=0}^{N_s-1} \exp\left[j \left[\phi_i + \omega_i t \right] \right] \qquad (3.26)$$

where $\omega_i = 2\pi f_D \cos(\theta_i)$. A computationally efficient form of complex gain generator equivalent to (3.26) is given by,

$$g(u) = \frac{1}{\sqrt{N_s}} \sum_{i=0}^{N_s-1} \exp\left[G_i + uG_{i+N_s} \right] \qquad (3.27)$$

where $u = x / \lambda = f_D t$ (λ is the wave length and f_D is the Doppler frequency), and $\boldsymbol{G}$ is a vector contains the state variables of the generator: the first half of $\boldsymbol{G}$ holds the randomized phases ϕ_n , and the second holds the Doppler shifts, also randomized by the selection of the first arrival angle θ_0 . The vector $\boldsymbol{G}$ is initialized using the algorithm given in Figure 3.11 [40].

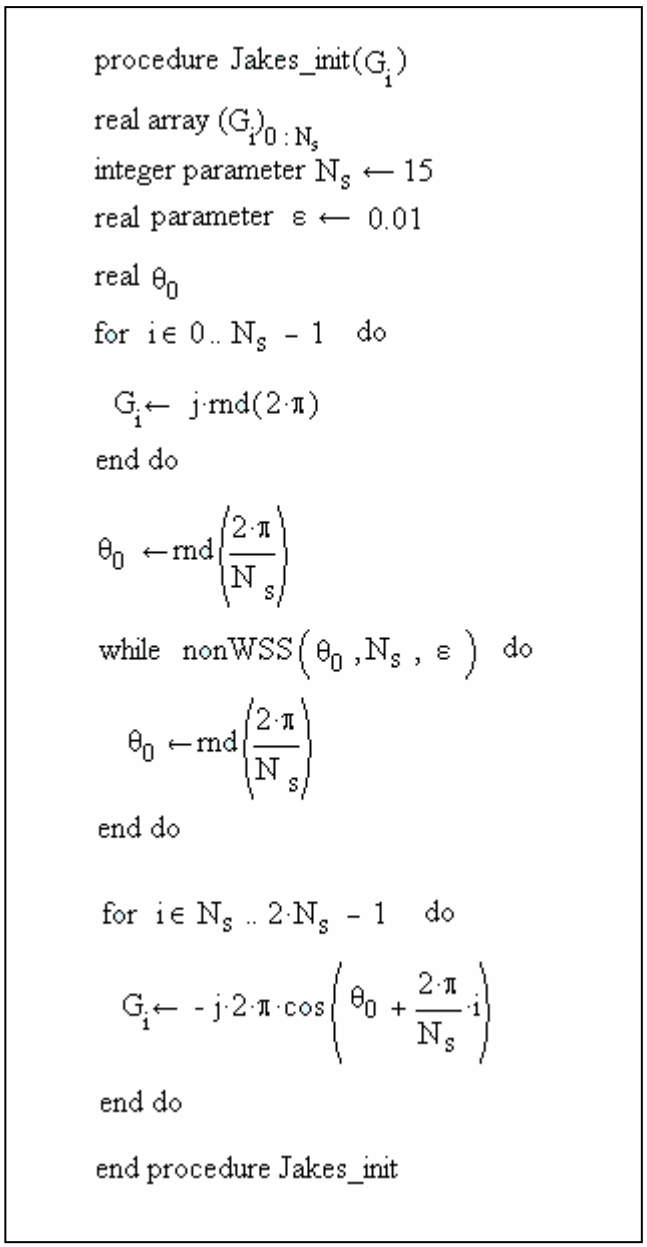

Figure 3.11: Algorithm of generating ***G***, the state variables of the Jakes-like generator.

This algorithm uses the function nonWSS to check if the initialized θ_0 generates a non-WSS behavior or not. Two conditions are examined for this purpose; if these

conditions are satisfied, this value of θ_0 is accepted. Otherwise, the algorithm needs to regenerate another value of θ_0. The conditions are [40]:

- The number of scatters N_s must be odd.
- No arrival angle equals to $\pi/2$ or $-\pi/2$.

The nonWSS($\theta_0, N_s, \varepsilon$) procedure does these checks (ε is a threshold for the "closeness" to the non-WSS behavior). This procedure is illustrated in Figure 3.12 and it will return 1 if it is close to the non-WSS behavior and 0 if not.

```
procedure nonWSS(θ0, Ns, ε)
integer Ns, i, flag
real θ, θ0, ε
flag ← 0
flag ← 1 if mod(Ns, 2) = 0
for i ∈ 0 .. Ns - 1 do
    θ ← θ0 + (2·π / Ns)·i
    flag ← 1 if |θ - π/2| < ε
    flag ← 1 if |θ + π/2| < ε
end do
end procedure nonWSS
```

Figure 3.12: Procedure to check for the WSS behavior of the Jake's-like generator.

We would like to make sure that our fading generators are uncorrelated. The method is simple: give the different generators different values of first angle θ_0. To prove that, let's define the process:

$$g1(t) = \frac{1}{\sqrt{N_s}} \cdot \sum_{i=0}^{N_s-1} \exp\left[j \cdot \left(\phi 1_i + \omega 1_i \cdot t\right)\right]$$

$$g2(t) = \frac{1}{\sqrt{N_s}} \cdot \sum_{i=0}^{N_s-1} \exp\left[j \cdot \left(\phi 2_i + \omega 2_i \cdot t\right)\right]$$

Their cross-correlation must be zero which is given by

$$\begin{aligned} \mathrm{Avg}_t\left(g1(t) \cdot \overline{g2(t-\tau)}\right) &= \frac{1}{N_s} \cdot \sum_{i=0}^{N_s-1} \sum_{k=0}^{N_s-1} e^{j \cdot \left(\phi 1_i - \phi 2_k\right)} \cdot \mathrm{Avg}_t\left[e^{j \cdot \omega_i \cdot t} \cdot e^{-j \cdot \omega_k \cdot (t-\tau)}\right] \\ &= \frac{1}{N_s} \cdot \sum_{i=0}^{N_s-1} \sum_{k=0}^{N_s-1} e^{j \cdot \left(\phi 1_i - \phi 2_k\right)} \cdot e^{j \cdot \omega_k} \cdot \mathrm{Avg}_t\left[e^{-j \cdot \left(\omega_k - \omega_i\right) \cdot t}\right] \end{aligned} \tag{3.28}$$

If the Doppler shifts ω_i and ω_k are all different, then the average is zero, as wanted. These Doppler shifts are dependent on the offset arrival angles. According to the algorithm, these angels are in the range $0 \le \theta 1_0, \theta 2_0 < \frac{2\pi}{N_s}$, and in order to have the Doppler shifts all different, we simply need to ensure that $\theta 1_0 \neq \theta 2_0$. In other words we have to make sure that the two angles are not too close together and this can be generalized to any pair of fading generators.

In broad terms, the time variability of a flat fading wireless channel depends on the relative velocity between transmitter and receiver or moving scatterers in the environment, with respect to the transmission rate. A common way to quantify this is to refer to the Doppler rate f_DT, which is defined as the product of the maximum Doppler frequency shift f_D experienced by a mobile receiver and the transmission symbol period T. Lower Doppler rates lead to slower varying channels, where the time correlation between successive channel gains is larger.

In our work, L identical and uncorrelated Jake's-like generators have been used, with Ns = 15 and ε = 0.01 and with different values of Doppler rate, to study the effect of outdated channel estimates. Figures 3.13 to 3.16 show the performance of the MC_AFEC system assuming that the CSI is delayed by duration of transmission of one block. In these figures there are five curves. Curve A displays the performance for the MC-AFEC system undergoing no outdated CSI while the effect of outdated CSI with different Doppler rates is shown in Curves B, C and D. On the other hand, the effect of outdated CSI on selective combing is illustrated in curves E and F. See Table 3.1 in which the definition of these curves are presented.

For the case of L = 2, Figures 3.13 and 3.15 demonstrate the effect of Doppler rate on the performance of the RS and BCH coded MC-AFEC system, respectively, in the presence of outdated channel estimates. Considering Figure 3.13, it can be observed that as the Doppler rate increases, the BER increases as well. While the reduction in performance, at $\overline{\gamma} = 30\,\text{dB}$, doesn't exceed 0.25 dB when $f_DT = 0.375\text{x}10^{-4}$ (Curve B), it

became around 2 dB when $f_D T$ is increased to 0.15×10^{-3} (Curve C) and higher than 4 dB if $f_D T$ is increased further to 0.375×10^{-3} (Curve D).

Observing Figure 3.13, one can notice that the increase in BER becomes more significant as the SNR gets higher. In case B, this behavior is not clear since the reduction in the performance is not that much. However, this effect can be seen clearly in case C, where, with almost 0 dB reduction in the performance at $\overline{\gamma}$ below 10 dB, the reduction becomes about 2 dB at $\overline{\gamma}$ = 30 dB. The situation get worst in case D; with almost 0 dB when $\overline{\gamma}$ is below 5 dB, the performance degraded as $\overline{\gamma}$ increases to be more than 4 dB when $\overline{\gamma}$ reaches 30 dB.

The selective combing system performs better than the MC-AFEC system in the presence of outdated estimates. From Figure 3.13, with $f_D T = 0.375 \times 10^{-4}$ (Curve F) and $\overline{\gamma}$ =30dB, the reduction in BER is still insignificant. One can conclude that SC is more immune to outdated estimate. However, the BER in MC-AFEC is still lower than the SC in most cases. As in case B, the MC-AFEC performs better than SC at all values of $\overline{\gamma}$. In this case, the MC-AFEC system outperforms SC by about 1 dB when $\overline{\gamma}$ =30 dB. Moreover, the MC-AFEC still performs better than SC in case B, but only when $\overline{\gamma}$ is below 25 dB, and when $\overline{\gamma}$ is below 20 dB in case D. However, the MC-AFEC system gets worse than the SC when $\overline{\gamma}$ is greater than 25 dB in case C and it gets worst in case D. The same comments can be said about the BCH coded system (Figure 3.15).

In the same way, the performance of the MC-AFEC with L = 3 deteriorates more as the Doppler rate increases in the presence of outdated channel estimates (Figures 3.14

and 3.16). In Figure 3.14, the RS coded system shows a very small deterioration in the performance (about 0.5 dB at $\overline{\gamma}$ = 30 dB) when $f_D T$ is as small as 0.375×10^{-4} (Curve B). This deterioration is enlarged to be about 3 dB for $f_D T = 0.15 \times 10^{-3}$ (Curve C). For $f_D T = 0.375 \times 10^{-3}$ (Curve D), the performance gets worse by about 6 dB. Like the case of L = 2, with L = 3 the increase in BER became more intense as the SNR gets higher, and it is even more sensitive than the case of L = 2. For example, consider case C. While there is no increase in the BER over the case of no outdated estimates if $\overline{\gamma}$ is below 20 dB, it grows to be worse by over 3dB at $\overline{\gamma}$ = 30dB. As another example, consider case D where the deterioration increases by more than 6 dB when $\overline{\gamma}$ is as high as 30 dB. While, it gets better as $\overline{\gamma}$ decreases to be equivalent to the case of no outdated estimates when $\overline{\gamma}$ decreases below 10 dB.

Consistently, SC shows more immunity to the effect of outdated estimates than the MC-AFEC system when L = 3. It is clear from Figure 3.14 that the deterioration in the performance of SC system caused by the outdated estimation is insignificant compared to the MC-AFEC even at $f_D T = 0.375 \times 10^{-3}$. Eventhough, the MC-AFEC system shows a better performance in most times specially at low $\overline{\gamma}$. Consider, for instance, case C, the system performs better than SC when $\overline{\gamma}$ is less than 28 dB and when $\overline{\gamma}$ is less than 21 dB in case D. However, in case B, the MC-AFEC shows a better performance at all values of $\overline{\gamma}$ to be about 2 dB better than SC at $\overline{\gamma}$ =30 dB. On the other hand, SC performs better than the MC-AFEC in the cases C and D at a very high $\overline{\gamma}$ as in the case of $\overline{\gamma}$ =30, where SC outperforms the MC-AFEC system by 0.7 dB and

3.4 dB, respectively. The same observations can be noted about the BCH-coded MC-AFEC system (Figure 3.16).

In short, the impact of outdated CSI on the performance is dependent on the values of f_DT and $\overline{\gamma}$. For smaller f_DT, the effect is less significant, but as f_DT increases the sensitivity to the outdated CSI increases as well. Similarly, at low $\overline{\gamma}$ the impact is very low while it becomes more intense as $\overline{\gamma}$ increases. On the other hand, SC shows more immunity to the outdated CSI, and its superiority appears at high $\overline{\gamma}$.

We conclude this section be answering two questions. The first question, is why does the increase of Doppler rate lead to a worse performance in the presence of outdated estimates? And the second is why the situation gets worse as the SNR gets higher? To answer the first question recall the autocorrelation function in Equation (3.25), sketched in Figure 3.17. In this figure, the autocorrelation function is drawn for the three values of f_D's: 10, 40 and 100 Hz. It is clear from the figure that as f_D increases the auto correlation function decays faster; thus, the correlation between fading samples decreases as f_D increases. As a result, when f_D gets smaller, the correlation between the actual (new) $\overline{\gamma}$ and its outdated estimate gets higher; hence the deterioration in the performance is minimal. However, when f_D is high, the correlation between the new $\overline{\gamma}$ and its estimate will be low; and hence an erroneous estimation may occur which result in a more degradation in the performance.

The answer of the second question is some how harder to explain. However, let's try to answer it from the concept of deep fade. As explained earlier, when one or more

channels has/have a very low instantaneous SNR (or in deep fade), the system tries to avoid that/those bad channels; that is, the system will use the ON/OFF code set. On the other hand, if all channels are in good conditions (high SNR), the system tries to utilize all channels with moderate coding.

Now, when the system has a low $\bar{\gamma}$, it will have the instantaneous SNR being low with a high probability, which means that the system will use the ON/OFF code set with a high probability. Using ON/OFF code set is equivalent to SC system where both systems are ignoring the bad channel and utilizing the good channel without employing any coding. With such code set, and with the strong correlation between fading samples, the switching between deep fade to good condition in the bad channel or from good condition to deep fade in the good channel is improbable. In addition, the influence of that switching on the performance is minimal. Hence, the degradation in the performance at low $\bar{\gamma}$ is insignificant.

On the other hand, if the system operates at high $\bar{\gamma}$, it means that the system is utilizing all channels with moderate coding with high probability. If the system is using all channels for transmission and the system is being in a deep fade, there will be errors for sure even though the occurrence of deep fades has a very low probability. The influence of these errors on the performance is significance at high $\bar{\gamma}$; hence, the degradation of the performance is large at high $\bar{\gamma}$.

Curve	System	Doppler rate (f_DT)
A	MC-AFEC (no outdated CSI)	$0.375\text{x}10^{-3}$
B	MC-AFEC	$0.375\text{x}10^{-4}$
C	MC-AFEC	$0.15\text{x}10^{-3}$
D	MC-AFEC	$0.375\text{x}10^{-3}$
E	SC (no outdated CSI)	$0.375\text{x}10^{-3}$
F	SC	$0.375\text{x}10^{-3}$

Table 3.1 Representation of the curves used in Figures 3.13 to 3.16.

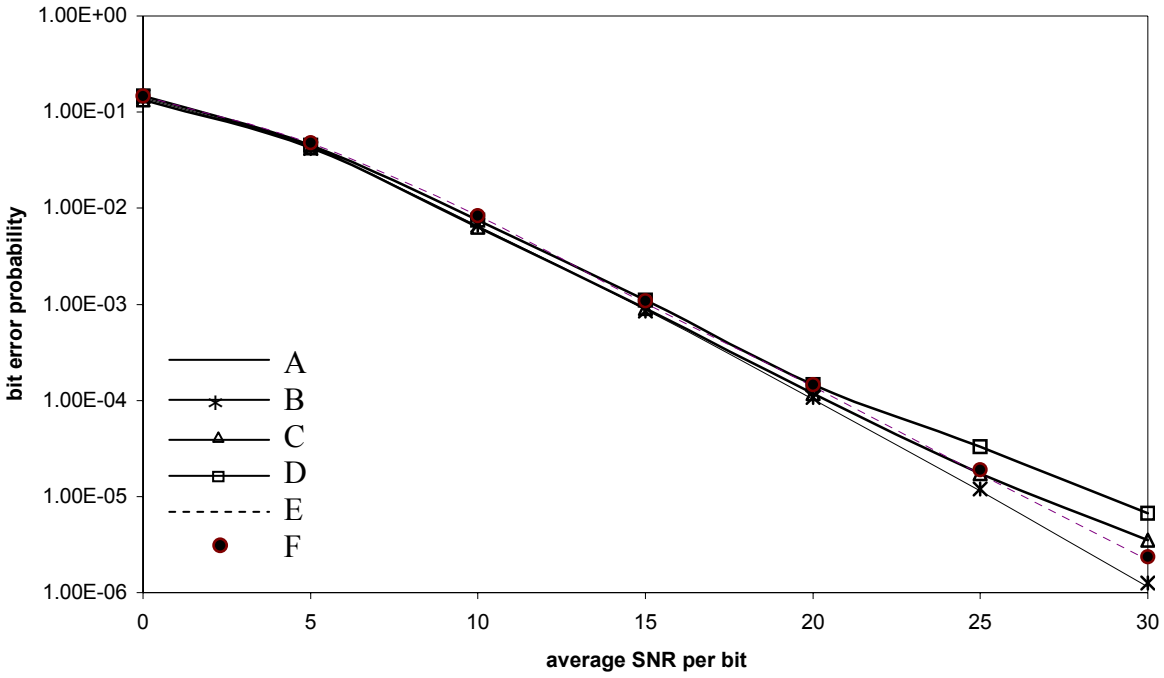

Figure 3.13: The effect of outdated CSI on the performance of the RS-coded MC-AFEC compared to SC over $L = 2$ channels modeled by Jakes like fading model.

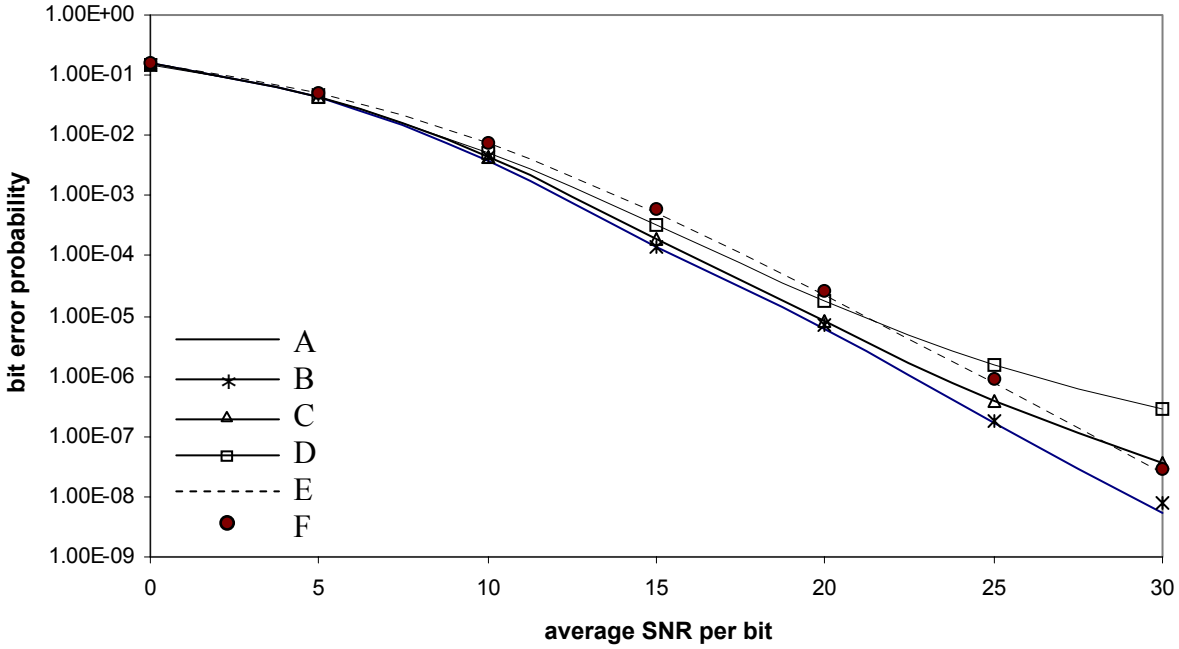

Figure 3.14: The effect of outdated CSI on the performance of the RS-coded MC-AFEC compared to SC over $L = 3$ channels modeled by Jakes like fading model.

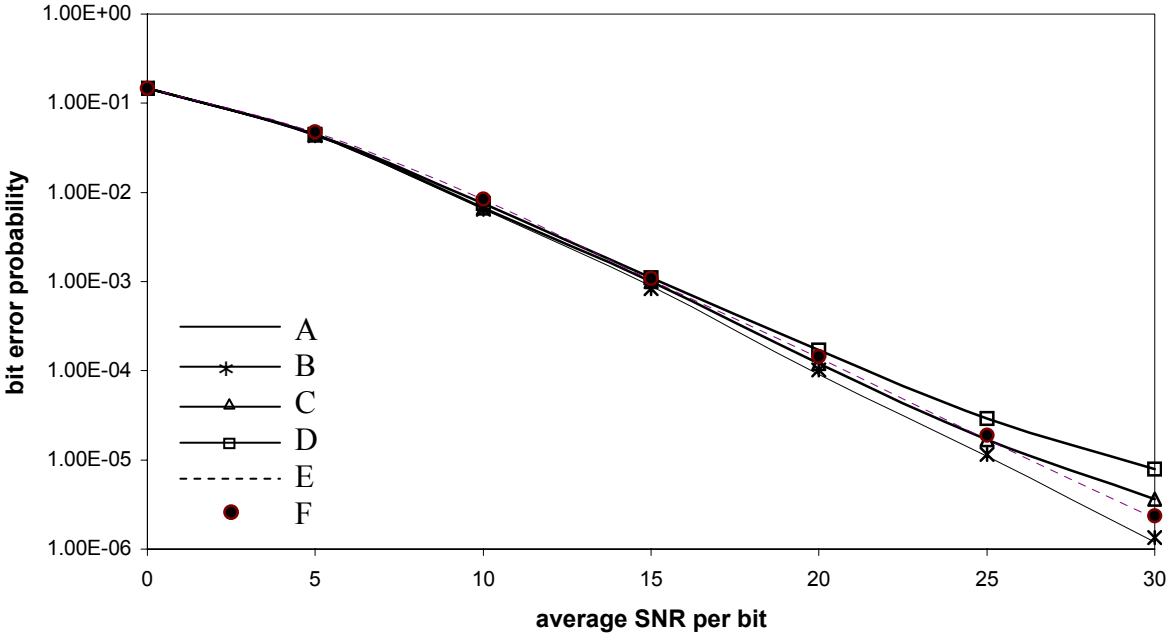

Figure 3.15: The effect of outdated CSI on the performance of the BCH-coded MC-AFEC compared to SC over $L = 2$ channels modeled by Jakes like fading model.

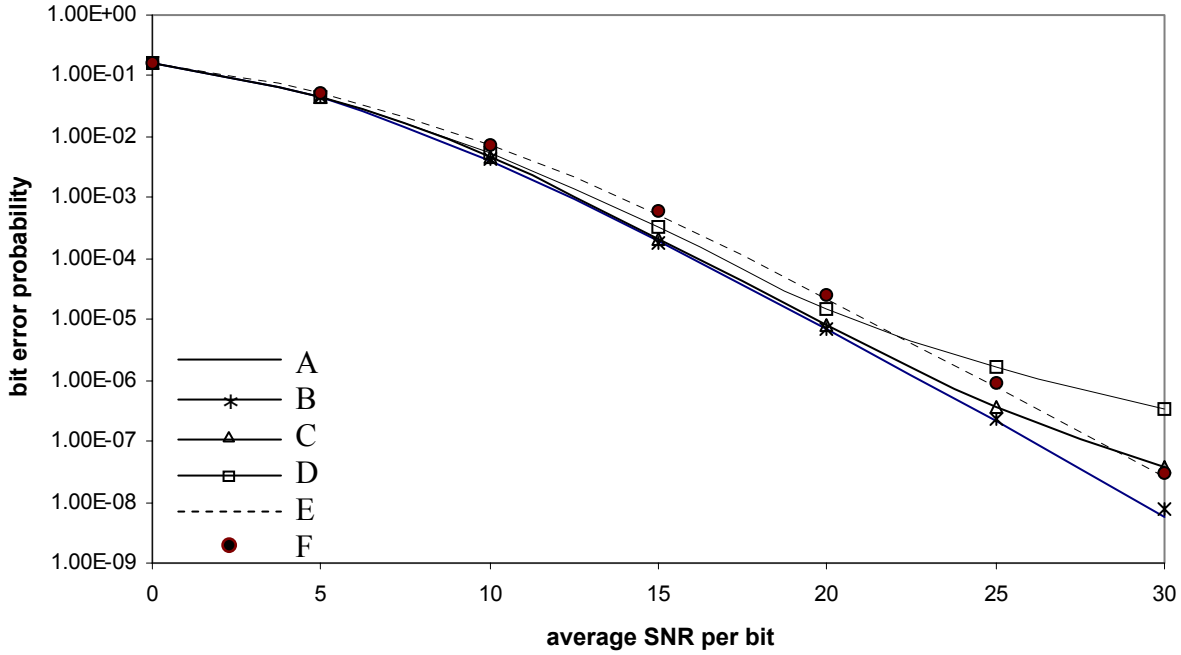

Figure 3.16: The effect of outdated CSI on the performance of the BCH-coded MC-AFEC compared to SC over $L = 3$ channels modeled by Jakes like fading model.

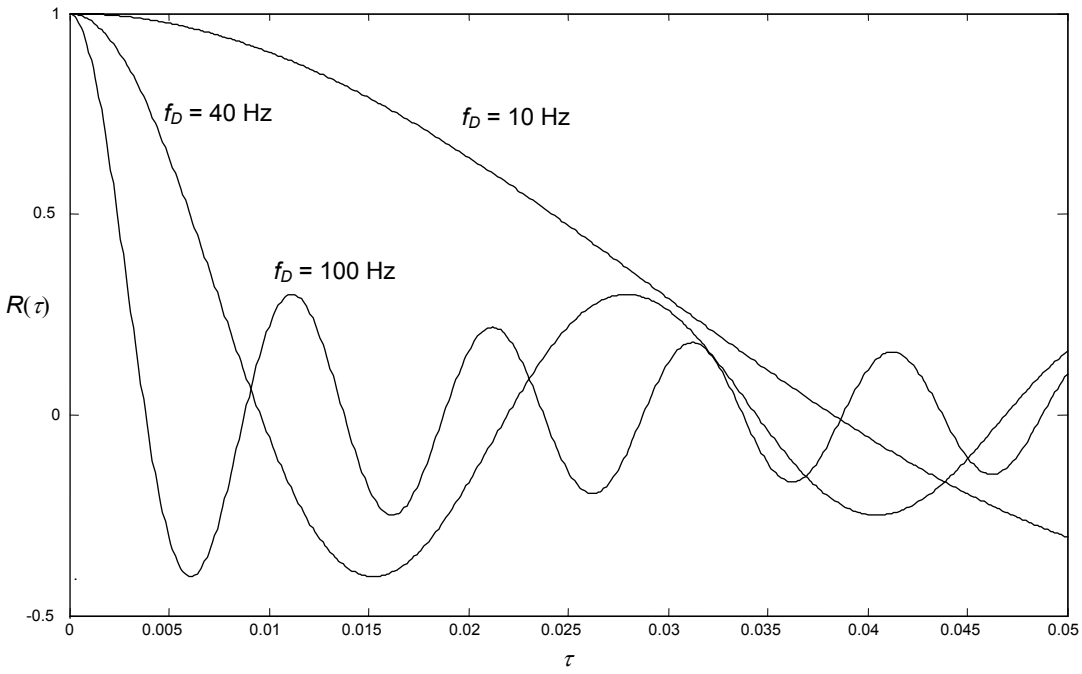

Figure 3.17: The auto correlation function $R(\tau) = J_0(2\pi f_D \tau)$ for different values of f_D.

3.5 Effect of fading severity

In this section, the effect of fading severity on the performance of the MC-AFEC will be investigated. For this purpose, the amount of fading (AF), or "fading figure", will be adopted. This term is associated with the fading pdf and it is defined by:

$$\mathrm{AF} = \frac{\mathrm{var}(\alpha^2)}{(\mathrm{E}(\alpha^2))^2} = \frac{\mathrm{E}(\gamma^2) - (\mathrm{E}(\gamma))^2}{(\mathrm{E}(\gamma))^2} \tag{3.29}$$

with E(.) denoting the statistical average and var(.) denoting variance. This term was introduced by Charash [39] as a unified measure of the severity of fading [3].

For the purpose of this study, the Nakagami-*m* fading model is utilized to examine the behavior of the MC-AFEC with different amounts of fading AF. The Nakagami-*m* distribution is given by

$$p_\alpha(\alpha) = \frac{2m^m \alpha^{2m-1}}{\Omega^m \Gamma(m)} \exp\left(-\frac{m\alpha^2}{\Omega}\right), \qquad \alpha \geq 0 \tag{3.30}$$

where *m* is the Nakagami-*m* fading parameter which ranges from 1/2 to ∞. Applying Equation (2.1) shows that the SNR per symbol, γ, is distributed according to the gamma distribution given by

$$p_\gamma(\gamma) = \frac{m^m \gamma^{m-1}}{\bar{\gamma}^m \Gamma(m)} \exp\left(-\frac{m\gamma}{\bar{\gamma}}\right), \qquad \gamma \geq 0 \tag{3.31}$$

The Nakagami-*m* distribution typically agrees with experimental data of land-mobile and indoor-mobile multipath propagation [3].

To calculate AF for the Nakagami-*m* distribution, the averages in Equation (3.29) need to be calculated. The moments of γ are given by [3]:

$$E[\gamma^k] = \frac{\Gamma(m+k)}{\Gamma(m)m^k}\overline{\gamma}^k \tag{3.32}$$

From the above equation, the first two moments are

$$E[\gamma] = \overline{\gamma} \tag{3.33}$$

$$E[\gamma^2] = \frac{\Gamma(m+2)}{\Gamma(m)m^2}\overline{\gamma}^2 = \frac{(m+1)(m)\Gamma(m)}{\Gamma(m)m^2}\overline{\gamma}^2 = (1+\frac{1}{m})\overline{\gamma}^2 \tag{3.34}$$

Substitute Equations (3.33) and (3.34) in (3.29) to get AF for Nakagami-*m* fading, yielding after simplification,

$$\mathrm{AF} = \frac{1}{m} \tag{3.35}$$

The performance of the MC-AFEC system will be evaluated with different values of AF. This will be done by changing the fading parameter *m*. In this work, three AF values will be considered: 1, 1/2 and 1/4, for *m* = 1,2 and 4, respectively. For each value of *m* and *L*, $\overline{P}_b$ of the MC-AFEC system is compared with SC and MRC systems with the same *m* and *L*. The evaluation will be carried out using the numerical evaluation method described in Section 2.6 with the following assumptions:

- The channels are slow and non-selective.
- All the diversity channels are identical on the average; i.e., $\mathrm{E}\left[\left|\alpha_{\mathrm{i}}\right|^2\right]=1$.
- The diversity channels are independent.
- Perfect channel state information CSI is assumed. That means the estimates are noise free and no time delay is encountered.

Figures 3.18 to 3.23 demonstrate the behavior of $\overline{P}_b$ of the MC-AFEC systems with different number of channels. In each figure, there are three groups of curves, corresponding to three values of the fading parameter, namely, *m*= 1 (AF = 1), *m*= 2 (AF= 1/2), and *m*= 4 (AF= 1/4). The effect of fading severity is clearly seen in these figures; that is as AF decreases the performance shows a significant improvement. However, the MC-AFEC shows more improvement compared to the other systems.

Consider the case of *L* = 2 (Figure 3.18), the RS coded system shows an improvement of about 1.5 order of magnitude (from 9×10^{-5} to 4×10^{-7}) at $\overline{\gamma}=20\,\mathrm{dB}$ when AF is reduced from 1 to 1/2; (i.e. m is increased from 1 to 2). Four orders of magnitudes are observed when *m* is increased from 2 to 4. The same observations are valid when *L* =3 (Figure 3.19). In this case, it can be noticed that with the decrease of AF from 1 to 1/2, two order of magnitude reduction in $\overline{P}_b$ is observed and more than four order of magnitudes reduction if AF reduced from 1/2 to 1/4 at $\overline{\gamma}\simeq19\,\mathrm{dB}$.

For the case *L*=4, a significant reduction of $\overline{P}_b$ is also remarked as AF decreases. Reducing AF from 1 to 1/2 causes a reduction in $\overline{P}_b$ of about three orders of magnitudes

(from 2×10^{-5} to 2.7×10^{-8}) and about four order of magnitudes reduction is observed when the AF reduced from 1/2 to 1/4 at $\overline{\gamma} \simeq 17\,\text{dB}$. The same observations can be noted for the BCH coded system (Figures 3.21 to 3.23).

To compare the performance of the MC-AFEC system with the SC and MRC systems as the amount of fading AF changes, consider the Figures 3.15 to 3.23 again. For the case of L = 2, Figures 3.18 and 3.21 shows the behavior of RS coded system and BCH coded system, respectively. While the improvement in the RS coded system over the SC doesn't exceed 0.5 dB in the case of m=1, an improvement of about 1.4 dB is observed when m= 2 and more than 2dB in the case of m= 4 at $\overline{P}_b \simeq 2\times10^{-6}$. However, the RS coded system lags MRC by about 0.3 dB at $\overline{P}_b \simeq 2\times10^{-6}$. This inferiority is reduced as m increases. Accordingly, the reduction in performance is lowered to be less than 0.2 dB when m= 2. If m became higher, MC-AFEC tends to outperform MRC as in the case of m= 4, where the RS coded system are better than MRC by more than 0.3 dB.

The same observations can be remarked about the BCH coded system (Figure 3.21) with more improvements. For instance, at m = 2, the BCH system behaves almost as the MRC system with no considerable difference. More improvement can be noticed when m= 4, with more than 3.4 dB over the SC system and about 1.1 dB over MRC.

Figures 3.19 and 3.22 demonstrate the performance of the MC-AFEC system with the two coding techniques. From these figures, it can be observed that the system shows more improvement. For example at m= 1 (AF= 1), around 1.8 dB superiority is noticed compared to SC. Still the lag to MRC is noticed of about 0.9 dB. Again, the lag

is reduces as AF decreases to be about 0.5 dB in the case of AF= 1/2. As in the case of *L*= 2, when *m*= 4 (AF= 1/4), the RS coded system provide a better performance compared to MRC system with about 0.4 dB at $\overline{P}_b \simeq 1\times10^{-10}$ and much better compared to the SC system with more than 4 dB. Similarly, the BCH system shows a significant improvement especially in the case of AF= 1/2 and more at AF= 1/4. In the case of *m* = 2 (AF = 1/2), the system provides 3 dB improvement over the SC and it again matches the performance of the MRC system. In the same way, more improvement can be figured out at AF = 1/4, where the system provides about 0.7 dB over the MRC system and about 4.3 dB over SC.

The same observations is noticed in the case of *L* = 4 (Figures 3.20 and 3.23), with more improvement. For example, at *m* = 4, the RS coded MC-AFEC system is more than 4.5 dB better than the SC system and more than that for BCH coded system. In addition, it outperforms MRC by about 0.9 dB in the case of BCH coded system.

We can summarize our observation in the following:

- By decreasing AF, more improvement in $\overline{P}_b$ is noticed for all systems.
- In all cases, the MC-AFEC system outperforms SC, and the superiority of the MC-AFEC system increases with the decreases of AF.
- In most cases, MRC performs better than the MC-AFEC system. However, the inferiority of the MC-AFEC system decreases as AF decreases to the point that it outperforms MRC when AF= 1/4.

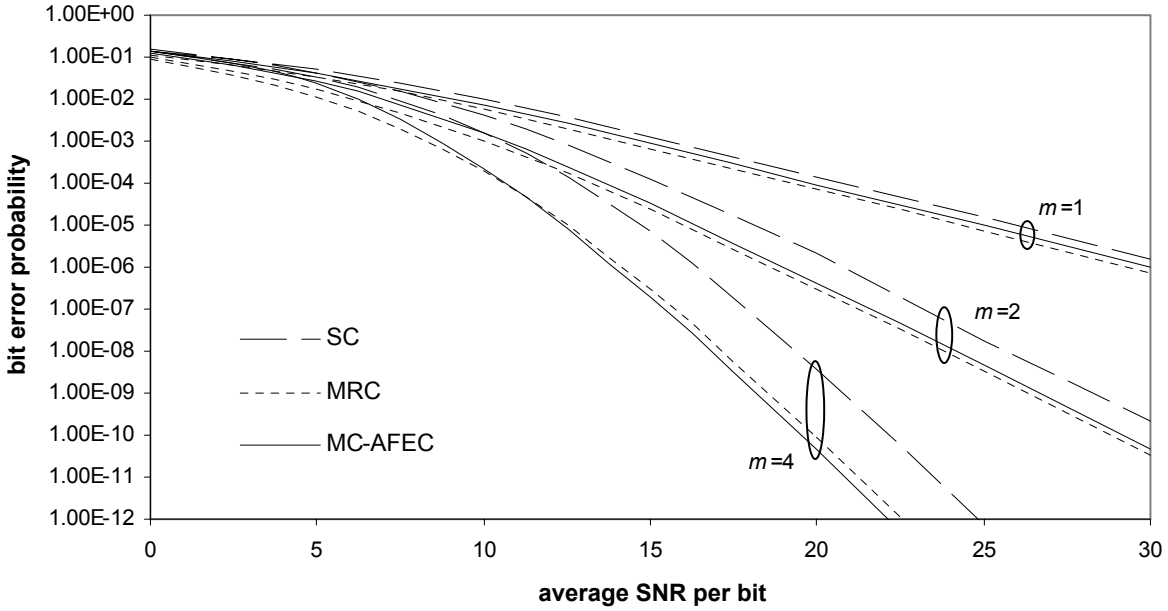

Figure 3.18: The performance of the RS-coded MC-AFEC system at R= 1/L compared to SC and MRC over L = 2 Nakagami fading channels with different values of m.

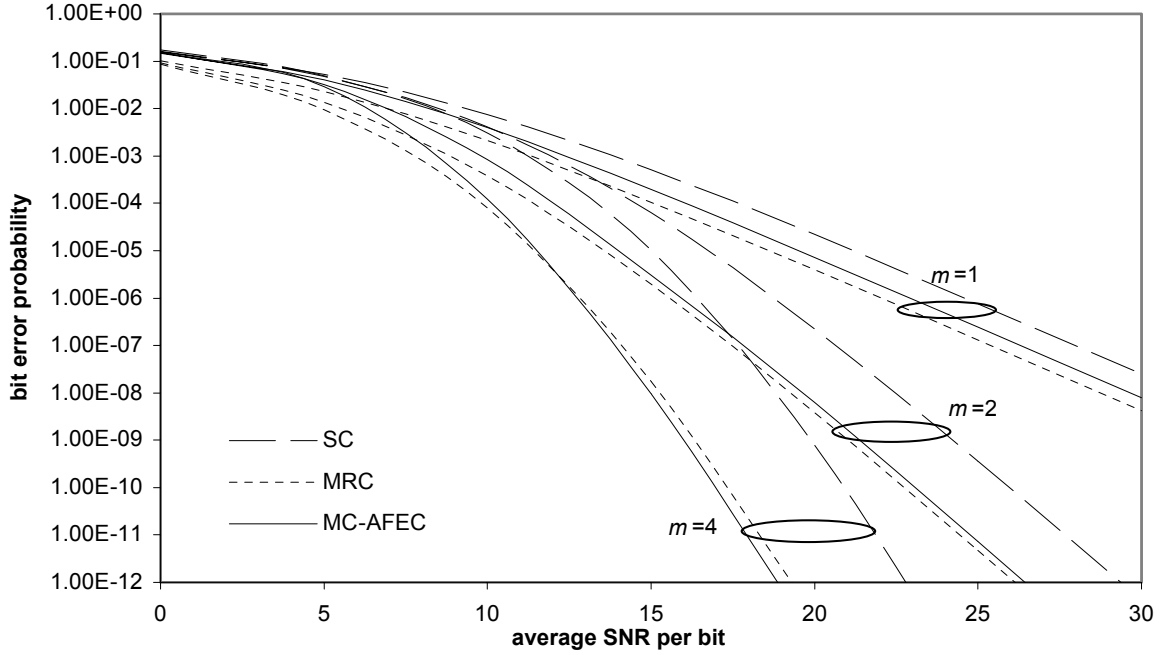

Figure 3.19: The performance of the RS-coded MC-AFEC system at R= 1/L compared to SC and MRC over L = 3 Nakagami fading channels with different values of m.

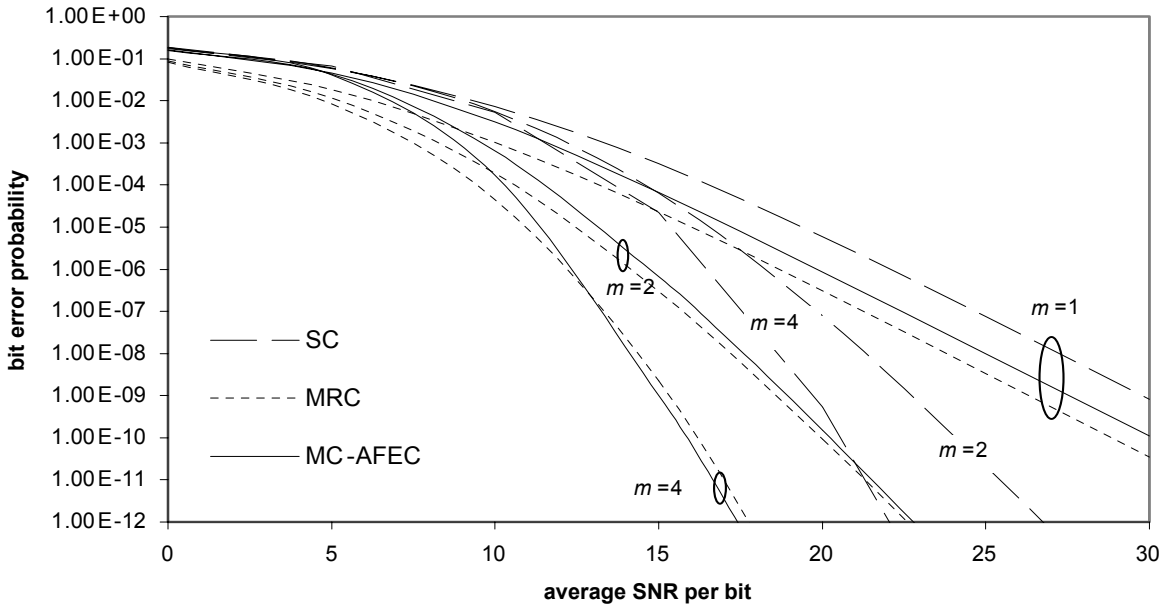

Figure 3.20: The performance of the RS-coded MC-AFEC system at R= 1/L compared to SC and MRC over L = 4 Nakagami fading channels with different values of m.

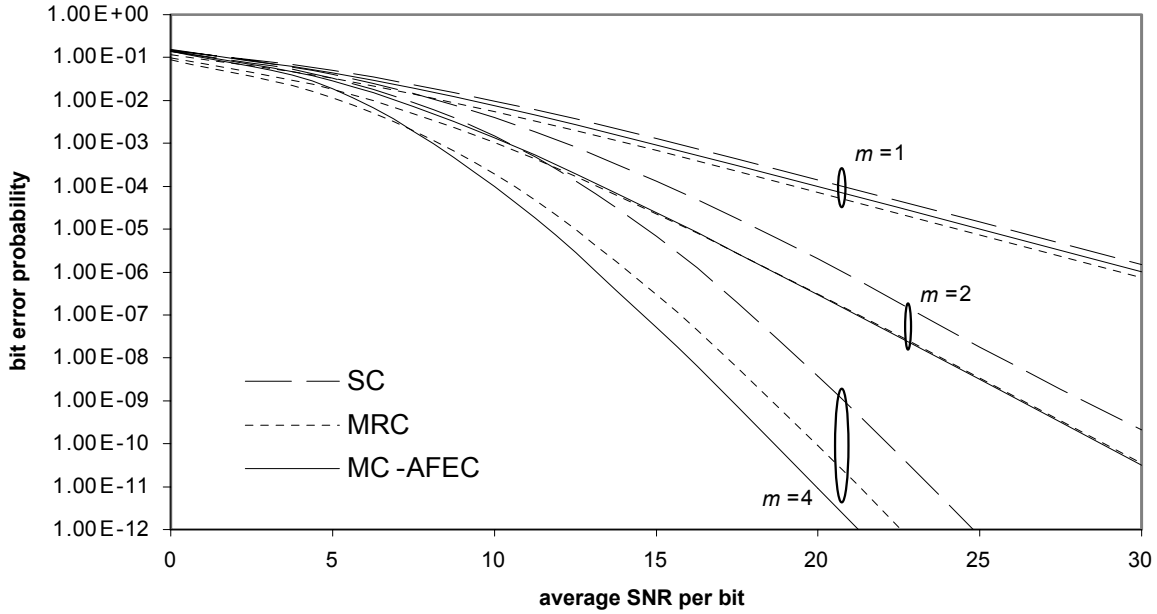

Figure 3.21: The performance of the BCH-coded MC-AFEC system at R= 1/L compared to SC and MRC over L = 2 Nakagami fading channels with different values of m.

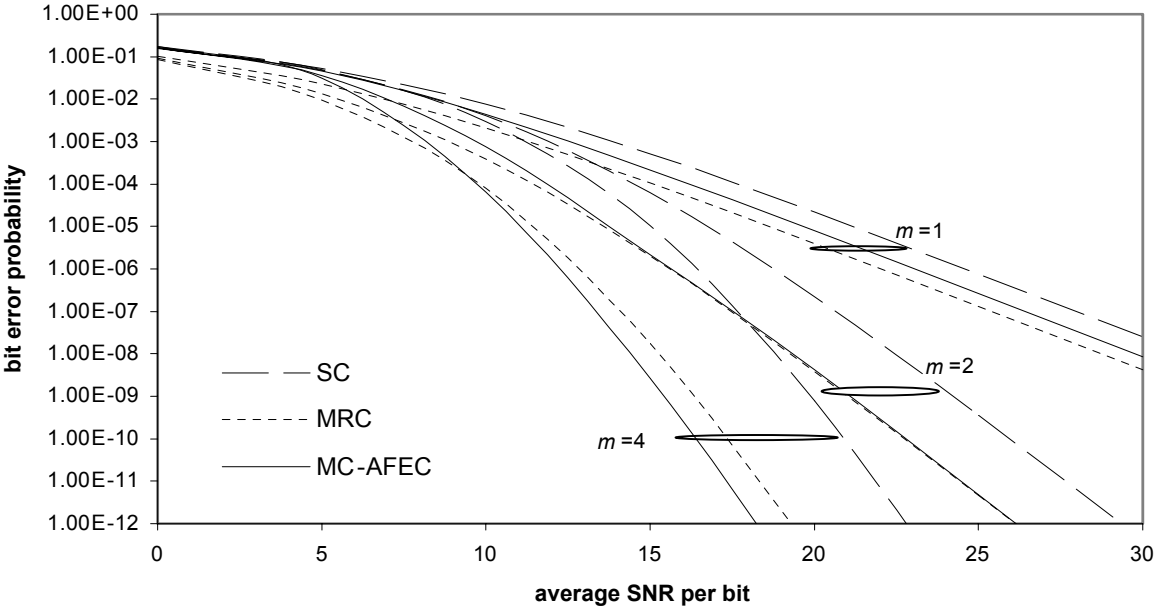

Figure 3.22: The performance of the BCH-coded MC-AFEC system at R= 1/L compared to SC and MRC over L = 3 Nakagami fading channels with different values of m.

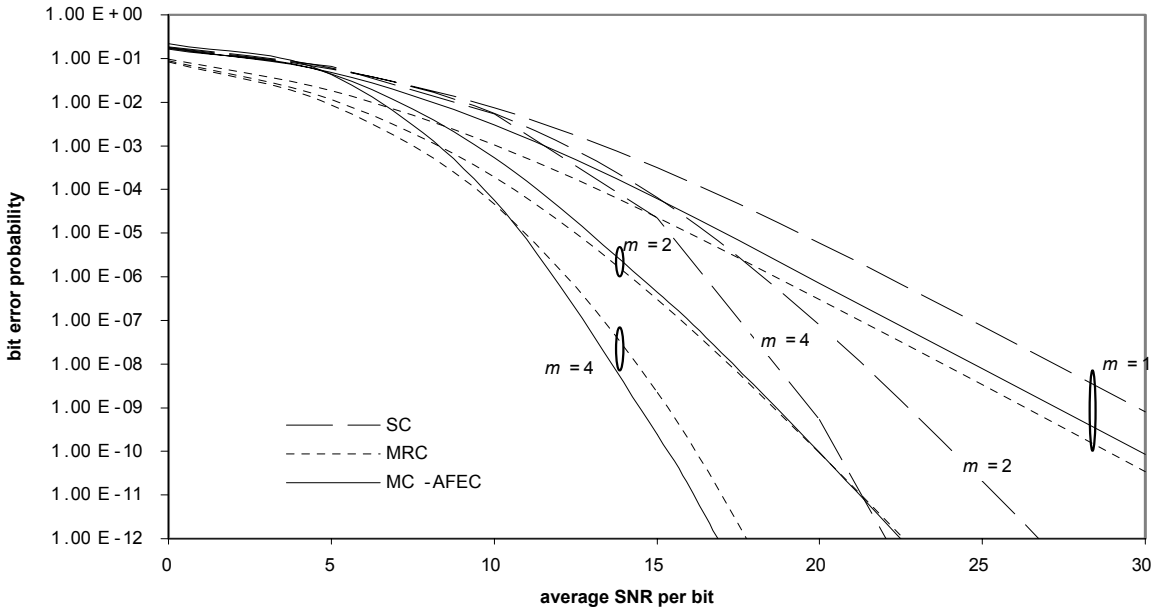

Figure 3.23: The performance of the BCH-coded MC-AFEC system at R= 1/L compared to SC and MRC over L = 4 Nakagami fading channels with different values of m.

To examine the effect of changing the number of diversity channels consider Figures 3.24 to 2.27. In each figure, the BER of the MC-AFEC is compared to the SC and MRC systems with different values of L for a certain value of m. Observing the figures we notice the following:

- As L increases the performance is increased as well.

- At a very low SNR, increasing the number of channels reduces the performance. This means that the MC-AFEC system, like the SC system, is inefficient at very low SNR.

- At a very low SNR the system tends to follow the SC system. This is not surprising since at a noisy environment the MC-AFEC system will more likely use the ON/OFF code set, the set that mimics the SC operation.

- At a very high SNR the system tends to follow the MRC system. That is because at high SNR the MC-AFEC tries to utilize the CSI of the channel efficiently by assigning the appropriate code set.

- As m increases, the improvement of the MC-AFEC system is more than that of MRC. That is because as m increases the channel tends to be Gaussian. In Gaussian environment, no significant improvement can be noticed in the MRC system since it just became a repetitive code. However, using BCH or RS code in Gaussian channels will improve the performance.

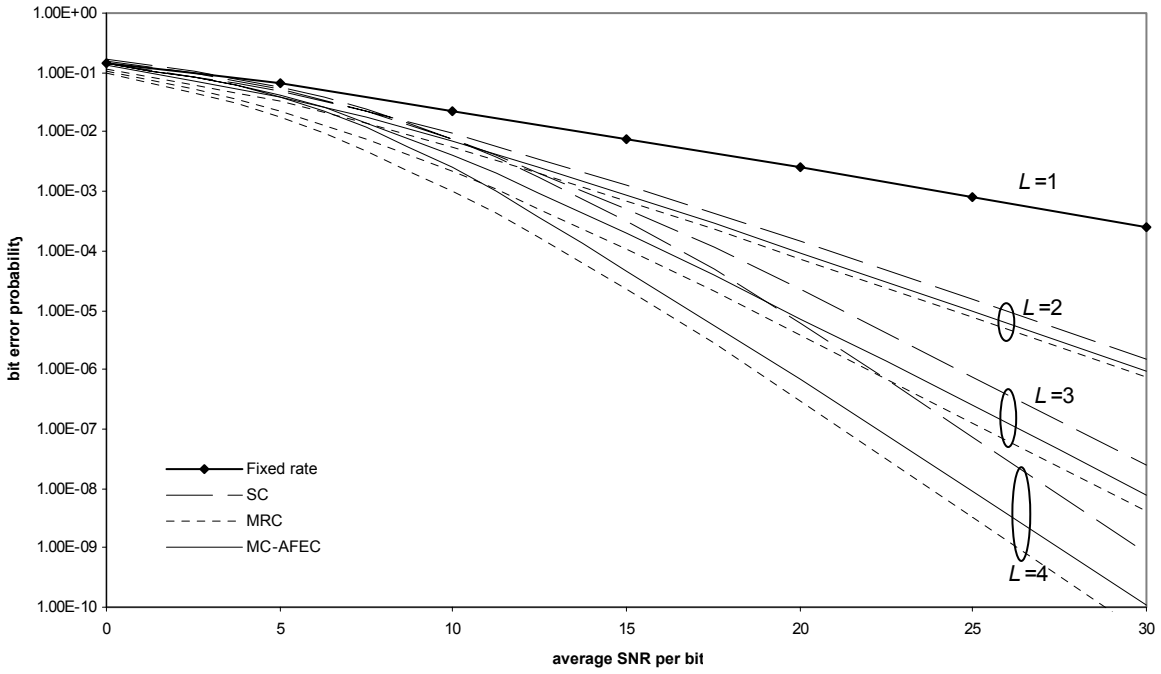

Figure 3.24: The performance of the RS-coded MC-AFEC system at R= 1/L compared to SC and MRC over different number of Nakagami fading channel with m = 1.

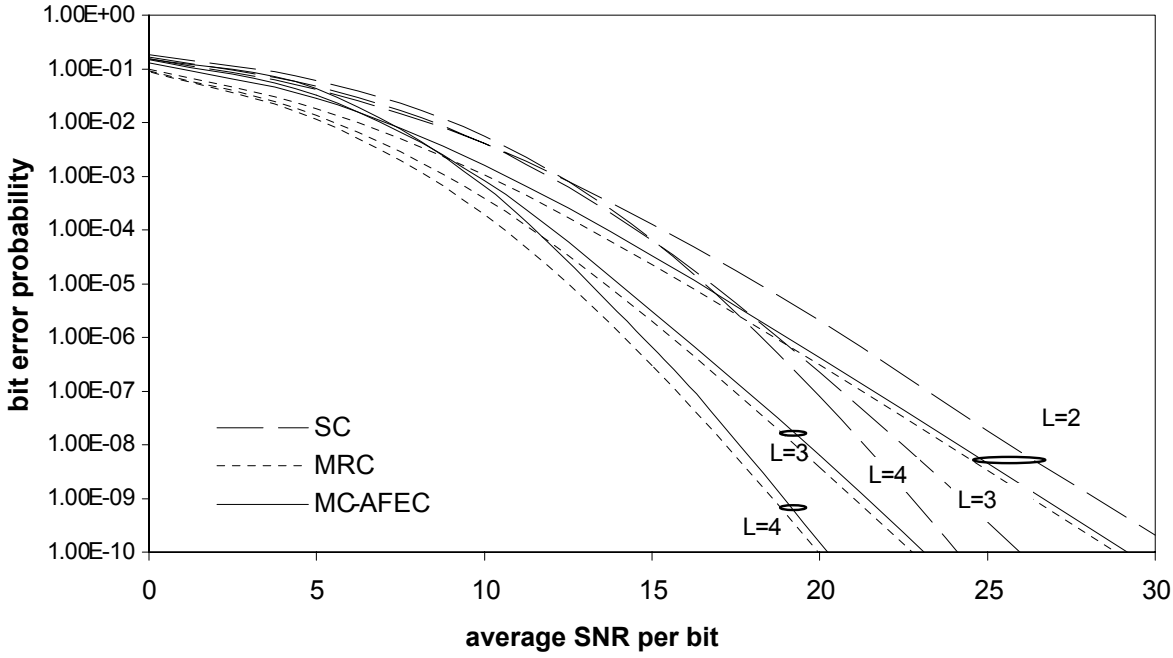

Figure 3.25: The performance of the RS-coded MC-AFEC system at *R*= 1/*L* compared to SC and MRC over different number of Nakagami fading channel with *m* = 2.

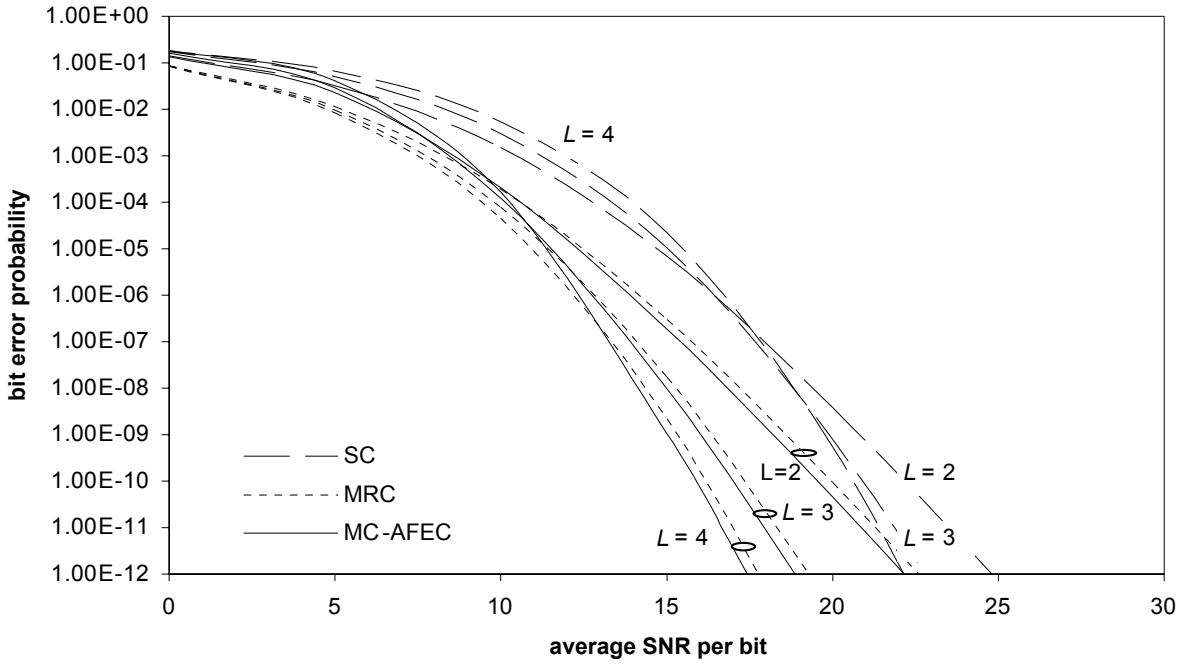

Figure 3.26: The performance of the RS-coded MC-AFEC system at R= 1/L compared to SC and MRC over different number of Nakagami fading channel with m = 4.

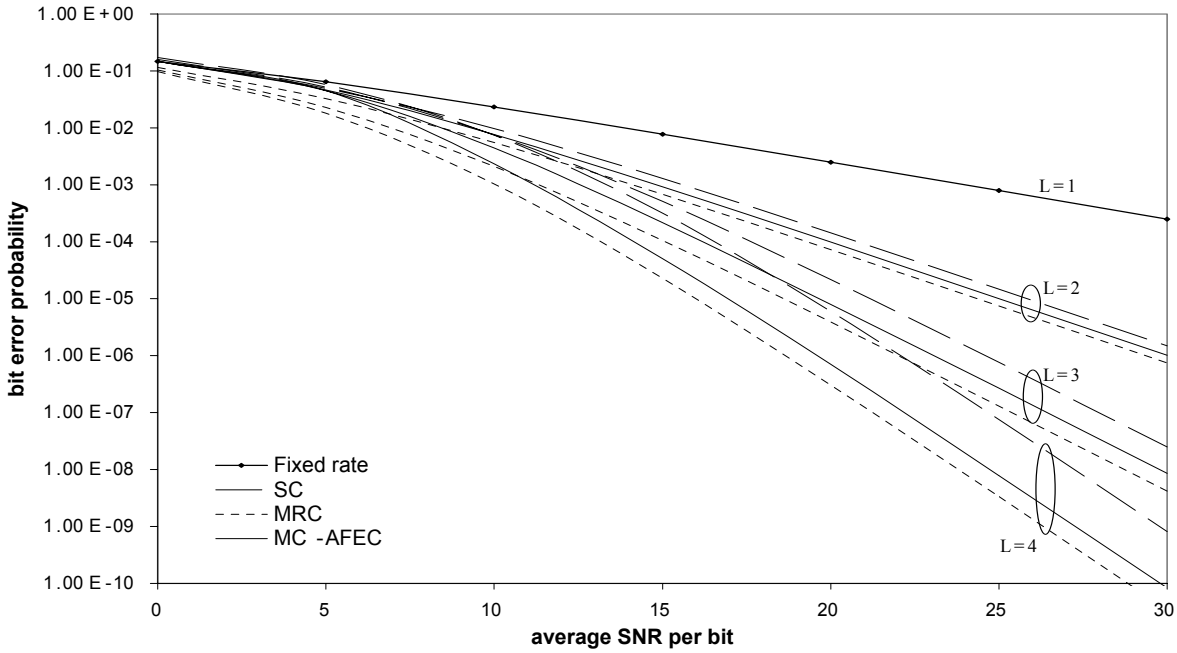

Figure 3.27: The performance of the BCH-coded MC-AFEC system at R= 1/L compared to SC and MRC over different number of Nakagami fading channel with m=1.

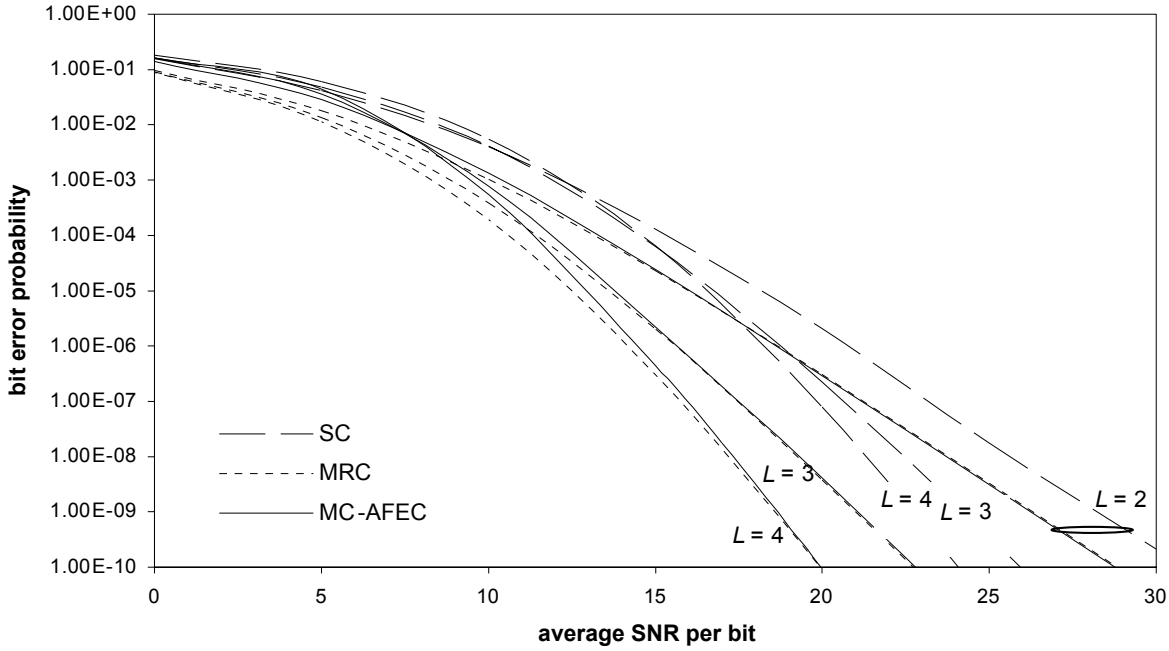

Figure 3.28: The performance of the BCH-coded MC-AFEC system at R= 1/L compared to SC and MRC over different number of Nakagami fading channel with m=2.

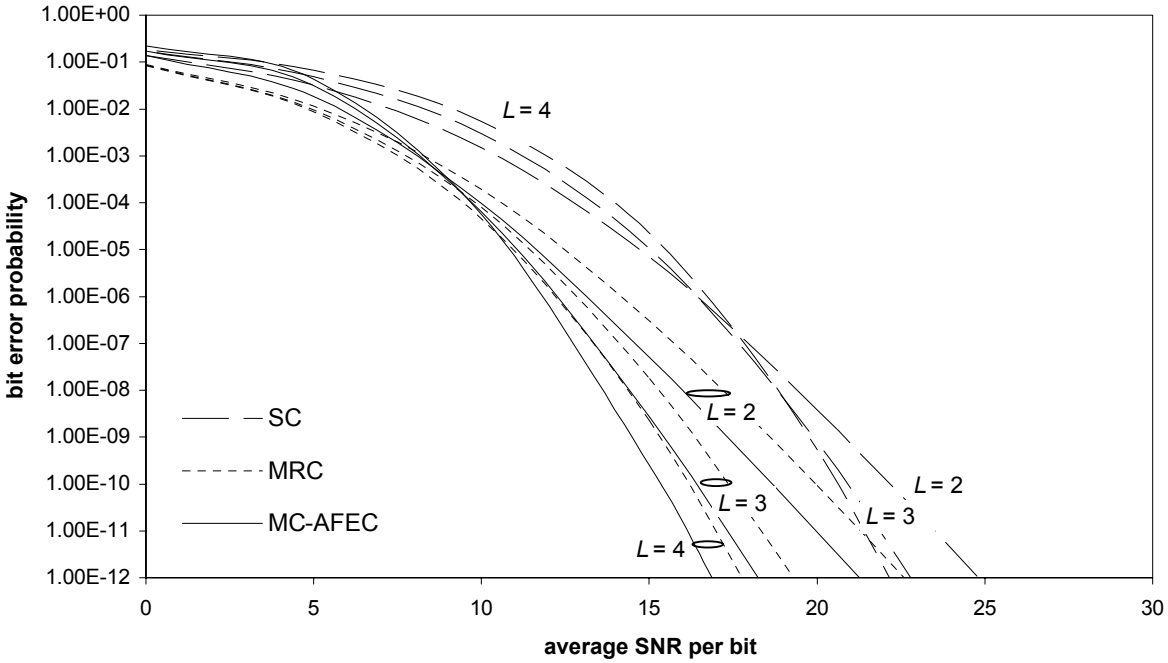

Figure 3.29: The performance of the BCH-coded MC-AFEC system at R= 1/L compared to SC and MRC over different number of Nakagami fading channel with m=4.

As a final point, consider Figures 3.30 to 3.35, where the performance of RS coded system is plotted versus the BCH system with different number of channels and with different fading parameters. It can be seen that with at m = 1 the two systems perform almost the same with RS system is getting slightly better at very low SNR. However, increasing m will make the BCH system superior to the RS system. The cause of this behavior is the ability to correct random noise, since the BCH codes are more powerful in random error correction than RS codes. And as m increases, the randomness of the noise increases as well. Hence, The BCH coded system will always perform better than RS coded system at higher m values.

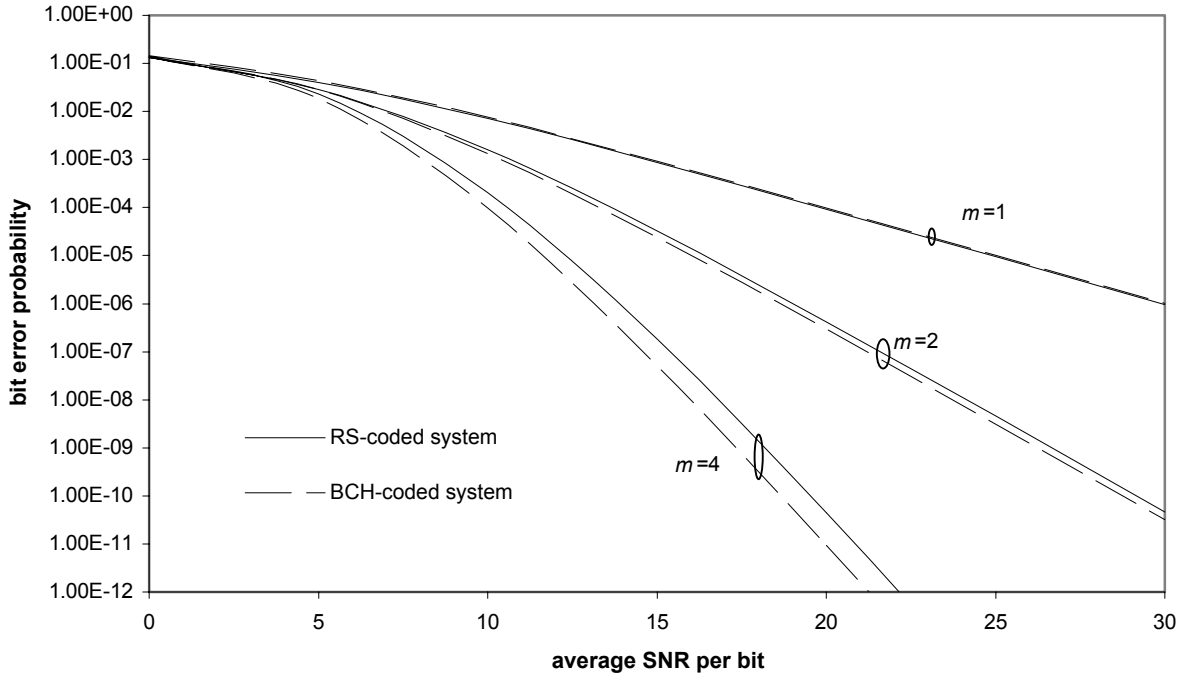

Figure 3.30: Comparison between RS-coded MC-AFEC and BCH coded system in Nakagami-m fading of different values of m with two diversity channels.

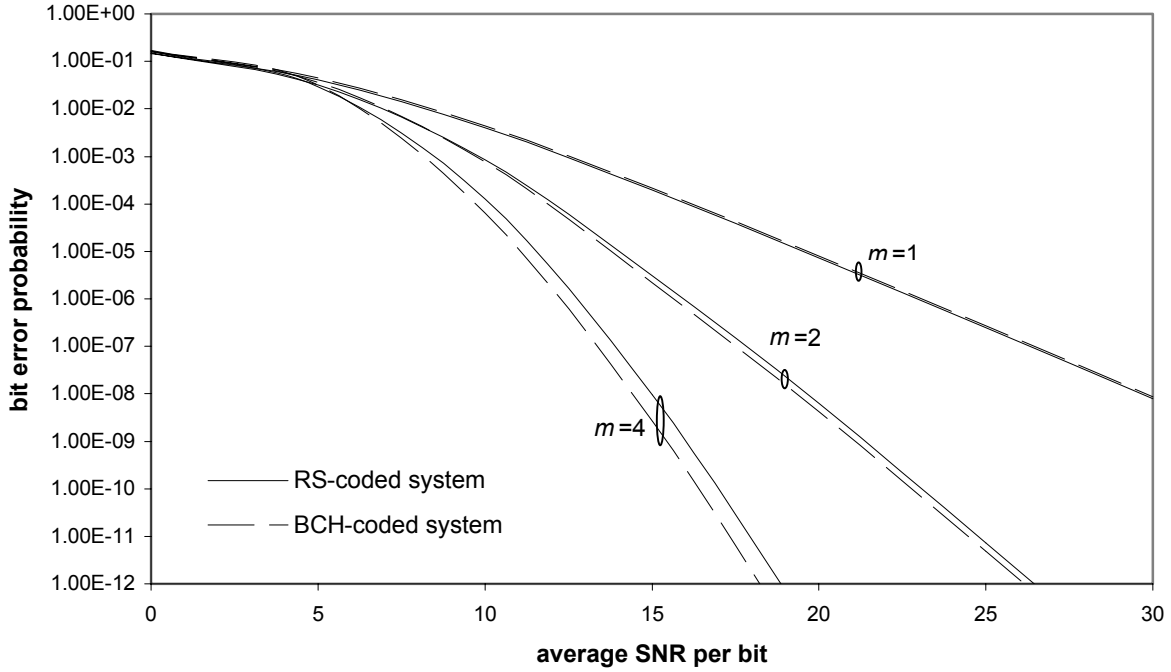

Figure 3.31: Comparison between RS-coded MC-AFEC and BCH coded system in Nakagami-*m* fading of different values of *m* with three diversity channels.

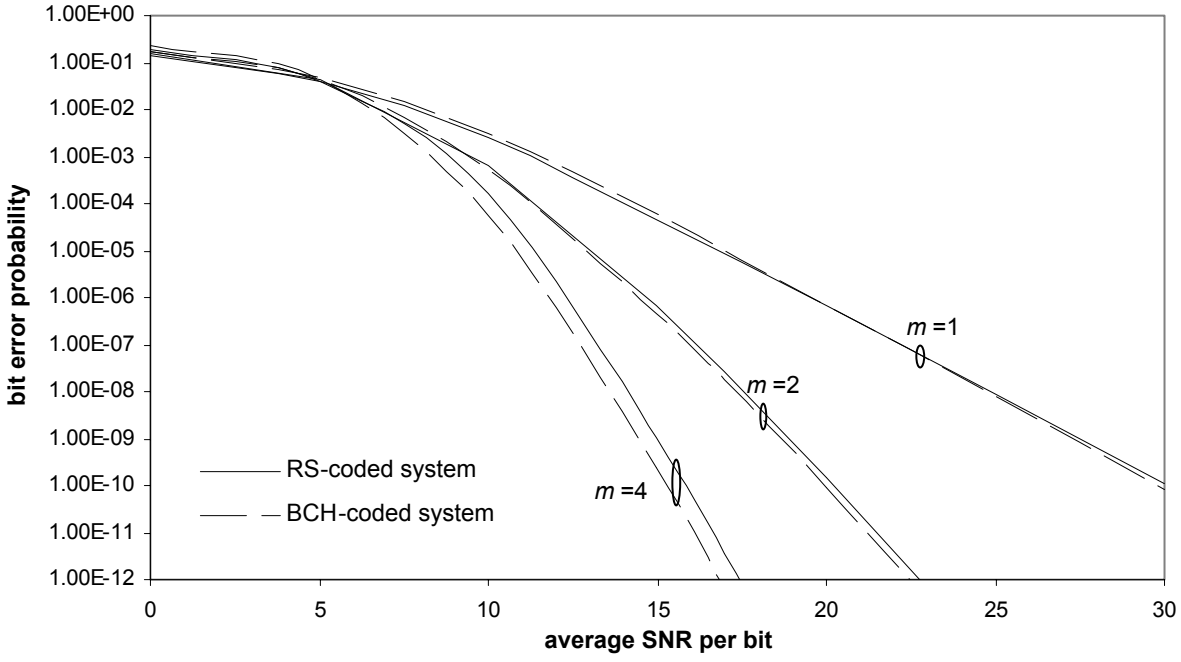

Figure 3.32: Comparison between RS-coded MC-AFEC and BCH coded system in Nakagami-*m* fading of different values of *m* with four diversity channels.

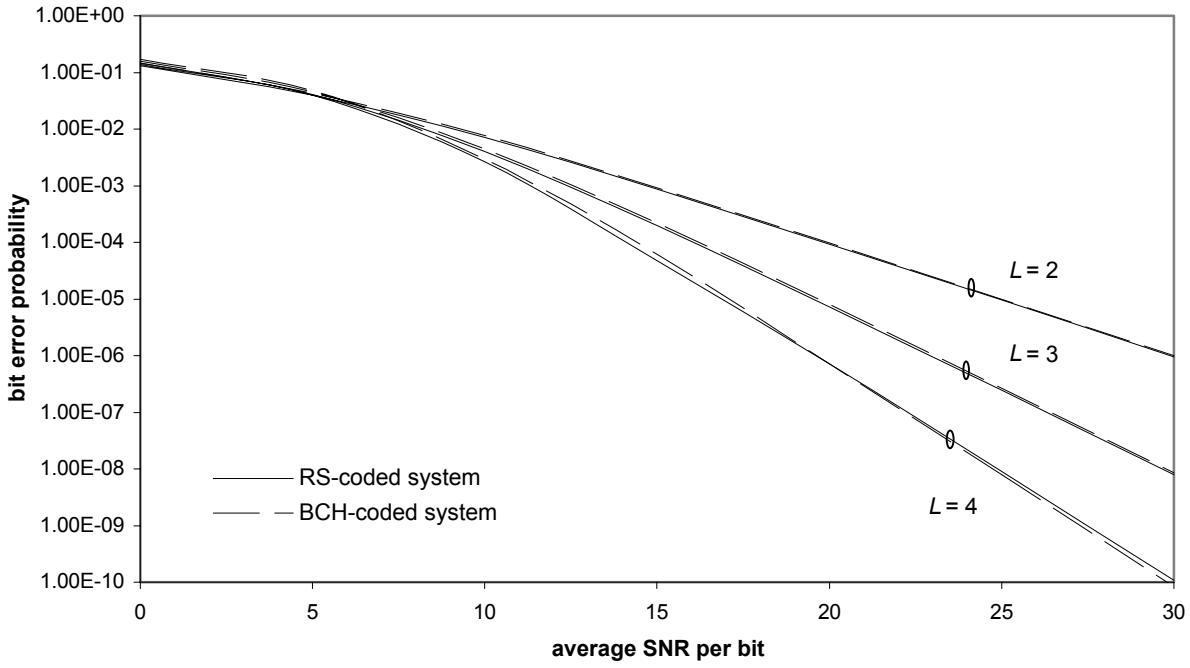

Figure 3.33: Comparison between RS-coded MC-AFEC and BCH coded system in Nakagami-*m* fading of *m* =1with different number of diversity channels.

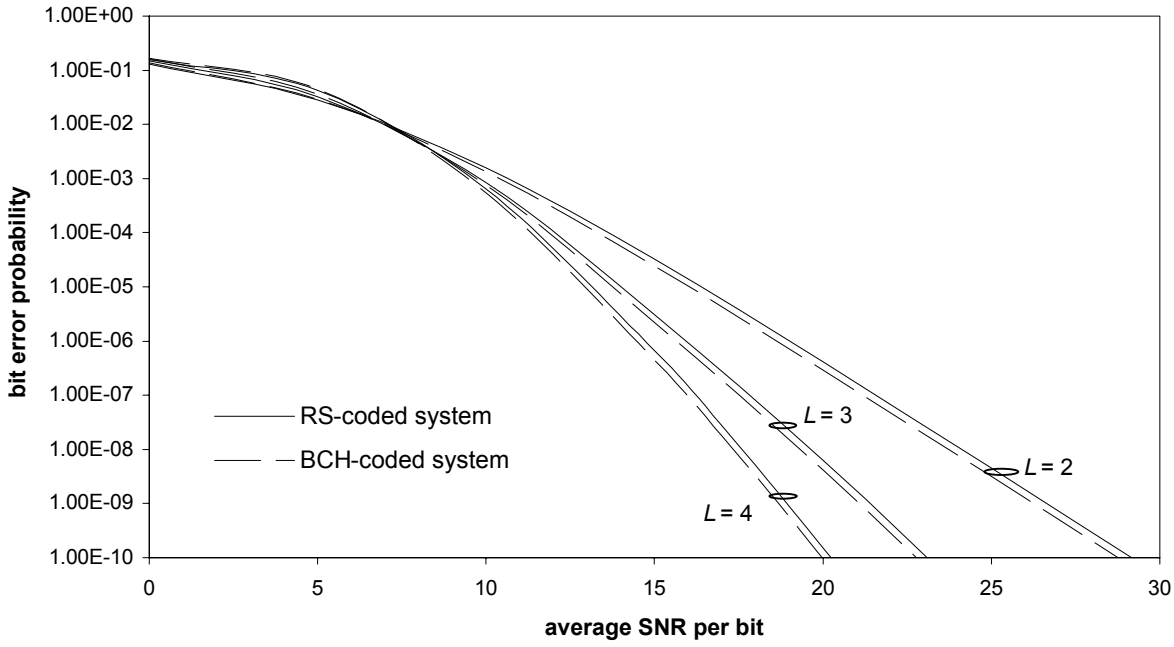

Figure 3.34: Comparison between RS-coded MC-AFEC and BCH coded system in Nakagami-*m* fading of *m* =2with different number of diversity channels.

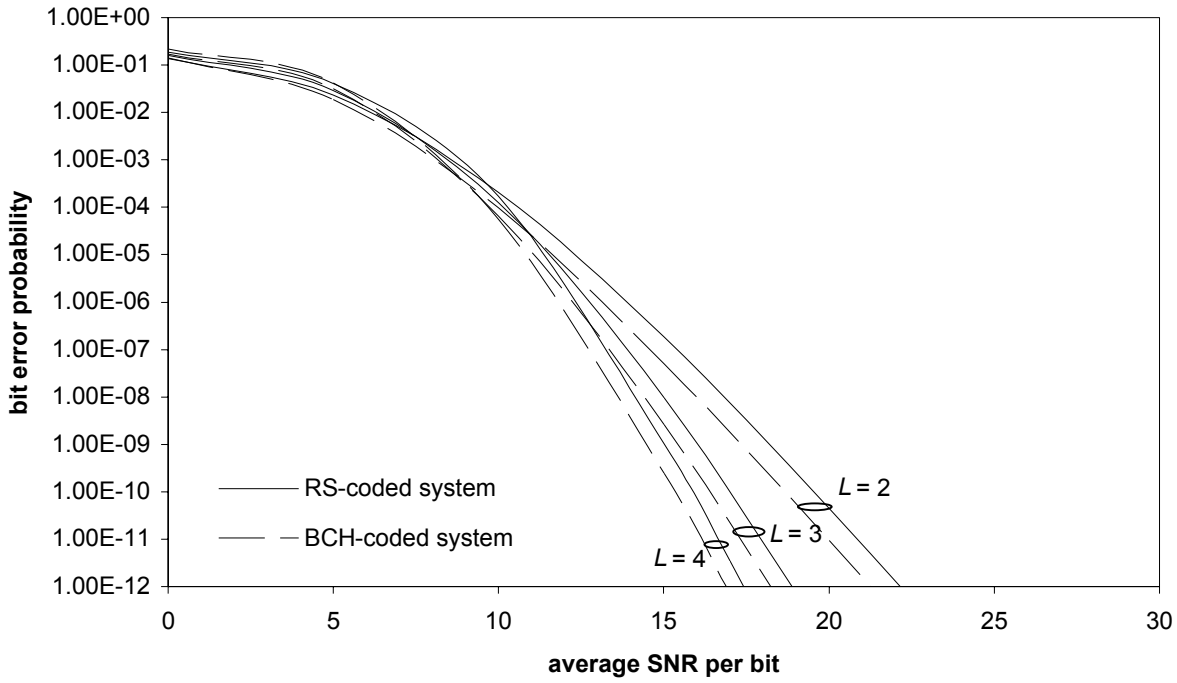

Figure 3.35: Comparison between RS-coded MC-AFEC and BCH coded system in Nakagami-*m* fading of *m* =4 with different number of diversity channels.

CHAPTER 4

CONCLUSIONS AND SUGGESTIONS FOR FURTHER WORK

4.1 Conclusions

In this thesis, forward error correction has been employed in an adaptive way to improve the performance of communication transmission over number of parallel channels perturbed by fading. The adaptive technique was applied to minimize the BER of the system under the constraint of fixed throughput; that is, the overall rate of flow of transmitted symbols from transmitter to the receiver was fixed, but the rates of the codes used for each channel was adjusted to match the prevailing channel state information

CSI. Channels having poor quality are allocated fewer information symbols and more check symbols, and better quality channels are allocated an increased number of information symbols and a reduced number of check symbols. This system, referred to as Multi-Channel Adaptive Forward Error-Correction (MC-AFEC) system has been studied under different environments. The performance of this system shows an improved performance compared to classical diversity systems with the advantage of having flexible throughput rate, but with the cost of increasing the complexity of the system, where the price is the added feedback channel and error correction coding.

In Chapter 2, the MC-AFEC system has been described and analyzed in details. In addition, the optimization technique and the evaluation methods used in this work have been explained. Two evaluation methods have been discussed: numerical integration and computer simulation. The results of the two methods are found matched. It has been found also that the performance of the MC-AFEC system does not improve linearly with increasing the number of channels or decreasing the throughput. In fact, the performance is dependent on the relative values of the throughput R and the number of channels L, where small and gradual changes in the BER have been noticed over the interval $\frac{i-1}{L} < R \le \frac{i}{L}$, $i = 1,2,\ldots,L$. However, at $R = i/L$, a large change has been remarked. It has been concluded that no decrease in R below $1/L$ will lead to an improvement in the performance; in fact the performance deteriorates as the system operates below $1/L$.

In the last section of Chapter 2, the effect of using one code set on the performance has been studied. It has been shown that by using a single code set selected in a particular way, most of the advantages of adaptation can be obtained, and the performance in this case is shown to be slightly inferior to that obtainable with larger number of code sets.

In chapter 3, the performance of the MC-AFEC system has been studied in different environments and compared to classical diversity systems. The chapter started by a comparison between the MC-AFEC system and SC over Rayleigh fading channels. It has been found that the MC-AFEC system outperforms SC for the same rate and the same number of channels, and in some cases the MC-AFEC with higher throughput can outperform SC at moderate and low SNR.

The effect of correlation has been investigated by means of numerical evaluation and computer simulation in the case of dual diversity. For the case of $L > 2$, simulation only has been employed to evaluate the BER of the system. In the evaluation, the same correlation coefficient ρ was assumed between channel pairs. The techniques of generating correlated branches have been explained for both evaluation methods. It has been found that the BER of both systems: MC-AFEC and SC, increases with the increase of the correlation between channels. It has been shown that both systems become more sensitive to the correlation as the number of diversity channels increases. It has been found also that the behavior of the MC-AFEC agrees with SC behavior. However, the performance of the MC-AFEC is still better than that of SC at all values of ρ.

The MC-AFEC system has been simulated in the presence of delayed channel state information CSI to study its impact on the performance. A Jakes-like algorithm has been utilized to model the channels. With different values of Doppler rate f_DT, the BER has been calculated and compared to SC. It has been shown that the impact of outdated CSI on the performance is dependent on the values of f_D and SNR. As f_DT increases the sensitivity to the outdated CSI increases as well. In the same way, at low SNR the effect of outdated CSI was found to be insignificant while it becomes more severe as SNR increases. On the other hand, SC shows more immunity to the outdated CSI, and its superiority appears at high SNR.

In the last section, the effect of fading severity has been studied and compared to MRC and SC. For this purpose, the amount of fading (AF) has been adopted to measure the severity of fading. The BER of the system has been evaluated over Nakagami-*m* fading channels with different AF (or *m*) values. It has been found that the system shows more improvement with the decrease in AF compared to MRC and SC. It has also been found that the MC-AFEC system outperforms SC in all cases, and the superiority of the MC-AFEC system increases with the decreases of AF. However, MRC was found to perform better than the MC-AFEC system in most cases. Nevertheless, the inferiority of the MC-AFEC system decreases as AF decreases to the point that it outperforms MRC when AF= 1/4.

The final section concluded by a comparison between the BCH-coded system and the RS-coded systems over Nakagami-*m* fading channels with different amounts of fading. It has been found that both systems have close performance when AF= 1.

However, at very low SNR, the RS-coded system shows a very small improvement over the BCH-coded system; whereas at high SNR the performance of BCH-coded systems tends to be better at higher SNR. Moreover, when AF decreases, the improvement of the performance of the BCH-coded system tends to be better than that of RS-coded system, which makes the BCH-coded system superior to the RS-coded system at AF > 1.

4.2 Suggestions for further work

In view of the findings of this work, the following suggestions is made for carrying out further work in this area:

1. The MC-AFEC system relies, to a large extent, on accurate channel state information CSI. In practice, CSI must be obtained in the presence of noise and delay. The effect of delayed CSI has been considered in Chapter 3. However, the effect of erroneous estimates has not been considered. The CSI has been assumed error free, which means that the estimates are perfect and the feedback channels are noise free. It would be worth studying the effect of errors in both cases. This actually would require evaluating the performance of the system employing a specific channel quality estimation method.

2. The channels were assumed to be perturbed by block fading. Block fading implies that the fading should be very slow, which makes the channels more likely frequency selective. That is because, in order to

have slow fading channel, the bandwidth of the transmitted signal should be much greater than the Doppler spread, and increasing the bandwidth of the signal increases the chance of the frequency selectivity of the channel. Thus, it would be valuable to investigate the behavior of the system over frequency selective block fading channels.

3. Coherent BPSK has been assumed as the modulation scheme of the MC-AFEC system. Since RS codes are non-binary codes, it would be worth studying the performance of the system using non-binary modulation scheme. In addition, ideal coherent phase detection was assumed. It would be valuable to study the impact of non-ideal coherent detection of the phase. In addition, the performance of the system can be studied for different modulation schemes and various error correcting codes.

4. In the study of the effect of branch correlation, outdated CSI and fading severity, each factor has been studied separately. It would be valuable to combine the effect of two or three factors together. For example, the effect of branch correlation or outdated estimates can be studied with different amount of fading.

References

[1] Sklar, B., "Rayleigh fading channels in mobile digital communication systems .I. Characterization," *IEEE Commun. Mag.*, Vol. 35, no. 7, pp. 90 –100, Jul 1997.

[2] Sklar, B., "Rayleigh fading channels in mobile digital communication systems .II. Mitigation," *IEEE Commun. Mag.*, Vol. 35, no. 7,pp. 102 –109, Jul 1997.

[3] Simon, M.K. and M-S. Alouini, *Digital Communication over Fading Channels: A Unified Approach to Performance Analysis*, New York: Wiley-Interscience, 2000.

[4] Sweeney, Peter, *Error Control Coding An Introduction*, Englewood Cliffs, NJ: Prentice-Hall, 1991.

[5] Peterson, W.W. and E.J. Weldon, Jr., *Error Correcting Codes*, Cambridge, MA: MIT Press, 1972.

[6] Michelson, A.M. and A.H. Levesque, *Error-Control Techniques for Digital Communications*, New York: Wiley-Interscience, 1985.

[7] Reed, Irving S. and Xuemin Chen, *Error-Control Coding for Data Networks*, Kluwer Academic Publishers, 1999.

[8] J. G. Proakis, *Digital Communications*, 3rd ed. New York: McGraw Hill, 1995.

[9] K. Ohno, Adachi, F.and Kawamura, K., "Combined effect of diversity reception/channel coding on error floor due to delay spread in DPSK mobile radio," *Electronics Letters* , vol. 28, no. 12 , pp. 1131 -1133, 4 June 1992.

[10] A.A. Abu-Dayya and Beaulieu, N.C. , "Correlated diversity versus simple block coding on frequency-selective fading channels," *Proc. Canadian Conf. Electrical and Comp. Eng.*, vol.1, pp. 202 -205, 1994.

[11] A.A. Abu-Dayya, and Beaulieu, N.C., "Dual diversity versus simple block coding for correlated frequency-selective fading channels," *IEEE Global TeleComm. Conf., GLOBECOM '94.*, vol. 1, pp. 430 -435,1994.

[12] A.A. Abu-Dayya .and Beaulieu, N.C., "Comparison of diversity with simple block coding on correlated frequency-selective fading channels," *IEEE Trans. Comm.*, vol. 43, no. 11 , pp. 2704 -2713, Nov. 1995.

[13] Hong Zhou, Deng, R.H. and Tjhung, T.T., "Performance of combined diversity reception and convolutional coding for QDPSK land mobile radio," *IEEE Trans.Vehicular Technology*, vol. 43 3 1-2, pp. 499 -508 , Aug. 1994.

[14] G. Taricco, Biglieri, E.M.and Caire, G., "Impact of channel-state information on coded transmission over fading channels with diversity reception," *IEEE Trans.Comm.* , vol. 47, no. 9 , pp. 1284 -1287 , Sept. 1999.

[15] Kang Byeong-Gwon and Myoung-Jin Kim, "Comparison of coding effects in a diversity combining DS/CDMA cellular system," 5th IEEE Intern. Conf. Universal Personal Comm., vol. 2 , pp. 989 -993, 1996.

[16] A. Abrardo, Benelli, G., Bini, A., and Garzelli, A., "Demodulation and decoding for diversity mobile radio systems," *IEE Proc. Comm.*, vol. 142, no. 5 , pp. 315 – 322, Oct. 1995.

[17] Hayoung Yang, Seoungkoo Lee, Bonjin Ku and Changeon Kang, "Combination of multiple turbo codes and multiple antennas for direct-sequence CDMA systems," *ICCE. Intern. Conf. Consumer Electronics*, pp. 316 -317, 1999.

[18] Hongjun Xu and F. Takwira, "Turbo Coded/Diversity Combining Scheme for Hybrid DS/SFH CDMA Systems," *IEEE AFRICON*, pp.75-80, 1999.

[19] J. Wang, and Moeneclaey, M., "Multiple hops/symbol FFH-SSMA with MFSK modulation and Reed-Solomon coding for indoor radio," *IEEE Trans. Commun.*, vol. 41, no. 5 , pp. 793 -801, May 1993.

[20] S. Sakakura, Wei Huang and Nakagawa, M., "Pre-diversity using coding, multi-carriers and multi-antennas," *Fourth IEEE Intern. Conf. Universal Personal Comm.*, pp. 605 –609, 1995 .

[21] Joonsuk Kim, Cimini, L.J., Jr. and Chuang, J.C., "Coding strategies for OFDM with antenna diversity high-bit-rate mobile data applications," *48th IEEE Vehicular Technology Conf, VTC 98.*, vol. 2 , pp. 763 -767, 1998.

[22] J. F. Hayes, "Adaptive feedback communication," *IEEE Trans. Comm. Tech.*, vol COM-16, no. 1, pp. 29-34, Feb 1968.

[23] A. Goldsmith and Chua, S.-G., "Adaptive coded modulation for fading channels," *IEEE Trans. Comm.*, vol. 46, no. 5 , pp. 595 -602, May 1998.

[24] A. Goldsmith and P. Varaiy, "Increasing Spectral efficiency through Power Control," *Proc. IEEE Intern. Comm. Conf.*, pp. 600-604, May 1993

[25] A. Goldsmith, "Joint source/channel coding for wireless channels," *45th IEEE Vehicular Technology Conf.*, vol. 2 , pp. 614 –618, 1995.

[26] A. Goldsmith, "Adaptive modulation and coding for fading channels," *Proc. of the 1999 IEEE Info. Theo. and Comm. Workshop*, pp. 24 -26 , 1999.

[27] R.H. Deng, Hong Zhou, "An adaptive coding scheme with code combining for mobile radio systems," *IEEE Trans. Vehicular Technology*, vol. 42, no. 4, pp. 469 -476, Nov. 1993.

[28] C. Mitchell, Swarts, F.and Aghdasi, F., "Adaptive coding in fading channels," *IEEE Africon*, vol. 1, pp. 81 -86, 1999.

[29] R. Chen, Chua, K.C., Tan, B.T., and Ng, C.S., "Adaptive error coding using channel prediction," *Seventh IEEE Intern. Symposium on Personal, Indoor and Mobile Radio Comm. PIMRC'96.,* vol. 2 , pp. 359 -363, 1996.

[30] M. A. Kousa and L. F. Turner, "Multichannel adaptive forward error correction system," IEE Proc-I, vol. 140, no. 5, pp. 357-64, Oct. 1993.

[31] M.A. Kousa and Al-Semari, S.A, "Adaptive binary coding for diversity communication systems," *IEEE Intern. Conf. Personal Wireless Comm*, pp. 80 - 84, 1997.

[32] M.A. Kousa. "Adaptive Forward Error Correction systems For Time-Varying Channels", Ph.D. thesis, Dept. of Elec. Eng., Imperial College of Science, Technology and Medicine, London, 1993

[33] J. E. Freund and R. E. Walpole, *Mathematical Statistics*. Englewood Cliffs, N. J.: Prentice Hall, 1980.

[34] Davis, Philip J., *Methods of Numerical Integration*, 2nd ed. New York: Academic Press, 1984.

[35] Q. T. Zhang. " A decomposition Technique for Efficient Generation of Correlated Nakagami Fading Channel," *IEEE Journal On Selected Areas In Commun.,* Vol. 18, No. 11, pp. 2385-2392, Nov. 2000.

[36] M. Nakagami, "The *m*-distribution: A general formula of intensity distribution of rapid fading," in Statistical Methods in Radio Wave Propagation. Oxford: Pergamon Press, pp. 3-36, 1960.

[37] V. A. Aalo, “Performance of maximal-ratio diversity systems in a correlated Nakagami-fading environment,” *IEEE Trans. Commun.*, vol. COM-43, pp. 2360-2369, Aug. 1995.

[38] A. Leon-Garcia, *Probability and Random Processes for Electrical Engineering.* Addison-Wesley, 1989.

[39] U. Charash, “A study of multipath reception with unknown delays.” Ph.D. dissertation, University of California, Berkeley, CA, Jan 1974.

[40] J. K. Cavers, *Mobile Channel Characteristics.* Norwell, MA: Kluwer Acadimic publishers, 2000.

[41] W. C. Jakes, ed., *Microwave Mobile Communications*, AT&T, 1974, reissued by IEEE, 1993.

[42] A. Ciofini, E. Del Re, L. S. Ronga, “W-CDMA Adaptive Receiver with Space-Frequency Diversity for Multi-path Fading Channels”, *VTC 2001 Spring Conference*, Rhodes, Greece, Vol.4, pp. 1538-1542, May 2001.

[43] S. Kaiser, ``OFDM code division multiplexing with unequal error protection and flexible data rate adaptation," in Proc. IEEE Global Telecommun. Conf. (GLOBECOM 2001), San Antonio, USA, pp. 861-865, Nov. 2001.

[44] Q. Liu, S. Zhou, and G. B. Giannakis, “Combining Adaptive Modulation and Coding with Truncated ARQ Enhances Throughput,” *Proc. of Signal Proc. Workshop on Advances in Wireless Communications (SPAWC)*, Rome, Italy, June 15-18, 2003.

[45] Q. Liu, S. Zhou, and G. B. Giannakis, “Jointly Adaptive Modulation and Packet Retransmission over Block Fading Channels with Robustness to Feedback Latency,” *Proc. of the 37th Conf. on Info. Sciences & Systems (CISS)*, Baltimore, Maryland, March 12-14, 2003.

[46] P. Xia, S. Zhou, and G. B. Giannakis, “MIMO OFDM with ST Coding and Beamforming Adapted to Partial CS,” *Proc. of the 37th Conf. on Info. Sciences & Systems (CISS)*, Baltimore, Maryland, March 12-14, 2003.

Vita

Saad Saeed Al. Abeedi was born in Saudi Arabia. He obtained a B. sc. Degree in Electrical Engineering from King Fahd University of Petroleum and Minerals (KFUPM), Dhahran, Saudi Arabia in 1998. he joined KFUPM as graduate student in 1998. his successful defense of this thesis at KFUPM in Dec, 2003 marks his acquisition of a Masters of Science degree in Electrical Engineering (Communications Option).